Molecular mechanism of xylose utilization in a plant growth-promoting bacterium *Pseudomonas fluorescens* SBW25

A thesis submitted in partial fulfillment of the requirements for the degree of Doctor of Philosophy in Genetics at Massey University, Auckland, New Zealand

Yunhao Liu

2015

Abstract

Pseudomonas fluorescens SBW25 is a plant growth-promoting bacterium that was originally isolated from the phyllosphere of field-grown sugar beet. It is capable of aggressively colonizing sugar beet and a number of other crops such as wheat, maize and peas, and inhibiting the damping-off disease caused by *Pythium ultimum*. *P. fluorescens* SBW25 has become an important model organism for studying the molecular interactions between bacteria and plants. Previous promoter-trapping analysis showed that SBW25 elevates expression of over 100 genes in its genome when colonizing sugar beet seedlings. These include a candidate gene for xylose utilization, suggesting that SBW25 colonization may be critically dependent on the presence and catabolism of plant-derived xylose. The overall aim of this project is to unravel the molecular basis of xylose utilization by *P. fluorescens* SBW25 and demonstrate its ecological significance for bacterial survival in complex plant experiments.

Bacterial degradation of xylose is sequentially mediated by two enzymes - an isomerase (XutA) and a xylulokinase (XutB) - with xylulose as an intermediate. *P. fluorescens* SBW25, though capable of growth on xylose as a sole carbon source, encodes only one degradative enzyme XutA in the xylose utilization (*xut*) locus. Here, using site-directed mutagenesis and transcriptional assays I identified two functional xylulokinase-encoding genes (*xutB1* and *xutB2*), and further showed that expression of *xutB1* is specifically induced by xylose. Surprisingly, the xylose-induced *xutB1* expression is mediated by the mannitol-responsive regulator MtlR, using xylulose rather than xylose as the direct inducer. In contrast, expression of the *xutA* operon is regulated by XutR in a xylose- and xylulose-dependent manner. Moreover, the data indicate a complex overlapping cellular responses to xylose and other structurally similar sugars such as mannitol, sorbitol, fructose as well as ribose.

Both XutR and MtlR are transcriptional activators of the AraC family, members of which typically use DNA-looping to modulate levels of gene expression. The functionality of XutR has been subjected to detailed genetic and biochemical

analyses, including promoter mapping, electrophoretic mobility shift assay (EMSA) and DNase I footprinting assay. My data leads to a XutR regulatory model that does not involve DNA-looping. XutR functions as a dimer, which recognizes two inverted repeat sequences; but binding to one half site is very weak requiring inducer molecules such as xylose for activation.

To determine the ecological significance of xylose utilization for bacterial colonization *in planta*, a Xut$^-$ mutant (Δ*xutA*) was subjected to competitive colonization on sugar beet seedlings together with a neutrally marked wild-type strain. Results showed that the Δ*xutA* mutant was significant less competitive than the wild-type strain both in the shoot and the rhizosphere. Together, the data show that xylose utilization is an important trait for *P. fluorescens* SBW25 to colonize surfaces of plants.

It should be noted that xylose can only support slow bacterial growth of *P. fluorescens* SBW25, and thus it is not the sugar of choice in the presence of other preferred carbon and energy sources such as succinate, glucose and arabinose. The underlying mechanism is called carbon catabolite repression (CCR). CCR has been well studied in *E. coli*, where it is mainly mediated by the catabolite-activation protein CAP charged with cAMP. However, CCR still remains elusive for non-enteric bacteria such as *Pseudomonas*. Previous studies in other *Pseudomonas* species indicate that CCR in *Pseudomonas* occurs at post-transcriptional levels and involves specific binding of the Crc protein to mRNAs of respective catabolic genes. However, genetic tools suitable for studying post-transcriptional gene expression are lacking, particularly vectors derived from mini-Tn*7*. Mini-Tn*7* vectors possess the advantage of delivering reporter fusions into the chromosome in a site- and orientation-specific manner.

To facilitate the study of CCR in *Pseudomonas*, I have successfully constructed and validated a panel of five mini-Tn7 vectors for analysis of post-transcriptional gene expression in *Pseudomonas*. Four vectors allow construction of translational fusions to β-galactosidase (*lacZ*), while the fifth is designed for functional analysis of noncoding RNA genes. Translational fusions can be constructed without a functional

promoter in the vector or from an inducible promoter of either P_{tac} or P_{dctA}. I show that promoterless fusions have value for determining levels of translation, whereas fusions to inducible promoters have utility in the analysis of mRNA-binding factors.

Next, a combination of site-directed mutagenesis and gene expression assays were used to identify regulators that are involved in the succinate-mediated repression of the *xut* operon. Succinate is an intermediate of the tricarboxylic acid (TCA) cycle and it is preferentially used by *P. fluorescens* SBW25 as a source of carbon and energy. In this work, I have successfully identified the major regulatory components of CCR in *P. fluorescens* SBW25. These include a two-component signal transduction system CbrAB, two small non-coding RNAs CrcY and CrcZ, and a two-protein complex composed of Crc and Hfq. Results showed that when succinate is present, the Crc/Hfq complex inhibits expression of *xut* genes via binding of the mRNA transcript; when succinate disappears, CbrAB activates the expression of CrcY and CrcZ, which in turn sequesters the Crc/Hfq complex and relieves repression of the *xut* operon.

Taken together, data presented in this thesis indicate novel mechanisms of xylose utilization in terms of not only the catabolic genes but also the mode of their regulation, and reveal complexity and redundancy of regulators involved in the succinate-mediated repression of xylose utilization genes.

Acknowledgements

I am very grateful to have worked in a highly productive and innovative research environment over the past few years. I would like to thank my supervisor Prof. Paul Rainey for his advice, encouragement and continued support throughout my project. I gratefully acknowledge my co-supervisor Dr. Xue-Xian Zhang for his encouragement, helpful discussion, and also his valuable insights and contribution to my research project. Thank you for providing me such a great opportunity to participate in this interesting and innovative research.

I appreciate the support from all other academic staffs and also my fellow students who have helped me a lot. Specifically, I would like to thank Dr. Jonathan C. Gauntlett for his help with solubilization and purification of proteins, and also thank Dr. Gayle Ferguson and Dr. Honour McCann for the critical reading of my manuscripts.

Lastly I would like to thank my family for their encouragement, endless patience and unconditional love.

Table of Contents

List of Figures

List of Tables

List of Abbreviations

APS	Ammonium persulphate
ATP	Adenosine triphoshpate
BLAST	Basic local alignment search tool
BSA	Bovine serum albumin
ºC	Degrees Celsius
bp	Base pairs
Da	Dalton
DNase I	Deoxyribonuclease I
dNTP	Deoxynucleotide triphosphate
EDTA	Ethylenediamine tetraacetic acid
g	Gravitational force
h	Hour
HEPES	n-2-hydroxylethylpiperazine-n'-2-ethanesulphonic acid
IPTG	Isopropyl-β-D-thiogalactoside
kb	Kilobase pairs
kDa	KiloDaltons
LB	Luria-Bertaini
M	Molar
mM	Millimolar
µM	Micromolar
mg	Milligram
ml	Millimeter
µl	Microlitre
min	Minute
MW	Molecular weight
MWCO	Molecular weight cut-off
nm	Nanometre
OD	Optical density
ORF	Open reading frames
PAGE	Polyacrylamide gel electrophoresis
PCR	Polymerase chain reaction

PMSF	Phenylmethylsulfonyl fluoride
rpm	Revolution per minute
SDS	Sodium dodecyl sulphate
TBE	Tris-borate-EDTA
TEMED	N,N,N',N'-Tetramethylethylenediamine
UV	Ultraviolet

Chapter 1

Introduction

1.1 Plant cell wall and xylose

Plant cell wall material is the major carbon source in the biosphere and is mainly composed of cellulose, hemicellulose and lignin (Wyman *et al.*, 2005). Cellulose is a homopolymer consisting of a linear chain of hundreds to thousands of β-(1→4)-linked glucose monomers (Wyman *et al.*, 2005). Hemicellulose is a mixture of polysaccharides which includes xylans, xyloglucans, mannans, glucomannans and glucans (Scheller & Ulvskov, 2010). Lignin is a polymer of aromatic alcohols covalently bound to hemicelluloses to provide the necessary strength and rigidity to the plant cell wall, and transport water and solutes (Vanholme *et al.*, 2008). Polysaccharides of the plant cell wall are degraded mainly by a group of hydrolases to a variety of sugar residues including glucose, xylose, galactose, mannose and arabinose (Heredia *et al.*, 1995; Lee, 1997). The approximate monosaccharide composition of various lignocelluosic materials is shown in Table 1.1.

Table 1.1. Composition of various lignocellulosic raw materials

	Corn stover	**Wheat straw**	**Rice straw**	**Rice hults**	**Bagasse fiber**	**Newsprint**	**Populus tristis**	**Douglas fir**
Carbohydrate (%)								
Glucose	39	36.6	41.0	36.1	38.1	64.4	40.0	50.0
Xylose	14.8	19.2	14.8	14.0	23.3	4.6	13.0	3.4
Arabinose	3.2	2.4	4.5	2.6	2.5	0.5	2.0	1.1
Galactose	0.8	2.4	0.4	0.1	1.1	-	-	1.3
Mannose	0.3	0.8	1.8	3.0	-	16.6	8.0	12.0

Adapted from (Lee, 1997).

Xylose is the second most abundant sugar in lignocellulosic biomass after glucose and it forms the backbone of xylan, the major component of hemicellulose (Lee, 1997;

Scheller & Ulvskov, 2010). Due to the complex structure and heterogeneity of xylan, complete breakdown of this polymer into its constituent sugars needs the action of a group of hydrolytic xylanases. These extracellular xylanases are mainly produced by bacteria and fungi and function cooperatively to degrade xylan (Sunna & Antranikian, 1997; Nguyen *et al.*, 2011). Moreover, xylanase-producing microorganisms have been isolated from a wide variety of habitats such as soil and ruminant animals, suggesting that these microbes play a key role in the decomposition and recycling of plant residues, and in providing nutrients for mammals (Hespell & Whitehead, 1990; Ueki *et al.*, 2007; Wang *et al.*, 2010). Since lignocellulosic biomass has been recognized as the most abundant renewable resources for biofuels and chemicals (Himmel *et al.*, 2007) and there is a considerable amount of xylose in the plant-derived sugars, the metabolic pathway and regulatory mechanisms of xylose utilization genes have been characterized in model microorganisms including *Escherichia coli* and *Bacillus subtilis* (Jeffries, 1983; Hastrup, 1988; Song & Park, 1997).

1.2 Metabolism of D-xylose in *Escherichia coli*

In *E. coli*, xylose utilization genes are organized into three major transcriptional units: *xylAB, xylFGHR* and *xylE* (Davis & Henderson, 1987; Song & Park, 1997). In addition, there is a weak promoter located in the front of *xylR* (Song & Park, 1997). Gene array analysis showed that expression of these genes is induced by xylose (Gonzalez *et al.*, 2002). The uptake of xylose into *E. coli* is mediated through three different pathways. (1) The first transport system encoded by *xylFGH* is a high-affinity transporter for xylose (K_m = 0.2-0.4 μM, Sumiya *et al.*, 1995) (Figure 1.1). Amino acid sequence homology analysis showed that XylFGH belong to the ATP-binding cassette (ABC) transporter family. *XylF* encodes a periplasmic xylose-binding protein, *xylG* encodes an ATP-binding protein and *xylH* encodes a membrane component of the ABC transporter (Ahlem *et al.*, 1982; Sofia *et al.*, 1994). (2) The secondary transport system encoded by *xylE* is a xylose/H^+ symporter (Davis & Henderson, 1987) (Figure 1.1) and has a relatively low affinity for xylose (K_m = 63-169 μM, Sumiya *et al.*, 1995). (3) The third transport system, which is presumably via facilitated diffusion and/or an alternative but less efficient transporter, is likely to function under a high concentration of xylose since the xylose degradative product is

notably detected when both *xylG* and *xylE* are absent (Khankal *et al.*, 2008). Among three transport routes, Hasona *et al.* (2004) suggests that xylose is primarily transported into *E. coli* cells by the XylFGH system based on a comparison of *E. coli* strains carrying a deletion of either *xylG* or *xylE*. Deletion of *xylG* led to a decrease in the growth rate by 47% on xylose under aerobic conditions while inactivation of *xylE* only reduced the growth rate by 8.5% under the same conditions (Hasona *et al.*, 2004).

After xylose is transported into *E. coli* cells, it is first isomerized to xylulose by xylose isomerase (encoded by *xylA*) and then phosphorylated by xylulokinase (encoded by *xylB*) to xylulose 5-phosphate before entry to the pentose phosphate pathway for further catabolism (Figure 1.1). Inactivation of either *xylA* or *xylB* by Tn*phoA'*-1 transposon insertions eliminated the ability of mutants to utilize xylose although transport of xylose was still maintained (Song & Park, 1997).

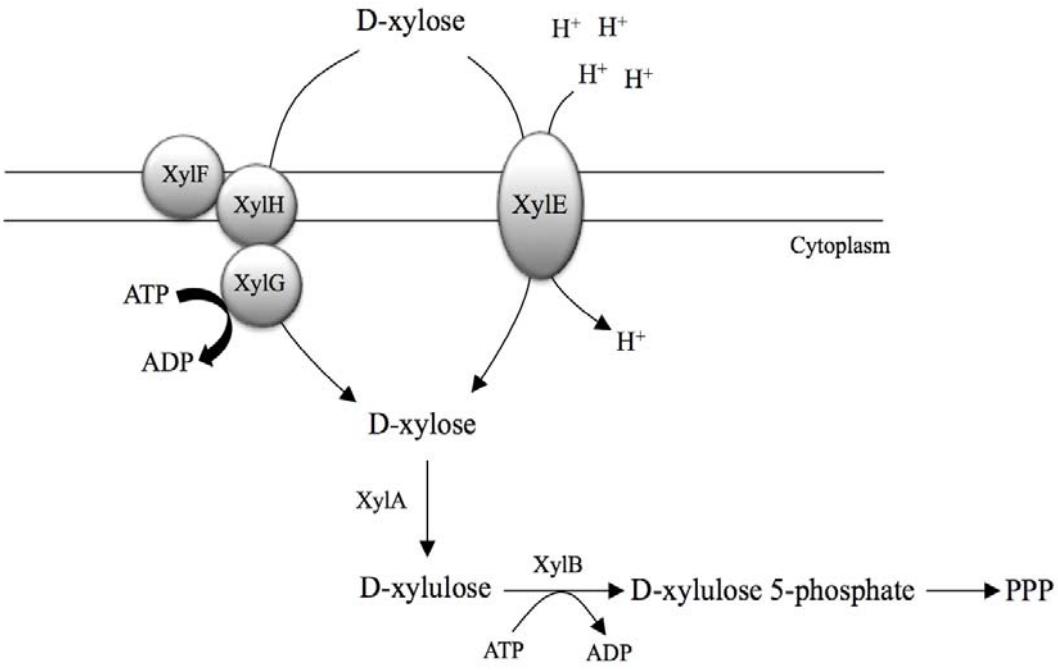

Figure 1.1. The transport and metabolic pathway of D-xylose in *E. coli.* D-xylose is transported into cells by either XylFGH or XylE. Gene products involved in the metabolism of D-xylose are: XylA--xylose isomerase; XylB--xylulokinase.

1.3 Regulatory mechanisms of D-xylose in *E. coli*

At the *xyl* locus, *xylR* encodes an AraC/XylS-type regulator since the C-terminal portion of the amino acid sequence of XylR shows considerable homology to the consensus sequence of the AraC/XylS family (Gallegos *et al.*, 1997; Song & Park, 1997). The highly conserved C-terminal domain of the AraC/XylS family regulators consists of two α-helix-turn-α-helix (HTH) DNA binding motifs based on the secondary-structure predication. Comparison of the HTH motifs of each member in the AraC/XylS family showed that the amino acid sequence at the first HTH motif is divergent whereas it is relatively conserved at the secondary HTH motif (Gallegos *et al.*, 1997). This comparison suggests that the first HTH motif is believed to be involved in recognition of promoters by different regulators and the conserved secondary HTH motif would have a common function for all members of the AraC/XylS family (Gallegos *et al.*, 1997). Mutagenesis analysis of some AraC/XylS regulators (AraC, MelR, SoxS, RhaR) revealed that both HTH motifs are able to bind the cognate promoters and that the second HTH motif interacts with RNA polymerase to activate gene expression (Gallegos *et al.*, 1997; Griffith & Wolf, 2002; Grainger *et al.*, 2004; Kolin *et al.*, 2008). Moreover, although amino acid sequence conservation is observed at the C-terminal region of AraC/XylS members, the N-terminal region of the regulators is highly divergent. This domain is presumed to have ligand-binding sites and confer substrate specificity (Gallegos *et al.*, 1997).

The crystal structure of XylR from *E. coli* has been solved and shows that the DNA-binding domain of XylR organized as two HTH motifs is located at the C-terminal end. The non-homologous N-terminal domain of XylR binds xylose, resulting in dimerization of XylR and activation of structural genes (Ni *et al.*, 2013). Transposon insertions in *xylR* resulted in a growth defect on xylose and completely abolished xylose-inducible expression from *xylA* and *xylF* promoters, suggesting that XylR functions as a transcriptional activator of the *xyl* operon. Xylose-bound XylR is also believed to activate transcription of *xylR* and *xylE* (Song & Park, 1997; Gonzalez *et al.*, 2002).

Binding of XylR to both *xylA* and *xylF* promoters has been demonstrated by electrophoresis mobility shift assays (Song & Park, 1997). The XylR-binding site has been determined by *in vivo* DMS footprinting assays and is composed of two direct repeats (with a consensus sequence: ---gaAa-a--a-AAT). It is located just upstream of the -35 DNA element of the σ^{70}-dependent promoter. A study of regulatory mechanisms of XylR by atomic force microscopy and crystal structure analysis suggests that XylR forms a dimer and binds to xylose in a specific manner, causing simultaneous activation of the two divergent promoters of *xylA* and *xylF* (Ni *et al.*, 2013). The activation involves DNA looping, which is typical for an AraC-type activator (Schleif, 2003).

1.4 Metabolism of D-xylose in *Bacillus subtilis*

In *B. subtilis*, utilization of xylose involves the isomerization of xylose to xylulose followed by phosphorylation to xylulose 5-phosphate. The *xyl* locus, that encodes this degradation pathway, is composed of three genes encoding for xylose isomerase (XylA), xylulokinase (XylB) and a regulatory protein (XylR) (Wilhelm & Hollenberg, 1984; Gärtner *et al.*, 1988; Hastrup, 1988). Deletion mapping showed the genetic organization of two genes: *xylB* is located downstream of *xylA* (Wilhelm & Hollenberg, 1984). *In silico* analysis of the intercistronic region between *xylA* and *xylB* did not show any sequences that resemble a transcription terminator, suggesting that these genes are organized in a single transcriptional unit (Hastrup, 1988). Consistent with this result, integration of a *lacUV5* promoter-operator fragment in front of *xylA* induced the expression of both *xylA* and *xylB* (Wilhelm & Hollenberg, 1984). Furthermore, *xylR* forms a single operon and is transcribed in the opposite direction of *xylAB* (Hastrup, 1988). Although *B. subtilis* has xylose isomerase and xylulokinase for xylose utilization, the wild-type strain is unable to grow on xylose as a sole carbon source, probably owing to lack of a xylose transporter (Lindner *et al.*, 1994). A study on xylose uptake of wild-type *B. subtilis* and spontaneous xyl^+ mutants exhibited that xylose uptake is not inducible by xylose and confirmed that there are no specific transport systems for xylose in *B. subtilis* (Schmiedel & Hillen, 1996).

A *B. subtilis* mutant obtained by random transposon mutagenesis was able to grow on xylose as a sole carbon source and the mutation was linked to *araE* (Schmiedel & Hillen, 1996). The *B. subtilis araE* gene encodes an arabinose/H^+ symporter involved in the L-arabinose transport and its expression is repressed by a regulator AraR (Sá-Nogueira & Ramos, 1997). Wild-type *B. subtilis* is capable of utilizing xylose in the presence of arabinose, suggesting that AraE induced by arabinose is likely to be involved in the transport of xylose (Schmiedel & Hillen, 1996). This is consistent with the result that inactivation of *araR* enables *B. subtilis* to grow on xylose as the sole carbon source since expression of *araE* is induced in a *ΔaraR* mutant (Sá-Nogueira & Ramos, 1997; Krispin & Allmansberger, 1998). The effect of AraE on xylose consumption and cell growth of *B. subtilis* has been examined in batch fermentation. Expression of *araE* led to a considerably high xylose consumption rate and an increase in the growth of *B. subtilis*, suggesting that metabolism of xylose is strongly dependent on the expression of *araE*. The study implies that the AraE protein is able to efficiently transport xylose into *B. subtilis* (Park *et al.*, 2012). In nature, hemicellulose, which is a major component of plant cell wall, contains mainly L-arabinose and D-xylose. The AraE protein with broad substrate specificity renders *B. subtilis* able to survive in a complex environment.

1.5 Regulatory mechanisms of D-xylose in *B. subtilis*

Regulation of the *xyl* genes in *B. subtilis* has been studied. Expression of a chromosomally integrated *xylA-lacZ* fusion was derepressed when titrated with the *xyl* regulatory DNA in *trans* on a multicopy plasmid, suggesting a negative regulation of the *xyl* genes in *B. subtilis* (Gärtner *et al.*, 1988). In the absence of xylose, the expression of *xylA* is repressed by XylR while the inhibition is relieved by inactivation of *xylR*. The result indicates that XylR functions as a repressor of the *xyl* operon (Kreuzer *et al.*, 1989). The *xyl* operator was identified by deletion analysis of the *xyl* regulatory region. It consists of a 25 bp palindromic sequence (TTAGTTTGTTTGATCAACAAACTAA) and is located 10 bp downstream from the *xylAB* promoter (Kreuzer *et al.*, 1989). Crude protein extract of *B. subtilis* was able to bind the *xyl* operator whereas the interaction between the Xyl repressor and the *xyl* operator was not observed using the crude extract from Δ*xylR* mutants in gel mobility

shift assays. The sequence of *xyl* operator was further verified by the copper-phenanthroline footprinting of the *xyl* regulatory region (Gärtner *et al.*, 1992). Inspection of the *xyl* operator in *B. subtilis* by methylation and hydroxyl radical protection and ethylation interference revealed that the *xyl* operator contains two shorter tandem-overlapping palindromes spaced by four base-pairs (Dahl *et al.*, 1994). Mutational analysis of their function by DNA retardation and β-galactosidase assays showed that there are two XylR-binding sites in the *xyl* operator and both of them co-operate in the repressor binding to maximize repression of the *xyl* genes (Dahl *et al.*, 1994).

It has been reported that XylR contains a putative helix-turn-helix (HTH) DNA binding motif between residues 27 and 47 (Dodd & Egan, 1990). It suggests that XylR makes sequence-specific contacts to the *xyl* operator via this motif. This is consistent with the finding that XylR with mutations in the HTH motif was operator-binding negative (Kauder *et al.*, 1993). Furthermore, XylR is able to bind to the palindromic *xyl* operator but not to a half-site of the operator, suggesting that the active repressor is likely to be a dimer (Gärtner *et al.*, 1992).

1.6 Carbon catabolite repression

In nature, bacteria often encounter a mixture of carbon sources and thus display a physiological and metabolic versatility that allows them to use a variety of substrates. These carbon sources can be co-metabolized, but some bacteria preferentially utilize one specific carbon source over another: that providing fastest growth is typically used first. Selective carbon usage has been named carbon catabolite repression (CCR). CCR is an important regulatory system for the hierarchical metabolism of sugars in bacteria. Regulation is achieved through inhibition or reduction of the activity of enzymes required for catabolism of non-preferred carbon sources (Brückner & Titgemeyer, 2002; Görke & Stülke, 2008). CCR is believed to be important for the competition of different bacterial species in natural niches because selection of the preferred carbon source optimizes metabolism and growth rate (Görke & Stülke, 2008).

1.6.1 Mechanism of CCR and CCR of xylose utilization in *E. coli*

In *E. coli*, glucose is the preferred carbon source and enters the cell through a phosphenolpyruvate-carbohydrate phosphotransferase system (PTS) (Postma *et al.*, 1993). The PTS system consists of two general proteins, enzyme I (EI) and histidine-containing protein (HPr), and sugar specific permeases (enzyme II). This system couples the transport of carbohydrates with simultaneous phosphorylation (Postma *et al.*, 1993). In *E. coli*, the glucose-specific permease EII is composed of three domains: a cytoplasmic domain $EIIA^{Glc}$ and membrane-bound domains $EIIBC^{Glc}$ (Postma *et al.*, 1993). The phosphate group of phosphoenolpyruvate (PEP) is sequentially transferred to EI, HPr and finally to $EIIA^{Glc}$. CCR is mediated by modulation of the phosphorylation state of $EIIA^{Glc}$ and is achieved by different regulatory mechanisms: inducer exclusion, and transcription activation by catabolite activation protein (CAP) complex (Figure 1.2) (Brückner & Titgemeyer, 2002; Görke & Stülke, 2008). In the presence of glucose, $EIIA^{Glc}$ is predominantly dephosphorylated because the phosphate group of PTS proteins is transferred to glucose. Consequently, $EIIA^{Glc}$ is able to bind to non-PTS sugar permeases and inhibits the transport of these sugars. Due to lack of an inducer, genes related to utilization of non-PTS sugars are poorly expressed.

In addition to inducer exclusion, $EIIA^{Glc}$ is also involved in CAP-cAMP-mediated activation of catabolic genes for non-PTS sugars (Figure 1.2). The intracellular cAMP level is controlled by adenylate cyclase (AC) whose activity depends on the phosphorylation state of $EIIA^{Glc}$ (Postma *et al.*, 1993). When glucose is exhausted, the concentration of nonphosphorylated $EIIA^{Glc}$ decreases and the effect of inducer exclusion is relieved. It allows transport of the inducer and induction of corresponding catabolic genes; however, the expression of genes for non-PTS sugars is usually low. Full induction of these genes often requires transcriptional activation by the CAP-cAMP complex. Under these conditions, phosphorylated $EIIA^{Glc}$ activates AC, which in turn converts ATP to cAMP (Yang & Epstein, 1983; Bettenbrock *et al.*, 2006). CAP then interacts with cAMP and activates respective operons of non-PTS sugars such as lactose, glycerol or maltose (Görke & Stülke, 2008).

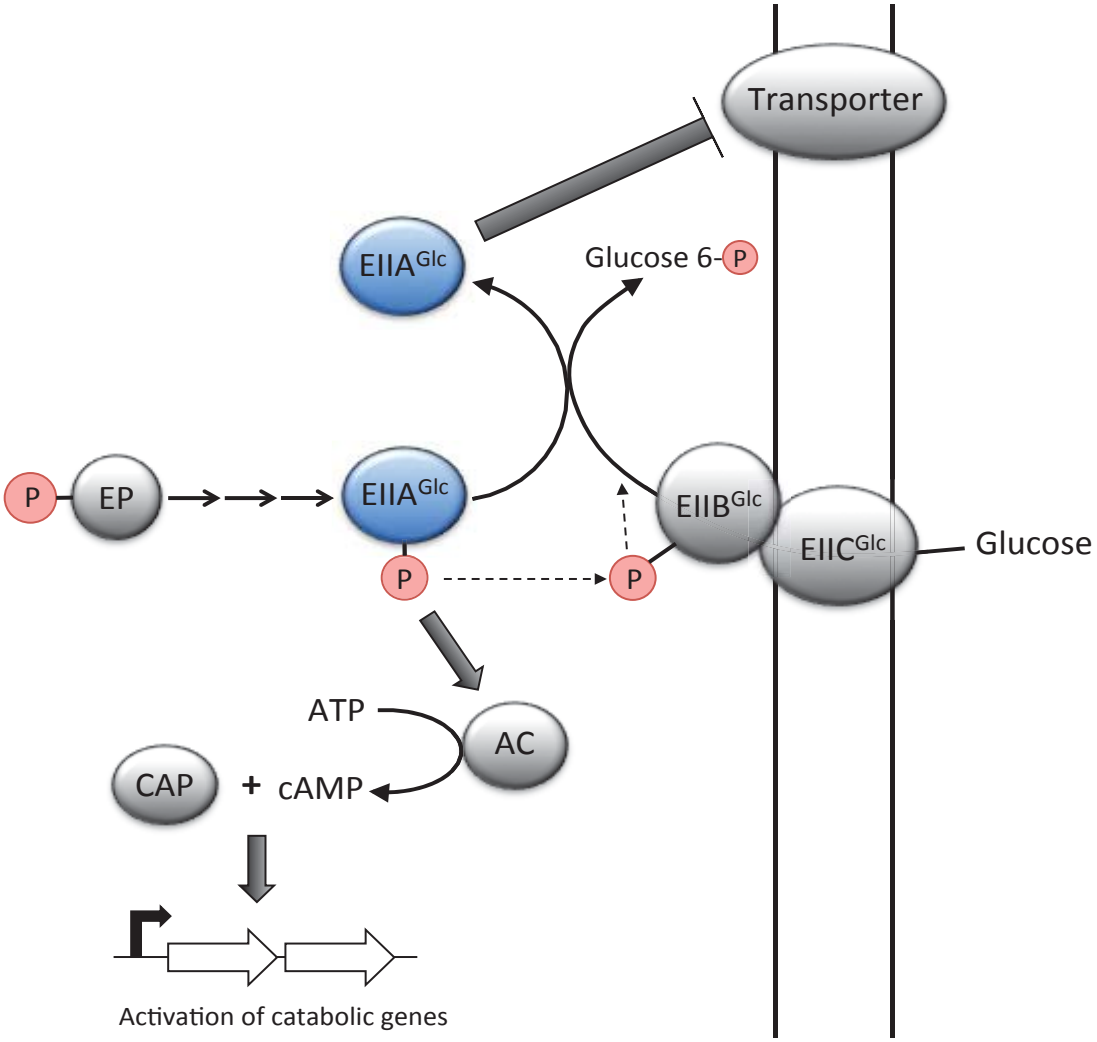

Figure 1.2. Carbon catabolite repression in *E. coli.* CCR is primarily determined by the phosphorylation state of $EIIA^{Glc}$. In the presence of glucose, the phosphate group is transferred from phosphoenolpyruvate (PEP) to glucose, resulting in dephosphorylation of $EIIA^{Glc}$. Nonphosphorylated $EIIA^{Glc}$ exerts inducer exclusion by binding and inactivating the transporters of non-preferred carbon sources. In the absence of glucose, phosphorylated $EIIA^{Glc}$ accumulates and activates adenylate cyclase (AC), which synthesizes cyclic AMP (cAMP) from ATP. Expression of genes responsible for catabolism of non-preferred sugars is stimulated by the transcriptional regulator CAP-cAMP.

In *E. coli*, it has been reported that expression of xylose utilization genes (*xylA* and *xylF*) is significantly repressed by glucose (Song & Park, 1997). As the PTS system plays a central role in the regulatory process of CCR, the effect of mutations in *ptsG* (encoding $EIIBC^{Glc}$) on assimilation of sugar mixtures has been studied (Nichols *et*

al., 2001). The wild-type strain utilized glucose and xylose sequentially while *ptsG* mutants metabolized these sugar mixtures simultaneously. In addition, the similar patterns of sugar use in ethanol fermentation were also observed (Nichols *et al.*, 2001).

1.6.2 Mechanisms of CCR and CCR of xylose utilization in *B. subtilis*

In *B. subtilis* and other related Gram-positive bacteria, glucose is also the preferred carbon source and is transported into cells by the PTS system. The major transcriptional regulator of CCR in *B. subtilis* is the catabolite control protein A (CcpA) and the signal transduction regulator is HPr, rather than $EIIA^{Glc}$ (Warner & Lolkema, 2003) (Figure 1.3). The HPr protein can be phosphorylated at a histidine residue and a serine residue, respectively. In the presence of glucose, the phosphate group of PEP is sequentially transferred to EI, HPr(His-P) and finally to glucose. Meanwhile, the HPr kinase (HPrK) phosphorylates HPr at residue Ser-46 at the expense of ATP. The resulting HPr(Ser-P) interacts with the CcpA protein, forming a complex that binds to a catabolite responsive element (*cre* site) in the promoter region of target genes. Binding of the HPr(Ser-P)-CcpA complex to the *cre* site inhibits transcription of the genes responsible for metabolism of non-preferred carbon sources (Warner & Lolkema, 2003).

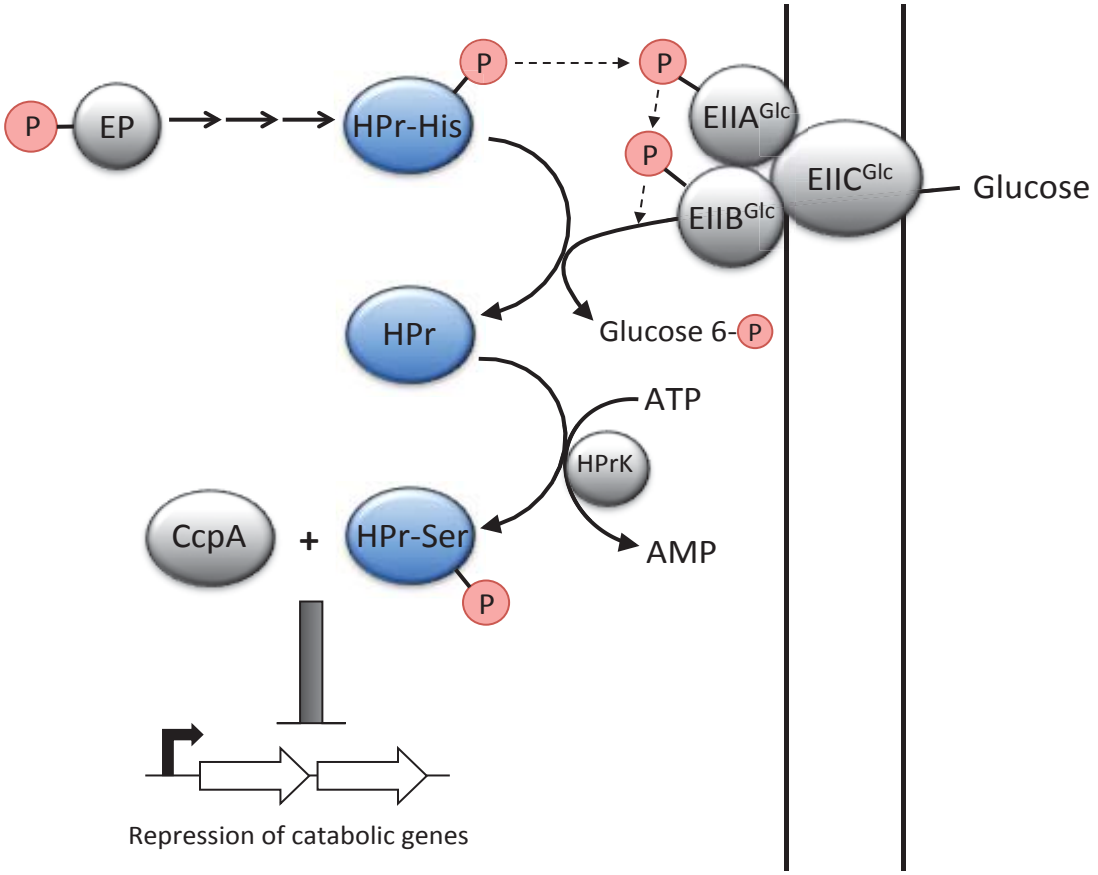

Figure 1.3. Carbon catabolite repression in *B. subtilis*. CCR is mainly determined by the phosphorylation state of HPr. This protein can be phosphorylated at a histidine residue and a serine residue, respectively. When glucose is available, the phosphate group is transferred from phosphoenolpyruvate (PEP), via HPr(His-P), to glucose. This results in dephosphorylation of the HPr protein. Meanwhile, it is phosphorylated by HPr kinase (HPrK) at the residue serine-46 and then interacts with catabolite control protein A (CcpA). The complex of HPr(Ser-P) and CcpA binds to the *cre* site, leading to repression of catabolic genes of non-preferred carbon sources.

Carbon catabolite repression of *xyl* genes is also observed in *B. subtilis*. Expression of *xylA* is significantly repressed in the presence of glucose and the inhibitory effect is mediated at the transcription level (Jacob *et al.*, 1991). Deletion analysis of *xylA-lacZ* transcriptional fusions identified a *cre* site that is necessary for CCR of *xyl* genes. This element is located in the coding region of *xylA* and has 2 bp differences from the consensus sequence (Jacob *et al.*, 1991; Kraus *et al.*, 1994). Repression extent of the *xylA-lacZ* transcriptional fusion increased with increasing identity of the *cre* site to the consensus sequence. Consistent with the results, deletion of the *cre* site markedly relieved the glucose repression, although a 13-fold repression of *xylA* was still

observed. These findings suggest that CCR of *xyl* genes in *B. subtilis* is mediated by the transcriptional factor CcpA that likely binds to the *cre* site (Kraus *et al.*, 1994). Moreover, deletion of both the *cre* site and the repressor *xylR* abolished the glucose repression of *xylA* expression, suggesting that CCR of the *xyl* operon is also mediated by an inducer exclusion mechanism in *B. subtilis* (Kraus *et al.*, 1994).

1.7 Plant-associated *Pseudomonas* and xylose

Although the xylose utilization genes and regulatory mechanisms have been studied in model bacteria including *E. coli* and *B. subtilis* (Jeffries, 1983; Hastrup, 1988; Song & Park, 1997), no empirical work has been reported for bacteria that form close associations with plants. Bacteria belonging to the genus of *Pseudomonas* are metabolically versatile. They are capable of colonizing a wide range of environments such as soil and water as well as eukaryotic hosts (Isnansetyo & Kamei, 2009; Silby *et al.*, 2011). Some *Pseudomonas* strains (e.g. *P. syringae*) are pathogenic and can infect many plant species, resulting in a variety of disease symptoms (Kennelly *et al.*, 2007). On the other hand, other members of *Pseudomonas*, for example *P. fluorescens*, can promote plant health and display disease-suppressing activities through the production of antimicrobial compounds (Haas & Defago, 2005). As plant-associated bacteria, colonization is an important step in microbial pathogenesis and biocontrol (Chin-A-Woeng *et al.*, 2000; Lugtenberg *et al.*, 2001). Successful colonization of *Pseudomonas in planta* is dependent on fast detection of and response to specific signals of the plant environment, including availability of nutritional substrates (Lugtenberg *et al.*, 2001; Espinosa-Urgel *et al.*, 2002). The ability to assimilate plant-derived nutrients is of critical importance for the ecological success of *Pseudomonas* as plant colonizers (Gal *et al.*, 2003; Silby & Levy, 2004; Fernandez *et al.*, 2013).

P. fluorescens SBW25 is a plant growth-promoting rhizobacterium (PGPR), which was originally isolated from a field-grown sugar beet plant (Rainey & Bailey, 1996; Alsohim *et al.*, 2014). It protects peas from seedling damping-off caused by *Pythium ultimum* (Naseby *et al.*, 2001; Nikel *et al.*, 2014). To determine the molecular mechanism responsible for the ecological success of *P. fluorescens* SBW25, *in vivo*

expression technology (IVET) was used to identify candidate genes whose expression is elevated during colonization of sugar beet seedlings (Rainey, 1999; Gal *et al.*, 2003). Of particular interest, one IVET fusion (*rhi-17*) includes 123 nucleotides from the 3' end of a gene that encodes a protein showing strong similarity to *xylA* (Rainey, 1999). The IVET data suggest that xylose utilization genes contribute to the increased ecological performance in the plant environment, prompting further investigation into the molecular mechanism of xylose catabolism in *P. fluorescens* SBW25.

1.8 Objectives of this study

The overall aim of this project is to elucidate the molecular basis of xylose metabolism in bacteria with a focus on its role in plant colonization. The research will be performed with the model plant growth-promoting bacterium *P. fluorescens* SBW25. Specific aims of this work are listed below:

1. **Genetic identification of *xut* genes involved in xylose uptake and degradation by *P. fluorescens* SBW25.** This will be achieved by computational analysis of *xut* catabolic genes and transporters encoded in the genome of *P. fluorescens* SBW25, followed by site-directed mutagenesis analysis and transcriptional assays using the *lacZ* reporter gene.
2. **Identification of regulator(s) involved in the control of *xut* catabolic genes.** Expression of *xut* genes is expected to be induced by the presence of xylose in the medium, and the induction is likely mediated by regulator(s) belonging to the AraC family. After the regulatory gene(s) are identified by genetic characterization, I will determine the transcriptional organization of *xut* genes, transcriptional start sites and also the minimum critical sequence for promoter activities.
3. **Biochemical and genetic characterization of the xylose responsive regulator XutR.** XutR is an AraC-type transcriptional activator, but it does not recognize the DNA target sequence of its counterpart XylR in *E. coli*, thus suggesting a novel mechanism of action. Molecular techniques such as

electrophoretic mobility shift assay (EMSA) and DNase I footprinting will be used to demonstrate the precise mode of XutR action.

4. **Construction of mini-Tn7 vectors for studying post-transcriptional gene regulation in *Pseudomonas*.** Such vectors are essentially required for the study of carbon catabolic repression of xylose utilization genes, which occurs at the post-transcriptional level.

5. **Elucidation of the molecular mechanism of succinate-mediated repression of *xut* genes for xylose utilization.** The work will be performed on the basis of our previous finding that the two-component signal transduction system CbrA / CbrB is involved in the global control of xylose utilization. Experiments will be designed to identify and characterize the regulator(s) that enable CbrAB to activate expression of *xut* genes in response to the presence of succinate, the most preferred carbon source for *P. fluorescens* SBW25.

1.9 References

Ahlem, C., Huisman, W., Neslund, G., & Dahms, A. S. (1982). Purification and properties of a periplasmic D-xylose-binding protein from Escherichia coli K-12. *J Biol Chem, 257*(6), 2926-2931.

Alsohim, A. S., Taylor, T. B., Barrett, G. A., Gallie, J., Zhang, X. X., Altamirano-Junqueira, A. E., Johnson, L. J., Rainey, P. B., & Jackson, R. W. (2014). The biosurfactant viscosin produced by *Pseudomonas fluorescens* SBW25 aids spreading motility and plant growth promotion. *Environ Microbiol, 16*(7), 2267-2281.

Bettenbrock, K., Fischer, S., Kremling, A., Jahreis, K., Sauter, T., & Gilles, E. D. (2006). A quantitative approach to catabolite repression in *Escherichia coli*. *J Biol Chem, 281*(5), 2578-2584.

Brückner, R., & Titgemeyer, F. (2002). Carbon catabolite repression in bacteria: choice of the carbon source and autoregulatory limitation of sugar utilization. *FEMS Microbiol Lett, 209*(2), 141-148.

Chin-A-Woeng, Thomas F. C., Bloemberg, Guido V., Mulders, Ine H. M., Dekkers, Linda C., & Lugtenberg, Ben J. J. (2000). Root Colonization by Phenazine-1-Carboxamide-Producing Bacterium *Pseudomonas chlororaphis* PCL1391 Is Essential for Biocontrol of Tomato Foot and Root Rot. *Molecular Plant-Microbe Interactions, 13*(12), 1340-1345.

Dahl, M. K., Degenkolb, J., & Hillen, W. (1994). Transcription of the xyl operon is controlled in *Bacillus subtilis* by tandem overlapping operators spaced by four base-pairs. *J Mol Biol, 243*(3), 413-424.

Davis, E. O., & Henderson, P. J. (1987). The cloning and DNA sequence of the gene xylE for xylose-proton symport in *Escherichia coli* K12. *J Biol Chem, 262*(29), 13928-13932.

Dodd, I. B., & Egan, J. B. (1990). Improved detection of helix-turn-helix DNA-binding motifs in protein sequences. *Nucleic Acids Res, 18*(17), 5019-5026.

Espinosa-Urgel, M., Kolter, R., & Ramos, J. L. (2002). Root colonization by *Pseudomonas putida*: love at first sight. *Microbiology, 148*(Pt 2), 341-343.

Fernandez, M., Conde, S., Duque, E., & Ramos, J. L. (2013). In vivo gene expression of *Pseudomonas putida* KT2440 in the rhizosphere of different plants. *Microb Biotechnol, 6*(3), 307-313.

Gal, M., Preston, G. M., Massey, R. C., Spiers, A. J., & Rainey, P. B. (2003). Genes encoding a cellulosic polymer contribute toward the ecological success of *Pseudomonas fluorescens* SBW25 on plant surfaces. *Mol Ecol, 12*(11), 3109-3121.

Gallegos, M. T., Schleif, R., Bairoch, A., Hofmann, K., & Ramos, J. L. (1997). Arac/XylS family of transcriptional regulators. *Microbiol Mol Biol Rev, 61*(4), 393-410.

Gärtner, D., Geissendorfer, M., & Hillen, W. (1988). Expression of the *Bacillus subtilis xyl* operon is repressed at the level of transcription and is induced by xylose. *J Bacteriol, 170*(7), 3102-3109.

Gärtner, D., Degenkolb, J., Ripperger, J. A., Allmansberger, R., & Hillen, W. (1992). Regulation of the *Bacillus subtilis* W23 xylose utilization operon: interaction of the Xyl repressor with the xyl operator and the inducer xylose. *Mol Gen Genet, 232*(3), 415-422.

Gonzalez, R., Tao, H., Shanmugam, K. T., York, S. W., & Ingram, L. O. (2002). Global gene expression differences associated with changes in glycolytic flux

and growth rate in *Escherichia coli* during the fermentation of glucose and xylose. *Biotechnol Prog, 18*(1), 6-20.

Görke, B., & Stülke, J. (2008). Carbon catabolite repression in bacteria: many ways to make the most out of nutrients. *Nat Rev Microbiol, 6*(8), 613-624.

Grainger, David C., Webster, Christine L., Belyaeva, Tamara A., Hyde, Eva I., & Busby, Stephen J. W. (2004). Transcription activation at the *Escherichia coli melAB* promoter: interactions of MelR with its DNA target site and with domain 4 of the RNA polymerase σ subunit. *Mol Microbiol, 51*(5), 1297-1309.

Griffith, K. L., & Wolf, R. E., Jr. (2002). A comprehensive alanine scanning mutagenesis of the *Escherichia coli* transcriptional activator SoxS: identifying amino acids important for DNA binding and transcription activation. *J Mol Biol, 322*(2), 237-257.

Haas, D., & Defago, G. (2005). Biological control of soil-borne pathogens by fluorescent pseudomonads. *Nat Rev Microbiol, 3*(4), 307-319.

Hasona, A., Kim, Y., Healy, F. G., Ingram, L. O., & Shanmugam, K. T. (2004). Pyruvate formate lyase and acetate kinase are essential for anaerobic growth of *Escherichia coli* on xylose. *J Bacteriol, 186*(22), 7593-7600.

Hastrup, S. (1988). Analysis of the *Bacillus subtilis* xylose regulon. In A. T. Ganesan & J. A. Hoch (Eds.), *Genetics and Biotechnology of Bacilli* (pp. 79-83): Academic Press.

Heredia, A., Jimenez, A., & Guillen, R. (1995). Composition of plant cell walls. *Z Lebensm Unters Forsch, 200*(1), 24-31.

Hespell, R. B., & Whitehead, T. R. (1990). Physiology and genetics of xylan degradation by gastrointestinal tract bacteria. *J Dairy Sci, 73*(10), 3013-3022.

Himmel, M. E., Ding, S. Y., Johnson, D. K., Adney, W. S., Nimlos, M. R., Brady, J. W., & Foust, T. D. (2007). Biomass recalcitrance: engineering plants and enzymes for biofuels production. *Science, 315*(5813), 804-807.

Isnansetyo, A., & Kamei, Y. (2009). Bioactive substances produced by marine isolates of *Pseudomonas*. *J Ind Microbiol Biotechnol, 36*(10), 1239-1248.

Jacob, Sabine, Allmansberger, Rudolf, Gärtner, Dagmar, & Hillen, Wolfgang. (1991). Catabolite repression of the operon for xylose utilization from *Bacillus subtilis* W23 is mediated at the level of transcription and depends on a cis site in the xylA reading frame. *Molecular and General Genetics MGG, 229*(2), 189-196.

Jeffries, T. W. (1983). Utilization of xylose by bacteria, yeasts, and fungi. *Adv Biochem Eng Biotechnol, 27*, 1-32.

Kauder, C., Allmansberger, R., Gartner, D., Schmiedel, D., & Hillen, W. (1993). An operator binding-negative mutation of Xyl repressor from *Bacillus subtilis* is trans dominant in *Bacillus megaterium*. *FEMS Microbiol Lett, 109*(1), 81-84.

Kennelly, Megan M., Cazorla, Francisco M., de Vicente, Antonio, Ramos, Cayo, & Sundin, George W. (2007). *Pseudomonas syringae* Diseases of Fruit Trees: Progress Toward Understanding and Control. *Plant Disease, 91*(1), 4-17.

Khankal, R., Chin, J. W., & Cirino, P. C. (2008). Role of xylose transporters in xylitol production from engineered *Escherichia coli*. *J Biotechnol, 134*(3-4), 246-252.

Kolin, Ana, Balasubramaniam, Vinitha, Skredenske, Jeff M., Wickstrum, Jason R., & Egan, Susan M. (2008). Differences in the mechanism of the allosteric l-rhamnose responses of the AraC/XylS family transcription activators RhaS and RhaR. *Mol Microbiol, 68*(2), 448-461.

Kraus, A., Hueck, C., Gartner, D., & Hillen, W. (1994). Catabolite repression of the *Bacillus subtilis xyl* operon involves a cis element functional in the context of

an unrelated sequence, and glucose exerts additional xylR-dependent repression. *J Bacteriol, 176*(6), 1738-1745.

Kreuzer, P., Gartner, D., Allmansberger, R., & Hillen, W. (1989). Identification and sequence analysis of the *Bacillus subtilis* W23 xylR gene and xyl operator. *J Bacteriol, 171*(7), 3840-3845.

Krispin, O., & Allmansberger, R. (1998). The *Bacillus subtilis* AraE protein displays a broad substrate specificity for several different sugars. *J Bacteriol, 180*(12), 3250-3252.

Lee, J. (1997). Biological conversion of lignocellulosic biomass to ethanol. *J Biotechnol, 56*(1), 1-24.

Lindner, C., Stulke, J., & Hecker, M. (1994). Regulation of xylanolytic enzymes in *Bacillus subtilis*. *Microbiology, 140 (Pt 4)*, 753-757.

Lugtenberg, B. J., Dekkers, L., & Bloemberg, G. V. (2001). Molecular determinants of rhizosphere colonization by *Pseudomonas*. *Annu Rev Phytopathol, 39*, 461-490.

Naseby, D. C., Way, J. A., Bainton, N. J., & Lynch, J. M. (2001). Biocontrol of Pythium in the pea rhizosphere by antifungal metabolite producing and non-producing *Pseudomonas* strains. *J Appl Microbiol, 90*(3), 421-429.

Nguyen, Q. B., Itoh, K., Van Vu, B., Tosa, Y., & Nakayashiki, H. (2011). Simultaneous silencing of endo-beta-1,4 xylanase genes reveals their roles in the virulence of Magnaporthe oryzae. *Mol Microbiol, 81*(4), 1008-1019.

Ni, L., Tonthat, N. K., Chinnam, N., & Schumacher, M. A. (2013). Structures of the *Escherichia coli* transcription activator and regulator of diauxie, XylR: an AraC DNA-binding family member with a LacI/GalR ligand-binding domain. *Nucleic Acids Res, 41*(3), 1998-2008.

Nichols, N., Dien, B., & Bothast, R. (2001). Use of catabolite repression mutants for fermentation of sugar mixtures to ethanol. *Applied Microbiology and Biotechnology, 56*(1-2), 120-125.

Nikel, P. I., Martinez-Garcia, E., & de Lorenzo, V. (2014). Biotechnological domestication of pseudomonads using synthetic biology. *Nat Rev Microbiol, 12*(5), 368-379.

Park, Y. C., Jun, S. Y., & Seo, J. H. (2012). Construction and characterization of recombinant *Bacillus subtilis* JY123 able to transport xylose efficiently. *J Biotechnol, 161*(4), 402-406.

Postma, P. W., Lengeler, J. W., & Jacobson, G. R. (1993). Phosphoenolpyruvate:carbohydrate phosphotransferase systems of bacteria. *Microbiol Rev, 57*(3), 543-594.

Rainey, P. B., & Bailey, M. J. (1996). Physical and genetic map of the *Pseudomonas fluorescens* SBW25 chromosome. *Mol Microbiol, 19*(3), 521-533.

Rainey, P. B. (1999). Adaptation of *Pseudomonas fluorescens* to the plant rhizosphere. *Environ Microbiol, 1*(3), 243-257.

Sá-Nogueira, I., & Ramos, S. S. (1997). Cloning, functional analysis, and transcriptional regulation of the *Bacillus subtilis araE* gene involved in L-arabinose utilization. *J Bacteriol, 179*(24), 7705-7711.

Scheller, H. V., & Ulvskov, P. (2010). Hemicelluloses. *Annu Rev Plant Biol, 61*, 263-289.

Schleif, R. (2003). AraC protein: a love-hate relationship. *Bioessays, 25*(3), 274-282.

Schmiedel, Dagmar, & Hillen, Wolfgang. (1996). A *Bacillus subtilis* 168 mutant with increased xylose uptake can utilize xylose as sole carbon source. *FEMS Microbiol Lett, 135*(2–3), 175-178.

Silby, M. W., & Levy, S. B. (2004). Use of In vivo expression technology to identify genes important in growth and survival of *Pseudomonas fluorescens* Pf0-1 in soil: discovery of expressed sequences with novel genetic organization. *J Bacteriol, 186*(21), 7411-7419.

Silby, M. W., Winstanley, C., Godfrey, S. A., Levy, S. B., & Jackson, R. W. (2011). *Pseudomonas* genomes: diverse and adaptable. *FEMS Microbiol Rev, 35*(4), 652-680.

Sofia, H. J., Burland, V., Daniels, D. L., Plunkett, G., 3rd, & Blattner, F. R. (1994). Analysis of the *Escherichia coli* genome. V. DNA sequence of the region from 76.0 to 81.5 minutes. *Nucleic Acids Res, 22*(13), 2576-2586.

Song, S., & Park, C. (1997). Organization and regulation of the D-xylose operons in *Escherichia coli* K-12: XylR acts as a transcriptional activator. *J Bacteriol, 179*(22), 7025-7032.

Sumiya, M., Davis, E. O., Packman, L. C., McDonald, T. P., & Henderson, P. J. (1995). Molecular genetics of a receptor protein for D-xylose, encoded by the gene *xylF*, in *Escherichia coli*. *Receptors Channels, 3*(2), 117-128.

Sunna, A., & Antranikian, G. (1997). Xylanolytic enzymes from fungi and bacteria. *Crit Rev Biotechnol, 17*(1), 39-67.

Ueki, A., Akasaka, H., Satoh, A., Suzuki, D., & Ueki, K. (2007). *Prevotella paludivivens* sp. nov., a novel strictly anaerobic, Gram-negative, hemicellulose-decomposing bacterium isolated from plant residue and rice roots in irrigated rice-field soil. *Int J Syst Evol Microbiol, 57*(Pt 8), 1803-1809.

Vanholme, R., Morreel, K., Ralph, J., & Boerjan, W. (2008). Lignin engineering. *Curr Opin Plant Biol, 11*(3), 278-285.

Wang, G., Wang, Y., Yang, P., Luo, H., Huang, H., Shi, P., Meng, K., & Yao, B. (2010). Molecular detection and diversity of xylanase genes in alpine tundra soil. *Applied Microbiology and Biotechnology, 87*(4), 1383-1393.

Warner, J. B., & Lolkema, J. S. (2003). CcpA-dependent carbon catabolite repression in bacteria. *Microbiol Mol Biol Rev, 67*(4), 475-490.

Wilhelm, M., & Hollenberg, C. P. (1984). Selective cloning of *Bacillus subtilis* xylose isomerase and xylulokinase in *Escherichia coli* genes by IS5-mediated expression. *EMBO J, 3*(11), 2555-2560.

Yang, J. K., & Epstein, W. (1983). Purification and characterization of adenylate cyclase from *Escherichia coli* K12. *J Biol Chem, 258*(6), 3750-3758.

Chapter 2

Materials and Methods

2.1 Enzymes and chemicals

Reagents and chemicals were purchased from Bioline, Bio-Rad, New England Biolabs, Fermentas, GE healthcare, Sigma-Aldrich Chemicals, Invitrogen and Qiagen. All buffers and solutions were prepared using MilliQ water and filtered through a 0.22 μm cellulose filter (Millipore) if required.

2.2 Bacterial strains, plasmids and growth conditions

Major strains and plasmids used in this study are listed in Table 2.1. *Pseudomonas fluorescens* and *Escherichia coli* strains were routinely grown in Luria-Bertani (LB) at 28ºC and 37ºC, respectively. When *P. fluorescens* was grown in mininal M9 salt medium (Sambrook *et al.,* 1989) each carbon source was supplemented at the final concentration of 20 mM except where indicated. When required, antibiotics were added to the medium at the following concentrations: ampicillin (Ap), 100 μg ml^{-1}; tetracycline (Tc), 10 μg ml^{-1}; spectinomycin (Sp), 100 μg ml^{-1} (*E. coli*); kanamycin (Km), 50 μg ml^{-1}; gentamicin (Gm), 25 μg ml^{-1}; nitrofurantoin (NF) was dissolved in dimethyl sulfoxide (DMSO) to a final concentration of 100 μg ml^{-1}

Table 2.1. Bacterial strains and plasmids used in this work

Strain or plasmid	Genotypes and relevant characteristics	Reference
P. fluorescens		
SBW25	Wild-type strain isolated from phyllosphere of sugar beet	Bailey *et al.* (1995)
SBW25-*lacZ*	SBW25 harboring a *lacZ* marker	Zhang and Rainey (2007b)
PBR810	Δ*cbrB*, SBW25 with deletion of *pflu5237*	Zhang and Rainey (2007a)
MU12-58	Δ*crc*, SBW25 with deletion of *pflu5989*	This work
MU47-1	Δ*xutA*, SBW25 devoid of *pflu2301*	This work
MU47-2	Δ*xutR*, SBW25 devoid of *pflu2302*	This work

MU47-3	Δ*xutFGH*, SBW25 with deletion of the *pflu2298* - *pflu2300* DNA region	This work
MU47-4	Δ*xutB1*, SBW25 with deletion *pflu2740*	This work
MU47-5	Δ*xutB2*, SBW25 with deletion *pflu3115*	This work
MU47-6	Δ*xutB1* Δ*xutB2*, SBW25 with deletion *pflu2740* and *pflu3115*	This work
MU47-7	Δ*mtlR*::Km^r, SBW25 with *pflu2746* being replaced with a Km^r cassette from pUC4K	This work
MU47-8	Δ*mtlZ*::Km^r, SBW25 with *pflu2739* being replaced with a Km^r cassette from pUC4K	This work
MU47-9	Δ*xutB1* Δ*mtlZ*::Km^r, derived from MU47-4 with *pflu2739* being replaced with a Km^r cassette from pUC4K	This work
MU47-10	Δ*rbsK*::Km^r, SBW25 with *pflu4156* being replaced with a Km^r cassette from pUC4K	This work
MU47-11	Δ*cbrB*Δ*crc,* SBW25 with deletion *pflu5237* and *pflu5989*	This work
MU47-12	SBW25Δ*crcZ*	This work
MU47-13	SBW25Δ*crcY*	This work
MU47-14	SBW25Δ*crcZ*Δ*crcY*	This work
MU47-15	SBW25Δ*crc*Δ*crcZ*Δ*crcY*	This work
E. coli		
BL21(DE3)	F^- *ompT hsd*S_B($r_B^-m_B^-$)*gal dcm* (DE3)	Invitrogen
TOP10	F^- mcrA Δ(mrr-hsdRMS-mcrBC) Φ80*lacZ*ΔM15 Δ*lac*X74 recA1 araD139 Δ(*araleu*)7697 *gal*U *gal*K *rps*L (Str^R) *end*A1 *nup*G	Invitrogen
Plasmid		
pCR8/GW/TOPO	Cloning vector, Sp^r	Invitrogen
pUC4K	Donor of Km^r gene cassette, Km^r, Ap^r	Taylor and Rose (1988)
pRK2013	Helper plasmid, Tra^+, Km^r	Ditta *et al.* (1980)
pUC18-mini-Tn7T-LAC	Mini-Tn7 vector, Ap^r, Gm^r	Choi *et al.* (2005)
pUC18-mini-Tn7T-Gm-*lacZ*	Mini-Tn7 vector for transcriptional fusion to promoterless *lacZ*, Ap^r, Gm^r	Choi *et al.* (2005)
pUX-BF13	Helper plasmid for transposition of mini-Tn7 element, Ap^r	Bao *et al.* (1991)
pXY6-*xutR*	pUC18-mini-Tn7T-LAC containing *xutR* for complementation	This work
pXY6-*xutA*	pUC18-mini-Tn7T-LAC containing *xutA* for complementation	This work
pXY7-P_R	pUC18-mini-Tn7T-*lacZ* containing *lacZ* fusion to P_R promoter for *xutR*	This work
pXY7-P_A	pUC18-mini-Tn7T-*lacZ* containing *lacZ* fusion to P_A promoter for *xutA*	This work
pXY7-P_A1	pUC18-mini-Tn7T-*lacZ* containing *lacZ* fusion to P_A1 (-215 to +48)	This work

pXY7-P_A2	pUC18-mini-Tn7T-*lacZ* containing *lacZ* fusion to P_A1 (-129 to +48)	This work
pXY7-P_A3	pUC18-mini-Tn7T-*lacZ* containing *lacZ* fusion to P_A1 (-79 to +48)	This work
pXY7-P_A4	pUC18-mini-Tn7T-*lacZ* containing *lacZ* fusion to P_A1 (-61 to +48)	This work
pXY7-P_A1-1	pUC18-mini-Tn7T-*lacZ* containing *lacZ* fusion to P_A1-1, a derivative of P_A1 without the P_A-I half-site	This work
pXY7-P_A1-2	pUC18-mini-Tn7T-*lacZ* containing *lacZ* fusion to P_A1-2, a derivative of P_A1 without the P_A-II half-site	This work
pXY7-P_E	pUC18-mini-Tn7T-*lacZ* containing a 227-bp P_E promoter region fused to *lacZ* reporter.	This work
pXY7-P_E1	pUC18-mini-Tn7T-*lacZ* containing a 151-bp P_E promoter region fused to *lacZ* reporter.	This work
pXY7-P_{xutF}	pUC18-mini-Tn7T-*lacZ* containing *lacZ* fusion to putative promoter for *xutFGH*	This work
pXY7-P_{xutB1}	pUC18-mini-Tn7T-*lacZ* containing *lacZ* fusion to a 473 bp DNA fragment preceding *xutB1*	This work
pCR8-mtlR::Km	Recombinant plasmid for the deletion of *mtlR*	This work
pCR8-mtlZ::Km	Recombinant plasmid for the deletion of *mtlZ*	This work
pCR8-rbsK::Km	Recombinant plasmid for the deletion of *rbsK*	This work
pXY2	pUC18-mini-Tn7T-*lacZ* containing a *lacZ* translational fusion, Ap^R, Gm^R	Liu *et al.* (2014)
pXY3	pUC18-mini-Tn7T-LAC containing a *lacZ* translational fusion, Ap^R, Gm^R	Liu *et al.* (2014)
pXY2-*xutA*	pXY2 containing the P_{xutA}-*lacZ* translational fusion, Ap^R, Gm^R	This work
pXY2-*xutR*	pXY2 containing the P_{xutR}-*lacZ* translational fusion, Ap^R, Gm^R	This work
pXY2-*crc*	pXY2 containing the P_{crc}-*lacZ* translational fusion, Ap^R, Gm^R	This work
pXY3-*xutA*	pXY3 containing the P_{tac}-*xutA*-*lacZ* translational fusion, Ap^R, Gm^R	This work
pUIC3	Suicide vector with promoterless '*lacZ*, Mob^+, Tc^r	Rainey (1999)
pUIC3-43	pUIC3 containing *cbrB*-*lacZ* fusion, Tc^r	This work
pUIC3-65	pUIC3 containing *crcZ*-*lacZ* fusion, Tc^r	This work
pUIC3-148	pUIC3 containing *xutF*-*lacZ* fusion, Tc^r	This work
pUIC3-149	pUIC3 containing *xutB1*-*lacZ* fusion, Tc^r	This work
pUIC3-150	pUIC3 containing *xutB2*-*lacZ* fusion, Tc^r	This work
pUIC3-151	pUIC3 containing *rbsK*-*lacZ* fusion, Tc^r	This work
pUIC3-152	pUIC3 containing *crcY*-*lacZ* fusion, Tc^r	This work
pTrc99A	Protein expression vector, P_{tac} promoter, Ap^r	Amann *et al.* (1988)

pTrc99A-*xutR*	pTrc99A carrying $XutR_{His6}$, Ap^r	This work
pTrc99A-*crc*	pTrc99A carrying Crc_{His6}, Ap^r	This work

2.2.1 Measurement of growth kinetics in laboratory media

P. fluorescens SBW25 and derived mutants were initially grown in 5 ml LB broth at 28ºC overnight. 1 ml of the overnight cell culture was pelleted and washed with 1/4 strength Ringer's solution once. The cell culture was resuspended with 1/4 strength Ringer's solution, followed by incubation at 28ºC for 2 hours. 13 µl of resuspension was mixed with 1.3 ml of appropriate fresh media (1:100 folds dilution). A 200 µl aliquot of cell culture was added into a well of a 96-well microplate (6 replicates). Growth kinetics of *P. fluorescens* SBW25 and derived mutants were monitored at 28ºC using a Synergy 2 plate reader installed with Gen5 software (Bio-Tek). Absorbance at 450 nm was measured at 5 minutes intervals for a period of 48 or 72 hours. The plate was shaken for 10 seconds prior to each read.

2.3 Polymerase chain reaction (PCR)

2.3.1 Primer design

Nucleotide sequences of genes of interest were obtained from *Pseudomonas fluorescens* SBW25 genome sequence (http://www.sanger.ac.uk). Primer design was undertaken using Geneious Pro 5.5.6. DNA sequences and primers were analyzed to build a restriction enzyme profile and to check for the formation of primer secondary structure and melting temperature. All primers were supplied by Integrated DNA Technologies and are listed in Table 2.2.

Table 2.2. Oligonucleotides used in this study

Primer	**Sequence (5' - 3')**[a]	**Application**
xutA1	gagatctGATGATACCGATGGGCTTGG	*xutA* deletion
xutA2	tccgtcaacggatccgcatgctgCATGGCGTTTTCCTTATTGT	
xutA3	cagcatgcggatccgttgacggaCTGATAGGGGTAAACACTGGC	
xutA4	gagatctCACCTTGGCGTTGTTATCGG	

xutR-1	gagatCTTCACGGCCACCCCACAGCAC	*xutR* deletion
xutR-2	cagcatgcggatccgttgacggaTTTCATTGTTGTTGTCCTGG	
xutR-3	tccgtcaacggatccgcatgctgTAGGGCCTCGTATTCAGACTG	
xutR-4	gagatCTGGGCGCACGGGTCAAATACGAC	
xutA-lacZF	gactagtCATAAGGAATGCCCTTGGGGT	P_A transcriptional & translational fusion to *lacZ*
xutA-lacZR	gaagcttGACACCGGGGAAGTACGGCATGGC	
xutR-lacZF	gactagtTAGTAGTCGATGCCCAGTTTG	P_R transcriptional & translational fusion to promoterless *lacZ*
xutR-lacZR	gaagcttCACGGGCGGTAGGGTTTTCATTGT	
xutR-compF	gactagtggAGGACAACAACAATGAAAACCC	*xutR* complementation
xutR-compR	gaagcttTGAATACGAGGCCCTAGGCC	
xutA-compF	gactagtggAGGAAAACGCCATGCCGTAC	*xutA* complementation
xutA-compR	gaagcttCAGTGTTTACCCCTATCAGGT	
xutA-pmF1	ggactagtCGCACTGTCCTTTGGTGATT	Forward primer for *xutA* promoter mapping, with "xutA-lacZR" as the reverse primer
xutA-pmF2	ggactagtGGCGGTAGGGTTTTCATTGT	
xutA-pmF3	ggactagtGACCCTGCCACTCAAAATCG	
xutA-pmF4	ggactagtAAGTCGGCGATGATGCCGTC	
xutA-pmF5	ggactagtTGCTGCTCAGGTAGTTGCCGA	
xutR-ProF	aaatttggaattccatcatcatcatcatcatAAAACCCTACCGCCCGTGCAC	XutR protein expression
xutR-ProR	aaatttgaagcttTGAATACGAGGCCCTAGGCC	
xutR-RACE3	CCGCTTCGATCAAATGTTCG (+361 nt from the ATG start)	*xutR* 5'-RACE analysis
xutR-RACE4	AGGCGACAGAGAAAGTCCTC (+152 nt from the ATG start)	
xutA-RACE1	AGTAGTCGATGCCCAGTTTG (+289 nt from the ATG start)	*xutA* 5'-RACE analysis
xutA-RACE2	TTGAAGGTGCCTACACCGAA (+194 nt from the ATG start)	
xutFGH-1	gagatctTATCTTCGGCAGCATCGACG	*xutFGH* deletion
xutFGH-2	cagcatgcggatccgttgacggaCATGGTGGTGCGTCCTTTTA	
xutFGH-3	tccgtcaacggatccgcatgctgCGCTGAATCCACGCCAACGA	
xutFGH-4	gagatctGCAAACTGGCGGTGTAGAGAA	
xutF-lacZF	gactagtTATCTTCGGCAGCATCGACG	Cloning the *xutFGH* putative promoter
xutF-lacZR	gaagcttGGTACGTTTGAATGACTTCATGGT	
xutR-BSmut1	TAGACCCTGCCACgtcgctggtaACTGTCCTTTGGTGATTTTCAT	Mutagenizing XylR binding site I (P_A-I)
xutR-BSmut2	ACCAAAGGACAGTtaccagcgacGTGGCAGGGTCTAGTCTGTGGC	

xutR-BSmut3	GCACTGTCCTTTGtaccagcgacTAATCGGCAAGGCCGATGCCGT	Mutagenizing XylR binding site II (P_A-II)
xutR-BSmut4	GCCTTGCCGATTAgtcgctggtaCAAAGGACAGTGCGATTTTGAG	
xutA-DNaseF1	GTTGAAGAGCAAGGCAATGCG (biotin labelled)	Forward primer for cloning P_A for XutR binding assays, with "xutA-lacZR" as the reverse primer
xutB1-1	gagatctTCGTGCACGAGACCATGAAC	*xutB1* deletion *xutB1-lacZ* fusion in plasmid vector pUIC3
xutB1-2	cagcatgcggatccgttgacggaCATGAGGGTGTGCTCAGCAGT	
xutB1-3	tccgtcaacggatccgcatgctgACCCTTTAAGAGCGAACGAC	
xutB1-4	gagatctTAGAGCAGGTGCAGGTCTTC	
2739-1	ggagatCTGTTCGACCTCGACCTGGCC	*mtlZ* deletion
2739-2	cagcatgcggatccgttgacggaCAGATACATAGTCGTTCGCTC	
2739-3	tccgtcaacggatccgcatgctgGGATGAAGGTTTTGTCAGCCAG	
2739-4	ggagatctACACTCCACACCCACAGCAGC	
4156-1	ggagatCTGGTGCGTATCGATCACGAG	*rbsK* deletion *rbsK-lacZ* fusion in plasmid vector pUIC3
4156-2	cagcatgcggatccgttgacggaTGGCATACATCAGTACTCATC	
4156-3	tccgtcaacggatccgcatgctgCCCTCATGAAAAAGACACCTC	
4156-4	ggagatctATCGCGAACAGCAACGCCACC	
3115-1	ggagatctAACGAAATTCCCGCTGTGCTG	*xutB2* deletion *xutB2-lacZ* fusion in plasmid vector pUIC3
3115-2	cagcatgcggatccgttgacggaCATATGCAGGTCTTCCAATCA	
3115-3	tccgtcaacggatccgcatgctgATGGAGGCTACAGGGGCTTCG	
3115-4	gagatctGACAGGTATTCTAGGGACGTA	
xutB1-lacZF	gactagtGACGGTTCGTCGAAGTTTCC	Amplify the 473 bp DNA fragment for the construction of *xutB1-lacZ* in mini-Tn7
xutB1-lacZR	gaagcttGTACAGGTTTTGCTGGGTCATGAG	
mtlR-1	ggagatctAAGGCCACGGCCTTACACAACC	*mtlR* deletion
mtlR-2	cagcatgcggatccgttgacggaGGTCATGCTGCCGTCGCTTTAT	
mtlR-3	tccgtcaacggatccgcatgctgTTGGCTTAATGGTTTCAGCTGC	
mtlR-4	ggagatctAACCCTTGACTGACAAACCGTC	

mtlE-pmF1	ggactaGTGCAGCGCTTGACCGAGCAGA	Forward primer for pXY7-P_E
mtlE-pmF2	ggactagtCCAGTGCGCCCAAGGATTTGTC	Forward primer for pXY7-P_E1
mtlE-lacZR	ggaagcttTGCTGTGAACTTCATCGCGCAC	Reverse primer for pXY7- P_E and pXY7-P_E1
5'xutA-F	gactagtACCGCCAAGAACAATAAGG	P_{tac}-*xutA-lacZ* translational fusion in pXY3
5'xutA-R	gaagcttGTCGTAATGGCGAAAGGCGA	Reverse primer for P_{tac}-*xutA-lacZ* fusion in pXY3 & *xutA in vitro* transcription
xutA-T7F1	tgtaatacgactcactatagggAGACACCGCCAAGAACAATAAG	Forward primer for *xutA in vitro* transcription
xutA-T7F2	tgtaatacgactcactatagggaGAAAACGCCATGCCGTACTTCC	
xutR-T7F1	tgtaatacgactcactatagggaGACTGGCCCCAGGACAACAACA	Forward primer for *xutR in vitro* transcription
xutR-T7F2	tgtaatacgactcactatagggagaTGAAAACCCTACCGCCCGTG	
xutR-T7R	TGCTCAGGTAGTTGCCGATGC	Reverse primer for *xutR in vitro* transcription
crc1	gagatCTGCAGCACCTGGTTCAGCG	*crc* deletion
crc2	cagcatgcggatccgttgacggaAGGCTGGGTCGTCCAGTT	
crc3	tccgtcaacggatccgcatgctgGACATTGACCATCTGAGGTC	
crc4	gagatCTTGGTCGACGCACTGAAAG	
crc-lacZF	gactagtGGTGATCACGTCGTCGATGAT	P_{crc} translational fusion to promoterless *lacZ*
crc-lacZR	gaagcttGTTCACACTGATGATCCGCATAAA	
crc-ProF	gccatgggcCGGATCATCAGTGTGAACGTT	Crc protein expression
crc-ProR	gaagctttcagtggtggtggtggtggtgGATGGTCAATGTCCAGTCGTA	
crcZ-1	aggatcCTGGCCAAAATCGGCCAGTTCC	*crcZ* deletion
crcZ-2	cagcatgcagatctgttgacggaCCAGCAAAACCGGGAGGTTG	
crcZ-3	tccgtcaacagatctgcatgctgAGTTTCCGGGATTTGTCTGGC	
crcZ-4	aggatccTGCGAATGTCGTGTACGCCA	
3887Z1	gagatctCACGGAATCAGCGTGCGTGGT	*crcY* deletion,
3887Z2	cagcatgcggatccgttgacggaAACACATTGTCACGGCTACGC	
3888Z3	tccgtcaacggatccgcatgctgCGACAAATTAAAGGGGACCCTCG	

3888Z4	gagatctCCCACGGCTACGTGTGCATCG	
crcY-lacZR	gagatctCTGCGAAGCACATCTTCTCC	Reverse primer for *crcY-lacZ* fusion in plasmid vector pUIC3
crcY-RACE1	TCCCCTTTAATTTGTCGTTGCG (+353 nt from the transcriptional start)	*crcY* 5'-RACE analysis
crcY-RACE2	CTGCTTCTTCGTTATCGATCC (+210 nt from the transcriptional start)	
crcY-RACE3	CTAACCGGTTGCGGGTTTCG (+151 nt from the transcriptional start)	
pcnB1	gagatCTGGCGCGCAAATTGGGCGT	*crcZ-lacZ* fusion in plasmid vector pUIC3
pcnB11	gagaTCTCCAAAAGAATCAGTTAGCT	

[a] Artificial sequences integrated into the primers are shown in lowercase whereas with restriction sites underlined.

2.3.2 Standard PCR

The gene of interest was amplified by PCR from *P. fluorescens* SBW25 genomic DNA. A deoxyribonucleotide triphophate stock was prepared from a dNTP set (Bioline) containing four separate 100 mM of dNTP solutions to generate a final concentration of 10 mM for each dNTP. Taq DNA polymerase (Invitrogen) was used for PCR amplification. The annealing temperature for each pair of primers was determined based on the calculated Tm of primers. If no PCR products or non-specific PCR products were detected at initial annealing temperature, empirical tests were performed to find optimal annealing temperatures for the primers. Preparation of a typical 50 µl of PCR reaction was shown in Table 2.3. PCR reactions were carried out using a gradient thermal Palm-Cycler™ (Corbett Life Science) and reaction conditions were shown in Table 2.4.

Table 2.3. Reagents in 50 µl of PCR reaction

	Volume (µl)	**Final Concentration**
10x Buffer	5	1x
$MgCl_2$ (50 mM)	1.5	1.5 mM
dNTP (10 mM)	1	0.2 mM
Forward Primer (10 µM)	1	0.2 µM
Reverse Primer (10 µM)	1	0.2 µM
Taq DNA Polymerase (5 U/µl)	0.2	1 U
Template DNA	5	1 ~ 5 ng
MilliQ H_2O	35.3	--
Total Volume	50	--

Table 2.4. Typical PCR reaction conditions

	Temperature	**Time**	**Cycles**
Initial Denaturation	94ºC	3 min	1x
Denaturation	94ºC	45 s	30x
Annealing	56 ºC	45 s	
Elongation	72 ºC	1 min per kb	
Final Elongation	72 ºC	10 min	1x
Hold	4ºC		--

In case of amplification of longer DNA targets (≥3 kb), Elongase (Invitrogen) was used according to the manufacturer's instructions. In brief, two separate mixtures were prepared on ice as follows: 1) 1 µl dNTP mix (10 mM), 1 µl of each primer (10 µM), 100~200 ng template DNA, made up to 20 µl with distilled water, and 2) 5 µl of 5x buffer A and B (achieving 1.5 mM Mg^{2+}), 1 µl Elongase enzyme mix, made up to 30 µl with distilled water. Two mixtures were combined to a final volume of 50 µl. The DNA template was initially denatured at 94ºC for 30 seconds. PCR amplification was performed 35 cycles of denaturation at 94ºC for 30 seconds, annealing at 55-65ºC for 30 seconds and extension at 68ºC for 1 minute per kb of the target. If PCR products were to be used for pCR8/GW/TOPO® cloning (Invitrogen), 1 µl of *Taq*

DNA polymerase (Invitrogen) was added after completion of PCR amplification and the reaction was incubated at 72ºC for 10 minutes.

2.4 Cloning and transformation techniques

2.4.1 Preparation of plasmid DNA

Plasmid DNA was extracted from overnight bacterial cultures using QIAprep Spin Miniprep Kit (Qiagen) according to manufacturer's instructions. 30 µl or 50 µl of MilliQ H_2O was used to elute DNA.

2.4.2 Restriction enzyme digestion

DNA was digested with restriction enzymes (New England Biolabs) in the appropriate NEB buffers at 37ºC for at least 2 hours.

2.4.3 Agarose gel electrophoresis

DNA fragments were separated on 1% agarose gels in 1x TBE buffer (UltraPure™, Invitrogen) containing 1x SYBR Safe™ DNA gel stain (Invitrogen). Samples were mixed with 6x DNA loading dye (Fermentas) at ratio of 1:5 prior to loading onto the gel. Gels were run at 140 volts for 30-60 minutes. Lambda DNA/EcoRI+HindIII marker (Fermentas) was also loaded to estimate the size of DNA fragments. Visualization of DNA was undertaken using UV light generated from a High Performance Transilluminator (UVP, LLC) and gels were photographed using DigiDoc-It™ Imaging System with Doc-It LS Analysis Software (UVP, LLC).

2.4.4 Extraction of DNA from agarose gel

DNA samples were subjected to agarose gel electrophoresis. Desired bands were excised from the gel and purified using a QIAquick Gel Extraction kit (Qiagen) following recommendations from the manufacture.

2.4.5 DNA ligation

Insert DNA and vectors at the molar ratio of 3:1 were mixed with 2 µl of 5x ligation reaction buffer and 1 µl (1 U) of T4 DNA ligase (Invitrogen). MilliQ water was added to a final volume of 10 µl. Reactions were incubated at 16ºC overnight.

2.4.6 pCR8/GW/TOPO® cloning

To facilitate cloning of PCR products into destination vectors, PCR products were firstly cloned into pCR8/GW/TOPO® vectors using the pCR8/GW/TOPO® Cloning Kit from Invitrogen (Auckland). The desired insert DNA was then excised from pCR8/GW/TOPO® vector by restriction digestion and subcloned into the desired destination vectors.

2.4.7 Preparation of electrocompetent *E. coli* cells

Escherichia coli strains stored in glycerol-saline at -80ºC were streaked out on a LB plate and grown at 37ºC overnight. A single colony from the plate was inoculated into 5 ml of LB and grown at 37ºC with shaking overnight. 5 ml of overnight culture was added into 200 ml of fresh LB broth and grown at 37ºC with shaking to an OD_{600} of 0.6-0.7. Cells were first chilled on ice for 20 minutes and then harvested at 4,000 g for 20 minutes at 4ºC. The supernatant was discarded and the cell pellet was resuspended in 100 ml of ice-cold 10% glycerol. Cells were centrifuged at 4,000 g for 20 minutes at 4ºC and the supernatant was discarded. The cell pellet was further washed with 50 ml of ice-cold 10% glycerol twice. Cells were centrifuged at 4,000 g for 20 minutes at 4ºC and the supernatant was discarded. The cell pellet was resuspended in 2 ml of ice-cold 10% glycerol. 50 µl of aliquots were stored at -80ºC.

2.4.8 Preparation of chemically competent *E. coli* cells

E. coli strains stored in glycerol-saline at -80ºC were streaked out on a LB plate and grown at 37ºC overnight. A single colony from the plate was inoculated into 5 ml of SOB and grown at 37ºC with shaking overnight. 5 ml of overnight culture was added to a 1L flask containing 200 ml of SOB and grown at 37ºC with shaking to an OD_{600} of 0.6-0.7. The cell culture was collected in four 50 ml sterile tubes and chilled on ice for 15 minutes. Cells were harvested at 4,000 g for 20 minutes at 4ºC. The cell pellet

was resuspended in 16 ml of ice-cold transformation buffer I and then incubated on ice for 15 minutes. Cells were centrifuged at 4,000 g for 20 minutes at 4ºC and the supernatant was discarded. The cell pellet was resuspended in 4 ml of ice-cold transformation buffer II. 50 µl of aliquots was stored at -80ºC.

Transformation buffer I (250 ml)

RbCl	3.0 g
$MnCl_2 \cdot 4H_2O$	2.5 g
Potassium acetate (1M, pH 7.5)	7.5 ml
$CaCl_2 \cdot 2H_2O$	0.4 g
Glycerol	37.5 ml

Adjusted pH to 5.8 with 0.2 M acetic acid and sterilized by filtration through a 0.22 µm filter.

Transformation buffer II (250 ml)

MOPS (0.5 M, pH 6.8)	5.0 ml
$RbCl_2$	0.3 g
$CaCl_2 \cdot 2H_2O$	2.75 g
Glycerol	37.5 ml

Sterilized by filtration through a 0.22 µm filter.

2.4.9 Preparation of electrocompetent *P. fluorescens* cells

P. fluorescens strains stored in glycerol-saline at -80ºC were inoculated in 5 ml of LB broth and grown with shaking at 28ºC overnight. 1.5 ml of cell culture was centrifuged at 13,000 rpm for 1 minute. The cell pellet was washed with 1 ml of sterile, ice-cold glycerol/HEPES solution (10% glycerol and 1mM HEPES) three times. Cells were resuspended in 50 µl of glycerol/HEPES solution and ready for electroporation.

2.4.10 Transformation of *E. coli* or *P. fluorescens* by electroporation

5 µl of ligation products or plasmid DNA (100~200 ng) was added to 50 µl of electrocompetent cells that had been thawed on ice. Cells were placed between 0.1 cm electrodes of a pre-chilled gapped Gene Pulser® cuvette (Bio-Rad) and electroporated using Electroporator 2510 (Eppendorf) at 1.8 kV. 250 µl of SOC medium was immediately added and the cells were transferred to a 1.5 ml sterile eppendorf tube. After electroporation, cells were incubated at 37ºC for *E. coli* or 28ºC for *P.*

fluorescens with shaking for 1 hour. The culture was spread onto LB plates containing appropriate antibiotic and incubated overnight (*E. coli*) or 2 days (*P. fluorescens*). After incubation, transformants were inoculated into 5 ml of LB containing the appropriate antibiotic and grown 37ºC (*E. coli*) or 28ºC (*P. fluorescens*) with shaking overnight.

S.O.C medium

2% Bacto Tryptone	10 mM $MgCl_2$
0.5% Yeast Extract	10 mM $MgSO_4$
10 mM NaCl	2.5 mM KCl

Sterilized by autoclaving and added sterile glucose to 20 mM.

2.4.11 Transformation of *E. coli* by heat shock method

Chemically competent *E. coli* cells were thawed on ice and 2 µl of plasmid DNA or ligation products was added. Cells were incubated on ice for 30 minutes. DNA was transformed into cells by heating at 42ºC for 30 seconds. 250 µl of SOC medium was immediately added and cells were incubated at 37ºC with shaking for 1 hour. The culture was spread onto LB plates containing appropriate antibiotic and incubated at 37ºC overnight.

2.5 Glycerol-saline stock

Glycerol-saline stock was made for long-term storage of bacteria. *P. fluorescens* or *E. coli* strains were inoculated in LB containing appropriate antibiotic and grown at 28ºC or 37ºC, respectively. 1 ml of bacterial culture was added to 800 µl of glycerol saline, mixed thoroughly and stored at -80ºC.

Glycerol-saline

0.85% (w/v)	NaCl
70% (v/v)	Glycerol

2.6 β-galactosidase assays

2.6.1 Construction of transcriptional *lacZ* fusions

Promoter region of target DNA was amplified by PCR using primers listed in Table 2.2. PCR products were first cloned into pCR8/GW/TOPO®, and recombinant plasmids were then subjected to DNA sequencing. After the sequence identity was confirmed, the DNA fragment was retrieved by restriction digestion analysis and cloned into plasmids containing a promoterless *lacZ* gene such as pUC18-mini-Tn7T-Gm-*lacZ* and pUIC3 (Rainey, 1999; Choi *et al.*, 2005). The resultant recombinant plasmid was then introduced into *Pseudomonas* strains using the standard method of either electroporation or conjugation.

2.6.2 Assay for β-galactosidase activity

Expression of *lacZ* fusions was monitored by β-galactosidase assays with 4-methylumbelliferyl-β-D-galactosidase (4MUG) as an enzymatic substrate (Zhang *et al.,* 2006). The cleavage of 4MUG by β-galactosidase generates fluorescent molecules 7-hydroxy-4-methylcoumarin (4MU). 1 ml of cell culture was added to a microcentrifuge tube and then permeabilized with 20 µl of 0.1% SDS (sodium dodecyl sulfate) and 40 µl of chloroform. After vortexing for 10 seconds, samples were incubated at room temperature for 5 minutes. The samples were diluted 20 to 100 folds with water. 40 µl of samples was added to a new centrifuge tube and mixed with 160 µl of reaction cocktail. Reactions were incubated at 37ºC for 30 minutes and stopped by addition of 50 µl of 25% (w/v) trichloroacetic acid. The solution was cooled down on ice and clarified by centrifugation at 13,000 rpm for 1 minute. 10 µl of supernatant was added to 990 µl of glycine-carbonate stop buffer and mixed by vortexing. 4MU standards (0, 100, 200, 300, 400, 500, 600, 700, 800, 900 nM) were prepared with glycine-carbonate stop buffer. The fluorescent 4MU was detected at 460 nm with an excitation wavelength of 365 nm using a Synergy 2 plate reader (Bio-Tek).

Reaction cocktail solution

25 mM	Tris-HCl, pH 7.5
125 mM	NaCl
2 mM	$MgCl_2$
12 mM	β-mercaptoethanol

0.3 mM 4MUG
Dissolve 4MUG in absolute ethanol and then add it to cocktail solution

Glycine-carbonate stop buffer

133 mM Glycine
83 mM Na_2CO_3
Dissolve in MilliQ water and adjust pH to 10.7. Store at room temperature.

2.7 Mutational analysis and gene complementation

2.7.1 Splicing by overlap extension PCR (SOE-PCR)

SOE-PCR (Horton *et al.,* 1989) was used to construct *Pseudomonas* mutants. In this process, flanking regions (600~700 bp) on either side of the targeted gene were amplified using standard PCR with primers that are complementary for 23 bp at the join site. Equal amount of two overlapping PCR products was used as templates in the standard PCR reaction to produce a single PCR product. The PCR product was subsequently checked by sequencing, prior to ligation into pUIC3.

2.7.2 Tri-parental conjugation

Overnight cell cultures of *E. coli* DH5α (λπ) donor containing pUIC3-based plasmids, *E. coli* DH5α containing the helper plasmid pRK2013 and *P. fluorescens* recipient strains were grown in LB containing appropriate antibiotics overnight. 0.5 ml of the recipient culture was heat shocked at 45ºC for 20 minutes. Meanwhile, 0.5 ml of the donor and helper cell cultures was pelleted at 13,000 rpm for 1 minute. Both pellets were mixed together in 0.5 ml LB. After heat-shock, all cultures were spun down at 13,000 rpm for 1 minute and resuspended together 100 µl LB. The resulting resuspension was dropped and spread onto the center of a LB agar plate. The cell culture was incubated at 28ºC overnight. After incubation, the inoculum was removed from the plate and resuspended in 3 ml of sterile water. 100 µl of resuspension was plated onto LB plates containing NF and Tc to select for transconjugants. After growth for two days at 28ºC, individual colonies were selected and purified by re-streaking for cycloserine enrichment (described below).

2.7.3 Cycloserine enrichment

Cycloserine enrichment was used for isolation of strains with mutations. 20 µl of transconjugants *P. fluorescens* (section 2.7.2) culture was inoculated in 400 ml LB broth without antibiotics (allow loss of the chromosomally integrated pUIC3 construct) and was grown at 28ºC overnight with shaking. 400 µl of overnight culture was transferred into 20 ml fresh LB and incubated for 30 minutes at 28ºC with shaking. Tetracycline was added at the final concentration of 10 µg/ml. Following 2 hours incubation at 28ºC with shaking, D-cycloserine was added at the final concentration of 800 µg/ml and incubation continued for 4~5 hours. During this step, addition of cycloserine killed the growing tetracycline-resistant *P. fluorescens* cells and selected for cells that had undertaken the second round of homologous recombination, resulting in loss of either original pUIC3 construct or the targeted gene. Cells (1 ml) were harvested by centrifugation at 13,000 rpm for 1 minute, washed once and diluted in sterile water. The dilutions were plated onto LB plus X-gal (60 µg/ml) plates and incubated for two days at 28ºC. White colonies were picked and gene mutations were checked by PCR.

2.7.4 Gene complementation

Gene complementation was performed by cloning the PCR-amplified coding region of target genes into the multiple cloning site of pUC18-mini-Tn7T-LAC (Choi *et al.*, 2005). The resulting plasmid was introduced into deletion mutants by electroporation with the helper plasmid pUX-BF13 (Bao *et al.*, 1991).

2.8 Protein expression and solubility tests

2.8.1 Protein information

The deduced amino acid sequences of XutR or Crc with a hexa-histidine tag were analyzed for information such as the molecular weight, extinction coefficient and theoretical isoelectric point (pI) using the online tool ProtParam available from ExPASy (Gasteiger et al., 2003) (http://www.expasy.ch/tools/protparam.html).

2.8.2 Small-scale protein expression

A single colony was inoculated into 5 ml of LB containing appropriate antibiotics, and grown at 37ºC with shaking overnight. 1 ml of overnight bacterial culture was inoculated into 20 ml of LB containing the appropriate antibiotic in a 100 ml flask. The bacterial culture was grown at 37ºC with shaking to an optical density (OD_{600}) of 0.6-0.7. IPTG (isopropyl-β-D-thiogalactopyranoside) was added to a final concentration of 1 mM. Following further 4 hours growth for protein induction, 1 ml of aliquot was taken from the culture. Samples of aliquots were centrifuged at 13,000 rpm for 1 minute. Cell pellets were resuspended in 100 µl of 2x sample buffer and subjected to SDS-PAGE analysis. The rest of bacterial culture was harvested at 4,000 g for 20 minutes and the cell pellet was stored at -20ºC until use.

2.8.3 Cell lysis and protein solubility test

Frozen cell pellets were thawed on ice and resuspended in 10 ml of lysis buffer. Prior to incubation on ice for 30 minutes, lysozyme (1.0 mg/ml), DNase I (20 µg/ml) and PMSF (0.1 mM) were added. Cells were lysed by sonication on ice at 10 cycles of 30s bursts with 30s pauses using the Microtip™ of Sonicator S-4000 Ultrasonic Liquid Processor (Misonix, Inc) at amplitude of 60 mV. The resulting cell lysate was centrifuged at 4,000 g for 20 minutes. The supernatant was collected as the soluble fraction. The cell pellet was resuspended in 10 ml of lysis buffer and retained as the insoluble fraction. Soluble and insoluble samples were mixed with 2x sample buffer at 1:1 ratio and were subjected to SDS-PAGE analysis.

Lysis buffer

20 mM	HEPES, pH 7.5
500 mM	NaCl
10 mM	Imidazole

2.8.4 Large-scale protein expression

A single colony was inoculated into 10 ml of LB containing the appropriate antibiotic, and grown at 37ºC with shaking overnight. 10 ml of overnight bacterial culture was inoculated into 500 ml of LB containing the appropriate antibiotic in a 2 L flask. The

bacterial culture was grown at 37ºC with shaking to an OD_{600} of 0.6-0.7 and IPTG was added to a final concentration of 1mM. The bacterial culture was incubated at 25ºC overnight for protein induction and was harvested at 4,000 g for 20 minutes. The supernatant was discarded and the cell pellet was stored at -20ºC until use.

2.9 Sodium dodecyl sulfate – Polyacrylamide gel electrophoresis

2.9.1 Gel preparation

Protein samples were analyzed by SDS-PAGE (Lammili, 1970) using the XCell *SureLock*™ mini-cell system (Invitrogen). Components of buffers, 5% stacking gels and 12% resolving gels are listed below.

10x SDS-PAGE running buffer, pH8.3

30.3 g	Tris base
144.0 g	Glycine
10.0 g	Sodium dodecyl sulfate (SDS)
Added MilliQ H_2O up to 1L	

2x Sample buffer (Reducing buffer)

125 mM	Tris-HCl, pH6.8
20%	Glycerol
4% (w/v)	SDS
10% (v/v)	β-mercaptoethanol
0.02 (w/v)	Bromophenol blue

Stacking gel (5% acrylamide) (10 ml)

6.1 ml	MilliQ H_2O
1.25 ml	40% acrylamide/bis solution (29:1)
2.5 ml	0.5 M Tris-HCl, pH6.8
0.1 ml	10% (w/v) SDS
50 µl	10% (w/v) Ammonium persulfate (APS)
10 µl	TEMED

Resolving gel (12% acrylamide) (10ml)

4.4 ml	MilliQ H_2O
3.0 ml	40% acrylamide/bis solution (29:1)
2.5 ml	0.5 M Tris-HCl, pH6.8
0.1 ml	10% (w/v) SDS
50 µl	10% (w/v) APS
5 µl	TEMED

2.9.2 Sample preparation, gel running and staining

Protein samples were mixed with 2x sample buffer at 1:1 ratio. The sample was heated to 95ºC for 5 minutes prior to being loaded onto a stacking gel. SDS-PAGE was run at 150V until the front dye reached the bottom of a resolving gel. Gels were stained with Coomassie brilliant blue for 1 hour and destained overnight, shaken gently at room temperature.

Coomassie blue stain

0.125% Coomassie brilliant blue R250
50% Methanol
10% Acetic acid
Filtered the mixture

Detain

30% Methanol
10% Acetic acid

2.10 Purification of hexa-histidine-tagged proteins (XutR and Crc)

2.10.1 Sample preparation

Hexa-histidine-tagged proteins (His_6-XutR and His_6-Crc) were purified using TALON® metal affinity resin (Clontech laboratories, Inc.). Cell pellets (prepared from large-scale protein expression) were resuspended in 20 ml lysis buffer and disrupted by lysozymes and sonication. The resulting cell lysate was centrifuged at 4,000 g for 20 minutes at 4 ºC. The supernatant was passed through a 0.45 μm filter and clarified solution was collected and temporarily stored at 4 ºC.

2.10.2 Protein purification

The TALON resin was thoroughly resuspended and 2 ml of resin suspension was transferred to a 30 ml tube. The resin was pelleted at 700 g for 2 minutes and the supernatant was removed. The resin was washed with 10 ml of ice-cold lysis buffer twice and was spun down at 700 g for 2 minutes. The clarified protein sample was mixed with the resin and incubated at 4 ºC for 1 hour with gentle shaking. It allows his-tagged proteins to bind the resin. The resin was centrifuged at 700 g for 5 minutes and washed with 10 ml of ice-cold binding buffer twice. Prior to transferring it to a 2 ml gravity-flow column, the resin was resuspended with 1 ml of lysis buffer. The column was washed with 10 ml of ice-cold lysis buffer, followed by 10 ml of ice-cold

wash buffer. His-tagged proteins were eluted by adding 5 ml of ice-cold elution buffer to the column. 500 µl fractions of the eluate were collected.

Lysis buffer	
20 mM	HEPES, pH 7.5
500 mM	NaCl
10 mM	Imidazole

Wash buffer	
20 mM	HEPES, pH 7.5
500 mM	NaCl
50 mM	Imidazole

Elution buffer	
20 mM	HEPES, pH 7.5
500 mM	NaCl
200 mM	Imidazole

2.11 Concentration of proteins and buffer exchange

Proteins (XutR or Crc) were concentrated using Vivaspin 6 concentrators (GE healthcare) with 10 kDa molecular weight cut-off. The protein was loaded into a concentrator and centrifuged at 4,000 g at 4ºC until the desired concentration of protein was reached. For buffer exchange, proteins were repeatedly diluted with new buffer in a Vivaspin concentrator until the components of old buffer became negligible. The concentrated proteins were stored at -20ºC.

2.12 Determination of protein concentration

Protein concentration was estimated by Bradford assay (Bradford, 1976). A series of bovine serum albumin (BSA) protein standards (0, 125, 500, 750, 1000, 1500, 2000 µg/ml) was prepared in the protein storage buffer. 5 µl of BSA standards and proteins of unknown concentration were mixed with 250 µl of 1x Quick Start™ Bradford Dye Reagent (Bio-Rad) in a 96-well plate. Reactions were incubated at room temperature for 15 minutes. The absorbance of each sample was measured at 595 nm using a spectrophotometer and a standard curve was made by plotting absorbance versus BSA standards. The concentration of protein was estimated using this standard curve.

2.13 Electrophoresis mobility shift assay (EMSA)

2.13.1 Preparation of biotin end-labelled DNA probes

A 205 bp DNA fragment containing the *xutA* promoter region was amplified by PCR using 5'-biotinylated primers. Biotin end-labelled DNA probes were purified by adding an equal volume of 1:1 phenol/chloroform mixture. The upper layer solution was transferred to a microcentrifuge tube after 2-minute centrifugation at 10,000 g. An equal volume of chloroform was added to remove residual phenol. The DNA probe was precipitated by mixing with 1/10th volume of 3 M sodium acetate (pH 5.2) and three volumes of ethanol, followed by incubation at -20ºC for at least 1 hour. DNA was pelleted by centrifugation for 20 minutes at top speed. The pellet was washed with 500 µl of ice-cold 70% ethanol once. After air drying, the DNA pellet was resuspended in 20 µl distilled water and stored at -20ºC.

2.13.2 Preparation of EMSA reactions

Specific binding of XutR to the *xutA* promoter was examined using an electrophoresis mobility shift assay. Reactions including 0.1 µM biotin-labelled DNA and increasing concentrations of XutR proteins were set up in binding buffer in the final volume of 20 µl and incubated at room temperature for 30 minutes. 4 µl of loading buffer was added to each reaction. A 7% native polyacrylamide gel (8 cm x 8 cm x 0.15 cm) was prepared and pre-run in 0.5X TBE buffer for 20~30 minutes using the XCell *SureLock*^{TM} mini-cell system (Invitrogen). Samples were electrophoresed on the 7% native polyacrylamide gel in 0.5X TBE buffer at 80V at 4ºC until blue dye reached to the bottom of the plate.

7% native polyacrylamide gel (10 ml)

1.75 ml	40% acrylamide/bis solution (29:1)
0.5 ml	10X TBE
1 ml	50% Glycerol
50 µl	10% APS
10 µl	TEMED
6.7 ml	MilliQ H_2O

Binding buffer

20 mM	HEPES, pH7.5
1 mM	DTT
50 mM	KCl
1 µg	poly(dI-dC)

Loading buffer		0.5X TBE buffer	
60%	Glycerol	50 mM	Tris-HCl, pH 8.3
0.025%	Bromophenol blue	45 mM	Boric acid
		0.5 mM	EDTA

2.13.3 Electroblotting and detection

DNA in a native polyacrylamide gel was transferred to nylon blotting membranes (Whatman® Nytran™ SuPerCharge) with pore size 0.45 μm. Transfer of DNA was performed in 0.5x TBE buffer at 300 mA for 1 hour using the XCell *SureLock*™ mini-cell system (Invitrogen). The transferred DNA fragments were immobilized onto the membrane by baking at 80ºC for 30 minutes. LightShift™ chemiluminescent EMSA kit (Thermo Scientific) was used to detect the biotin-labelled DNA fragments.

2.14 DNase I footprinting assays

205 bp 5'-biotinylated DNA fragments which includes XutR-binding sites were obtained by PCR amplification. XutR-binding sites were determined by DNase I footprinting assays. Reactions including 2 μM biotin-labelled DNA and increasing concentrations of XutR proteins were set up in EMSA binding buffer in the final volume of 50 μl and incubated at room temperature for 30 minutes. 50 μl of cofactor solution was added and gently mixed by pipetting up and down. Each reaction was treated with 0.03 U DNase I (Invitrogen) for 5 minutes at room temperature. The reaction was terminated by the addition of 100 μl of DNase I stop solution. The DNA fragments were extracted by addition of an equal volume of phenol:chloroform (1:1) mixture and centrifuged at 10,000 g for 2 minute at 4ºC. The upper layer was collected in a centrifuge tube. DNA was precipitated by mixing with of 1μl of glycogen (20 mg/ml, Fermentas), 1/10th volume of 3 M sodium acetate (pH 5.2) and three volumes of ethanol, followed by incubation at -20ºC for at least 1 hour. DNA was pelleted by centrifugation for 20 minutes at top speed. The pellet was washed with 500 μl of ice-cold 70% ethanol. After air-drying, the DNA pellet was resuspended in 8 μl of loading buffer. Samples were heated at 95ºC for 10 minutes and loaded to a 5% sequencing gel which was pre-run in 1X TBE at 50W for at least 30 minutes using the Sequi-Gen® GT cell system (Bio-rad). The electrophoresis was performed in 1X TBE at 50W until blue dye reached to the bottom of glass plates.

DNA in the sequencing gel was transferred to positively charged nylon membranes (Whatman® Nytran™ SuPerCharge) by contact blotting. A glass plate was carefully removed from the gel and a dry nylon membrane was placed onto the gel. The nylon membrane was covered by three layers of Whatman 3MM papers, a glass plate and a weight of ~2 kg. DNA transfer was completed overnight. The transferred DNA fragments were immobilized onto the nylon membrane by baking at 80ºC for 30 minutes. LightShift™ chemiluminescent EMSA kit (Thermo Scientific) was used to detect the biotin-labelled DNA fragments.

Cofactor solution

5 mM	$CaCl_2$
10 mM	$MgCl_2$

DNase I stop solution

200 mM	NaCl
20 mM	EDTA, pH 8.0
1%	SDS

5% sequencing gel (40 ml)

5.0 ml	40% acrylamide/bis solution (29:1)
16.8 g	Urea
4.0 ml	10x TBE
40 µl	25% APS
40 µl	TEMED

Loading buffer

95%	Formamide
0.05%	Bromophenol blue
20 mM	EDTA

2.14.1 G+A marker

A G+A marker which shows the location of purines within the target DNA sequence was prepared using Maxam-Gilbert chemical sequencing reactions. 10 µl of 20 µM biotin-labelled target DNA was mixed with 25 µl of formic acid and the solution was incubated at 25ºC for 5 minutes. The reaction was stopped by addition of 200 µl of hydrazine stop buffer and 750 µl of ice-cold ethanol and incubated at -80ºC for 30 minutes. DNA fragments were collected by centrifugation at 15,000 g for 15 minutes. The supernatant was discarded and the pellet was washed with 700 µl of 70% ethanol twice. The pellet was dried and resuspended in 100 µl of 10% piperidine. The solution was incubated at 90ºC for 30 minutes. 10 µl of 3 M sodium acetate (pH 7.0) and 300 µl of ice-cold ethanol were added and the solution was incubated at -80ºC for 1 hour. DNA fragments were collected by centrifugation at 15,000 g for 15 minutes. The pellet was washed with 700 µl of 70% ethanol twice. After air-drying, the pellet was resuspended in 20 µl of loading buffer and stored at -20ºC.

Hydrazine stop buffer

300 mM	Sodium acetate, pH 7.0
0.1 mM	EDTA
20 µg/ml	yeast tRNA

Loading buffer

95%	Formamide
0.05%	Bromophenol blue
20 mM	EDTA

2.15 RNA manipulation

2.15.1 Synthesis of RNA fragments

RNA fragments were obtained by *in vitro* transcription. PCR products containing a T7 promoter in the correct orientation were cloned into pCR8/GW/TOPO® vectors using pCR8/GW/TOPO® Cloning Kit (Invitrogen). After sequence identity was verified by DNA sequencing, insert DNA was excised from the pCR8/GW/TOPO® vectors by restriction digestion and used as a template for *in vitro* transcription. Non-labelled RNA fragments were synthesized using a T7 Quick High Yield RNA Synthesis Kit (New England Biolabs). For synthesis of transcripts longer than 0.3 kb, the reaction was incubated at 37ºC for 2 hours. For synthesis of transcripts smaller than 0.3 kb, the reaction was incubated at 37ºC for 12-16 hours. DNase I (Invitrogen) treatment was performed to remove the DNA template on completion of RNA synthesis. The size of synthesized RNA was analyzed by polyacrylamide gel electrophoresis.

2.15.2 Gel purification of RNA fragments

After synthesis of RNAs was completed, RNA samples were mixed with an equal volume of 2x RNA loading dye (New England Biolabs) and denatured by heating at 70ºC for 5-10 minutes. The mixture was loaded onto a denaturing 6% polyacrylamide/7 M urea gel. The gel slice containing the band of interest was excised from the gel, cut to tiny pieces and transferred to a 1.5 ml centrifuge tube. Sufficient crush/soak buffer (0.3 M sodium acetate, pH 5.2) was added to cover the gel slice. This slurry was incubated at 4ºC overnight with shaking. The sample was then centrifuged at 10,000 g for 2 minute at 4ºC. The supernatant was transferred into a fresh tube. RNA probes were extracted by addition of an equal volume of 1:1 phenol:chloroform mixture and centrifuged at 10,000 g for 5 minute at 4ºC. The aqueous phase was collected and mixed with an equal volume of chloroform to remove any trace phenol. The sample was centrifuged at 10,000 g for 5 minute at 4ºC.

The aqueous phase was transferred into a fresh tube and mixed with 3 volumes of 100% ethanol to precipitate RNA at -20ºC overnight. RNA fragments were pelleted at maximum speed for 20 minutes at 4ºC. The pellet was washed with 500 µl of ice-cold 70% ethanol once. The purified RNA was resuspended in water and stored at -20ºC.

2.15.3 RNA band shift assay

Binding reaction in 20 µl contained RNA binding buffer, 0.1 µM biotin-labelled RNA, 1 µg yeast tRNA and the indicated amount of purified Crc. Competition assays contained same but unlabeled RNA fragments. After incubation at room temperature for 30 minutes, samples were mixed with 4 µl of loading buffer and loaded to native polyacrylamide gels (8 cm x 8 cm x 0.15 cm). The electrophoresis was performed in 0.5X TBE at 100V at 4ºC until blue dye reached to the bottom of the plate. A 6% nondenaturing polyacrylamide gel (29:1 acrylamide/bisacrylamide) was used for analysis of binding of Crc to *xutR* and *xutA* RNA fragments and a 5% nondenaturing polyacrylamide gel (80:1 acrylamide/bisacrylamide) for analysis of CrcZ and CrcY sRNAs. RNAs in the polyacrylamide gel were transferred to nylon blotting membranes (Whatman® Nytran™ SuPerCharge) with pore size 0.45 µm in 0.5x TBE buffer at 300 mA for 1 hour using the XCell *SureLock*™ mini-cell system (Invitrogen). The transferred RNA fragments were immobilized onto the membrane by baking at 80ºC for 30 minutes. LightShift™ chemiluminescent EMSA kit (Thermo Scientific) was used to detect the biotin-labelled RNA fragments.

RNA binding buffer

10 mM	HEPES, pH7.9
35 mM	KCl
2 mM	$MgCl_2$

6% native polyacrylamide gel (10 ml)

1.5 ml	40% acrylamide/bis solution (29:1)
0.5 ml	10X TBE
1 ml	50% Glycerol
50 µl	10% APS
10 µl	TEMED
6.94 ml	MilliQ H_2O

Loading buffer

60%	Glycerol
0.025%	Bromophenol blue

5% native polyacrylamide gel (10 ml)

1.25 ml	40% acrylamide/bis solution (80:1)
0.5 ml	10X TBE
1 ml	50% Glycerol
50 µl	10% APS
10 µl	TEMED
7.19 ml	MilliQ H_2O

0.5X TBE buffer

50 mM	Tris-HCl, pH 8.3
45 mM	Boric acid
0.5 mM	EDTA

2.16 Transposon mutagenesis

2.16.1 Generation of transposon mutants

Plasmid pSCR001 containing IS-Ω-Km/hah (Giddens *et al*., 2007) was introduced from *E. coli* S17-1 (λπ) donor strains to *ΔcbrB* mutants using a bi-parental conjugation method. Transconjugants were selected on minimal salts medium agar plates supplemented with xylose, NF and Km. Arbitrary primed-PCR (AP-PCR) and DNA sequencing were used to determine the genomic location of IS-Ω-Km/hah transposon insertions. The sequence data were mapped to the genome sequence of *P. fluorescens* SBW25 using Geneious Pro.

2.16.2 Arbitrary primed-PCR (AP-PCR)

AP-PCR involves two rounds of PCR. Reagents used in the first round PCR are listed in Table 2.5. Following initial denaturation of the DNA template at 94ºC for 10 minutes, PCR amplification was carried out by six cycles of denaturation at 94ºC for 30 seconds, annealing at 42ºC for 30 seconds and extension at 72ºC for 3 minutes, where the annealing temperature was decreased 1ºC after each cycle. PCR was continued by 25 cycles of 94ºC for 30 seconds, 65ºC for 30 seconds and 72ºC for 3 minutes. PCR products were diluted by addition of 80 µl of distilled water and used as a DNA template in the second round PCR. Reagents used in the second round PCR are listed in Table 2.6. PCR amplification was performed by initial denaturation of the template at 94ºC for 10 minutes, followed by 30 cycles of 94ºC for 30 seconds, 65ºC for 30 seconds and 72ºC for 3 minutes. PCR products were cooled to 4ºC and 5 µl of CIP/EXO solution (0.2 µl exonuclease I (20 U/µl), 0.1 µl alkaline phosphatase (10 U/µl) and 4.7 µl H_2O) was added to each sample. Reactions were incubated at 37ºC

for 3 minutes and then 80ºC for 20 minutes. Samples were cooled to 4ºC and prepared for sequencing.

Table 2.5. Reagents used in the 1st round of PCR

Reagents	**Volume (µl)**
10x Buffer	2.5
$MgCl_2$ (50 mM)	0.8
dNTP (10 mM)	1
TnphoA-II (10 pmol/µl)	2
Mixture of CEKG 2A, 2B, 2C (1:1:1) (10 pmol/µl)	2
Taq DNA Polymerase (5 U/µl)	0.25
Template DNA	3
MilliQ H_2O	13.45
Total Volume	25

Table 2.6. Reagents used in the 2nd round of PCR

Reagents	**Volume (µl)**
10x Buffer	2.5
$MgCl_2$ (50 mM)	0.8
dNTP (10 mM)	1
Hah-1 (10 pmol/µl)	2
CEKG 4 (10 pmol/µl)	2
Taq DNA Polymerase (5 U/µl)	0.25
Template DNA	2
MilliQ H_2O	14.45
Total Volume	25

2.17 References

Amann, E., Ochs, B., & Abel, K. J. (1988). Tightly regulated tac promoter vectors useful for the expression of unfused and fused proteins in *Escherichia coli*. *Gene, 69*(2), 301-315.

Bailey, M. J., Lilley, A. K., Thompson, I. P., Rainey, P. B., & Ellis, R. J. (1995). Site directed chromosomal marking of a fluorescent pseudomonad isolated from the phytosphere of sugar beet; stability and potential for marker gene transfer. *Mol Ecol, 4*(6), 755-763.

Bao, Y., Lies, D. P., Fu, H., & Roberts, G. P. (1991). An improved Tn7-based system for the single-copy insertion of cloned genes into chromosomes of gram-negative bacteria. *Gene, 109*(1), 167-168.

Choi, K. H., Gaynor, J. B., White, K. G., Lopez, C., Bosio, C. M., Karkhoff-Schweizer, R. R., & Schweizer, H. P. (2005). A Tn7-based broad-range bacterial cloning and expression system. *Nat Methods, 2*(6), 443-448.

Ditta, G., Stanfield, S., Corbin, D., & Helinski, D. R. (1980). Broad host range DNA cloning system for gram-negative bacteria: construction of a gene bank of *Rhizobium meliloti*. *Proc Natl Acad Sci U S A, 77*(12), 7347-7351.

Liu, Y., Rainey, P. B., & Zhang, X. X. (2014). Mini-Tn7 vectors for studying post-transcriptional gene expression in Pseudomonas. *J Microbiol Methods, 107*, 182-185.

Rainey, P. B. (1999). Adaptation of *Pseudomonas fluorescens* to the plant rhizosphere. *Environ Microbiol, 1*(3), 243-257.

Taylor, L. A., & Rose, R. E. (1988). A correction in the nucleotide sequence of the Tn903 kanamycin resistance determinant in pUC4K. *Nucleic Acids Res, 16*(1), 358.

Zhang, X. X., & Rainey, P. B. (2007a). Genetic analysis of the histidine utilization (*hut*) genes in *Pseudomonas fluorescens* SBW25. *Genetics, 176*(4), 2165-2176.

Zhang, X. X., & Rainey, P. B. (2007b). Construction and validation of a neutrally-marked strain of *Pseudomonas fluorescens* SBW25. *J Microbiol Methods, 71*(1), 78-81.

Chapter 3

Novel mechanisms of xylose utilization by a plant growth-promoting bacterium *Pseudomonas fluorescens* SBW25

Yunhao Liu[1,2], Paul B. Rainey[2,3] and Xue-Xian Zhang[1]*

[1]Institute of Natural and Mathematical Sciences, Massey University at Albany, Auckland 0745, New Zealand

[2]NZ Institute for Advanced Study, Massey University at Albany, Auckland 0745, New Zealand

[3]Max Planck Institute for Evolutionary Biology, Plön 24306, Germany

Running Title: Xylose Utilization in *Pseudomonas*

Key Words: Xylose utilization, XylR, MtlR, AraC-type regulator, *Pseudomonas*, Plant-derived nutrients

*Author for correspondence

(**This manuscript is currently under review by *Molecular Microbiology***)

3.1 Summary

Bacterial degradation of xylose is sequentially mediated by two enzymes - an isomerase (XutA) and a xylulokinase (XutB) - with xylulose as an intermediate. *Pseudomonas fluorescens* SBW25, though capable of growth on xylose as a sole carbon source, encodes only one degradative enzyme XutA in the xylose utilization (*xut*) locus. Here, using site-directed mutagenesis and transcriptional assays we have identified two functional xylulokinase-encoding genes (*xutB1* and *xutB2*), and further show that expression of *xutB1* is specifically induced by xylose. Surprisingly, xylose-induced *xutB1* expression is mediated by the mannitol-responsive regulator MtlR, using xylulose rather than xylose as the direct inducer. In contrast, expression of the *xutA* operon is regulated by XutR in a xylose- and xylulose-dependent manner. Both XutR and MtlR are transcriptional activators of the AraC family, member of which typically use DNA-looping to modulate levels of gene expression. The functionality of XutR has been subjected to detailed genetic and biochemical analyses, including DNase I footprinting assays. Our data led to an unconventional XutR regulatory model that does not involve DNA-looping. XutR functions as a dimer, which recognizes two inverted repeat sequences; but binding to one half site is very weak requiring an inducer molecule such as xylose for activation.

3.2 Introduction

Xylose is the backbone monomer of hemicellulose xylan, which is a major structural component of the plant cell wall and particularly prevalent in angiosperms (Rennie & Scheller, 2014). For herbaceous angiosperms, xylose can make up to 31% of the total dry weight (Jeffries & Shi, 1999). Consequently, xylose is considered the second most abundant carbohydrate moiety in nature after glucose, and microbial enzymes involved in the xylose catabolism have been subjected to extensive investigations. However, these studies were largely motivated by commercial use of these enzymes in the food and renewable energy industries (Binder *et al.*, 2010, Beg *et al.*, 2001, Wohlbach *et al.*, 2011). The biological significance of xylose utilization genes has been largely overlooked, particularly for bacteria that colonize plant surfaces, such as the plant growth-promoting bacterium *Pseudomonas fluorescens* SBW25 (Dahl *et al.*, 1994, Desai & Rao, 2010, Silby *et al.*, 2009).

In enteric bacteria, xylose enters the cell via a high-affinity ABC-type transport system consisting of a periplasmic substrate-binding protein (XylF), a cytoplasmic ATP-binding cassette (XylG) and a membrane-spanning component (XylH) (Hasona *et al.*, 2004). Subsequent breakdown of xylose is mediated by two enzymes (outlined in Figure. 3.1A): the xylose-specific isomerase (XylA) catalyses the conversion of xylose to xylulose, which is then phosphorylated by xylulokinase (XylB) (Lawlis *et al.*, 1984). The enzymatic product xylulose-5-phosphate (xylulose-5-P) is an intermediate of the non-oxidative branch of the pentose phosphate pathway, which generates cellular energy and precursor molecules for biosynthesis. Eukaryotic cells use a similar route to catabolize xylose, though the first step from xylose to xylulose is catalyzed by two enzymes (xylose reductase and xylitol dehydrogenase) with xylitol as an intermediate compound (Wohlbach et al., 2011).

The xylose utilization (*xyl*) genes in *E. coli* are organised in three transcriptional units: *xylAB*, *xylFGH* and *xylR* (Song & Park, 1997). Xylose-induced expression of the *xyl* structural genes is mediated by XylR, a transcriptional activator belonging to the AraC family (Desai & Rao, 2010, Song & Park, 1997). It possesses a N-terminal substrate binding domain and two C-terminal helix-turn-helix (HTH) DNA binding domains. XylR itself is constitutively expressed at low levels (Song & Park, 1997). In the presence of xylose, XylR forms a dimer that binds to xylose in a specific manner and causes simultaneous activation of two divergent promoters P_{xylAB} and P_{xylFGH} (Fig. 3.1B). Transcription is initiated via complex molecular interactions between XylR

and the two DNA operator sites. This current model of XylR action was proposed on the basis of crystal structure and atomic force microscopy analysis (Ni *et al.*, 2013). Importantly, it involves DNA looping, which is typical mode of action for an AraC-type activator (Schleif, 2003, Gallegos *et al.*, 1997).

In Gram-positive bacteria, xylose is also catabolised through isomerization to xylulose followed by phosphorylation to xylulose-5-P as in *E. coli*. However, the mechanism of *xyl* gene regulation is significantly different from those established in enteric bacteria (Dahl et al., 1994, Lokman *et al.*, 1994). The *xylAB* operons of *Bacillus subtilis* and *Lactobacillus* are subject to negative control mediated by a repressor protein (also called XylR). The $XylR_{B.subtilis}$ repressor binds to a palindromic sequence located immediately after the transcriptional start site, and the repression is relieved in the presence of xylose (Gärtner *et al.*, 1992, Lokman *et al.*, 1997).

Here, we report the genetic and biochemical characterization of genes and their products that are required for xylose utilization (*xut*) in the plant growth-promoting bacterium *P. fluorescens* SBW25. SBW25 was originally isolated from the phyllosphere of field-grown sugar beet (Bailey *et al.*, 1995). It is capable of aggressively colonising sugar beet and a number of other crops including wheat, maize and peas, and inhibits damping-off disease caused by *Pythium ultimum* (Ellis *et al.*, 2000, Jaderlund *et al.*, 2008, Humphris *et al.*, 2005). To gain insight into the molecular basis of this bacterium's success *in planta*, promoter-trapping techniques such as *in vivo* expression technologies (IVET) were used to identify genes whose expression are specifically induced during bacterial colonization on sugar beet seedlings (Rainey, 1999, Gal *et al.*, 2003). A total of 139 plant-inducible genes were identified, ~ 16% of which have predicted functions in nutrient scavenging (Giddens *et al.*, 2007, Silby et al., 2009). Of particular note was one IVET fusion (*rhi-17*) containing a DNA fragment that bears strong sequence similarity to the *E. coli* XylA gene (Rainey, 1999). It has previously been shown that xylose is a dominant constituent of root exudate for a wide range of plant species (Dakora & Phillips, 2002, Bhuvaneswari & Subba-Rao, 1959). It is also known that SBW25 is capable of growing on xylose as a sole source of carbon and energy (Zhang & Rainey, 2008). These findings cumulatively suggest that SBW25 colonization may be critically dependent on the presence and catabolism of plant-derived xylose, initiating our investigation into the genetic basis of xylose metabolism.

The present study began with an *in silico* prediction of xylose utilization (*xut*) genes encoded in the genome of *P. fluorescens* SBW25 (Silby et al., 2009). Surprisingly, we found that a crucial xylulokinase-encoding gene is missing in the *xut* locus, which contains only a xylose-specific isomerase, a transport system and a transcriptional regulator. Few xylulokinase-like genes are scattered in the genome and each is organized in an operonic structure with predicted functions in the catabolism of mannitol, arabitol, sorbitol, fructose and other yet unknown sugars. We characterized the function of the candidate *xut* genes using a combination of site-directed mutagenesis and chromosomally integrated *lacZ* fusions. We then performed a detailed genetic and biochemical analysis of the function of the xylose-responsive regulator (XutR). Based on our findings we propose a new regulatory model for this AraC-type regulator, which plays its functional role without the involvement of DNA-looping. Finally, we provide empirical evidence showing that xylose utilization genes contribute to the competitiveness of *P. fluorescens* SBW25 in the plant environment.

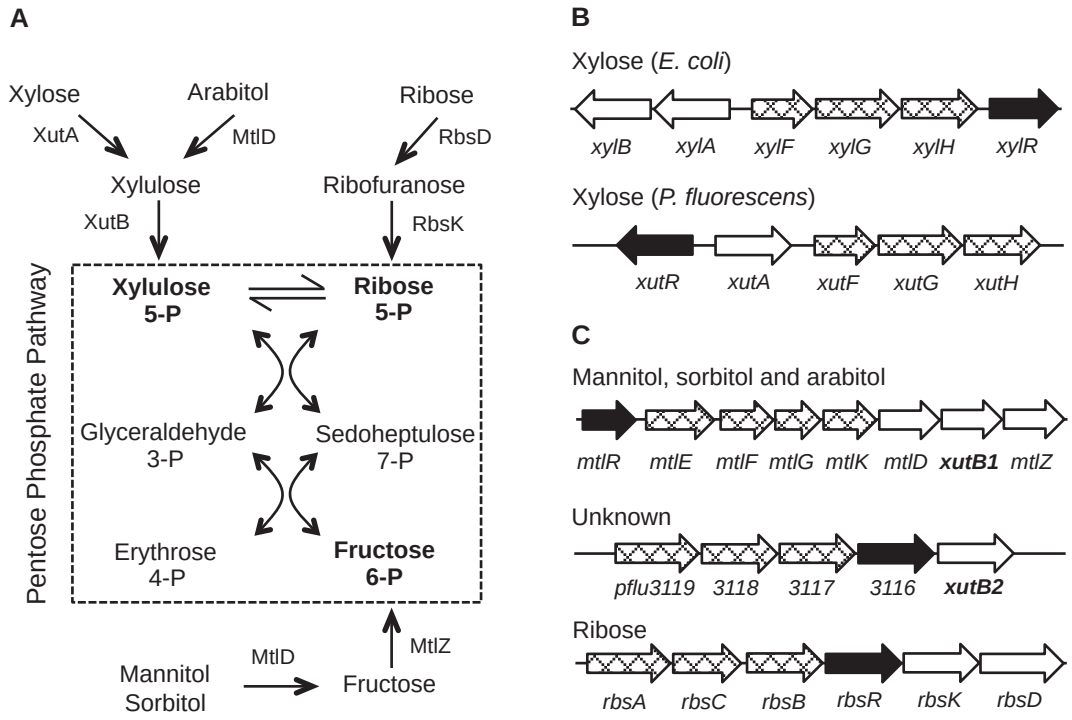

Figure 3.1. Metabolic pathways and genetic organization of genes for the utilization of xylose and five other related carbon substrates in *P. fluorescens* SBW25. The metabolic genes and regulators are shown by open and solid arrows, respectively. Crosshatched arrows represent putative transporters. **(A)** Xylose is degraded by the enzymatic activities of isomerase (XutA) and xylulose kinase (XutB). Breakdown of mannitol, sorbitol, arabitol, fructose and ribose involves 4 additional enzymes: mannitol / arabitol

dehydrogenase (MtlD), fructokinase (MtlZ), ribose pyranase (RbsD) and ribokinase (RbsK). The pentose phosphate pathway is partially shown here to highlight the enzymatic interconversion between the three end products of these utilization pathways: xylulose-5-phosphate, ribose-5-phosphate and fructose-6-phosphate. **(B)** A comparison of xylose utilization loci between *E. coli* and *P. fluorescens* SBW25. **(C)** *P. fluorescens* SBW25 loci related to the xylose catabolism.

3.3 Results

3.3.1 Genomic and genetic identification of xylose utilization genes

Xylose isomerase is a key enzyme for xylose utilization, as it catalyses the first step of the xylose degradation pathway (Fig. 3.1A). A BLASTp search of the *P. fluorescens* SBW25 genome using protein sequence of the functionally characterised isomerase (XylA) from *E. coli* K-12, revealed the presence of a XylA homologue (Pflu2301) with 68.3% sequence identity. As shown in Figure 3.1B, *pflu2301* is flanked by a putative transcriptional regulator and an ABC-type transporter, which are homologues to the *E. coli xylR* and *xylFGH* genes, respectively, suggesting this locus is likely responsible for xylose utilization. We designate these open reading frames *xut* genes for xylose utilization on the basis of the functional characterization described below. Of note, the gene name "*xyl*" has already been assigned in *Pseudomonas* to a group of plasmid-encoded genes, which are involved in the utilization of xylene and toluene and bear little sequence similarity with the *xyl* genes from *E. coli* (de Las Heras *et al.*, 2012).

To our surprise, we found that the *xut* locus of *P. fluorescens* SBW25 does not contain a homologue of the *E. coli* xylulokinase (XylB), which is required in the second step of the xylose degradation pathway (Fig. 3.1A). Instead, five putative xylulokinase-encoding genes are scattered throughout the genome. Each is organized in an operonic structure with other catabolic genes, transporters and transcriptional regulators. Thus, they are likely responsible for the utilization of other substrates like arabitol, which also requires xylulokinase for degradation. We explored their possible involvement in xylose utilization after first attaining a complete understanding of the function of xylose utilization genes located in the *xut* locus (Fig. 3.1B).

We first tested the predicted roles of *xutR*, *xutA*, and *xutFGH* in xylose utilization by site-directed mutagenesis (Fig. 3.1B). Three in-frame deletion mutants (Δ*xutR*, Δ*xutA* and Δ*xutFGH*) were constructed and used in growth assays in minimal medium with xylose as the sole carbon source

(Fig. 3.2A). Consistent with our expectations, deletion of *xutA* or *xutR* abolished growth on xylose (Xut$^-$). The growth defect of the Δ*xutA* and Δ*xutR* mutants on xylose was restored by the introduction of a cloned copy of *xutA* and *xutR*, respectively (Fig. 3.2B). The Δ*xutFGH* mutant displayed diminished growth on xylose, suggesting additional xylose transporters may be present elsewhere in the genome.

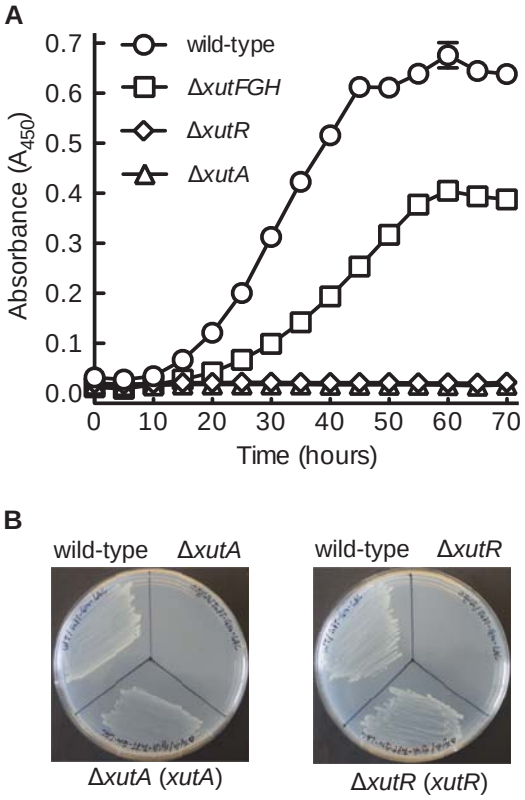

Figure 3.2. Mutational analysis of xylose utilization (*xut*) genes in *P. fluorescens* SBW25. **(A)** Growth dynamics of wild-type SBW25 and mutants MU47-1 (Δ*xutA*), MU47-2 (Δ*xutR*), MU47-3 (Δ*xutFGH*) were measured in minimal salt medium with xylose (20 mM) as sole carbon source. Results are means and standard errors of six independent cultures. **(B)** Growth of wild-type SBW25 and its derived mutants on agar plates of minimal salt medium with xylose (20 mM) as sole carbon source. The coding regions of *xutA* and *xutR* were cloned into pUC18-mini-Tn7T-LAC and their express was induced by IPTG (1 mM). Wild-type and mutants (Δ*xutA* or Δ*xutR*) contain the empty vector as controls.

Next we sought to determine the predicted role of XutR in regulating *xutA* expression in response to the presence of xylose. To this end, a 450-bp DNA fragment containing the putative *xutA* promoter (P_A) was cloned into vector pUC18-mini-Tn7T-Gm-*lacZ*, and the resultant P_A-*lacZ* fusion was introduced into wild-type SBW25 and its derived mutant Δ*xutR*. β-galactosidase activity was measured for cells grown in minimum salts medium supplemented with either glycerol or glycerol plus xylose. Glycerol was selected as a control substrate because it does not produce any detectable effects on *xutA* expression. In the wild-type background, *xutA* expression remained constant at low levels when grown on glycerol, but a significant increase over time was observed for bacteria grown on glycerol plus xylose (Fig. 3.3A). Significantly, xylose-induced *xutA* expression was abolished in the Δ*xutR* mutant background (Fig. 3.3B). This expression data is consistent with the observed Xut$^-$ phenotype of the Δ*xutR* mutant, which together show that XutR functions as an activator responsible for the xylose-induced transcription of *xutA*.

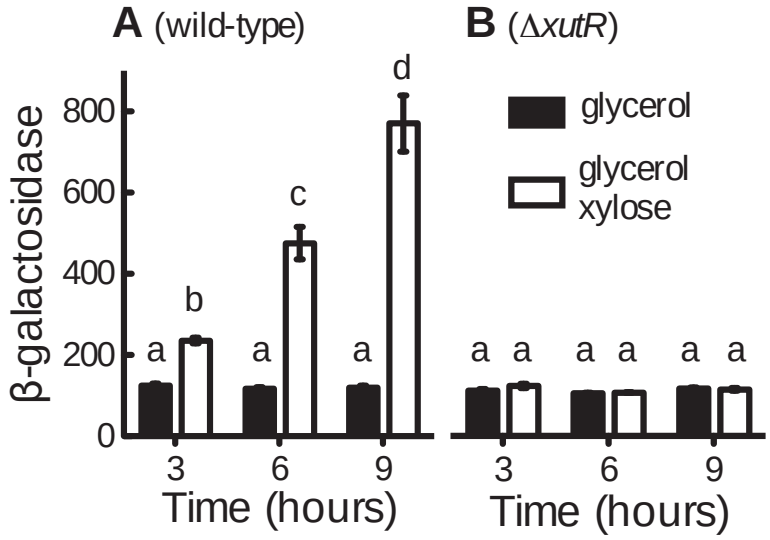

Figure 3.3. Xylose-induced expression of *xutA* in wild-type *P. fuorescens* SBW25 (A) and the *xutR* deletion mutant (B). β-galactosidase activities (μM 4MU min^{-1} OD_{600}^{-1}) were measured for cells grown in minimal salts medium supplemented with glycerol or glycerol plus xylose. Values are means and standard errors of three biological repeats. Three-way ANOVA revealed a significant interaction between genotype, medium and time ($F_{2,24} = 34.998$, $P < 0.001$]. Bars that are not connected by the same letter (shown above each) are significantly different ($P < 0.05$) by Tukey's HSD test.

3.3.2 Transcriptional organization of *xut* genes

xutR must be transcribed as a single unit from a promoter located in the intergentic region of *xutR* and *xutA* (Fig. 3.1B). To test the xylose responsiveness of this *xutR* promoter (P_R), a mini-Tn7 P_R-*lacZ* fusion was constructed in *P. fluorescens* SBW25, and β-galactosidase activity was assayed for cells grown on two minimal media (glycerol vs. glycerol plus xylose) at three time points (i.e. 3, 6 and 9 hours after inoculation). The results revealed no significant effects of cultivation medium and time (Fig. S3.1A), indicating that the P_R promoter is constitutively active. Therefore, unlike *xutA*, transcription of *xutR* is not subject to regulation by xylose.

xutFGH and *xutA* are organized in the same orientation. Thus, it is likely that *xutFGH* and *xutA* are transcribed as a single mRNA (Fig. 3.1B). However, the intergenic region between *xutFGH* and *xutA* is of 225 bp in length, which is long enough to harbour an additional promoter specific for *xutFGH* transcription. To test this possibility, a 700 bp DNA fragment spanning the 3' end of *xutA* to the 5' end of *xutF* was cloned into pUC18-mini-Tn7T-Gm-lacZ (Fig. S3.2). The resultant P_{xutF}-*lacZ* fusion was then introduced into the chromosome of *P. fluorescens* SBW25 at the Tn7 insertion site located downstream of *glmS* (Liu *et al.*, 2014). Results of β-galactosidase assay revealed no significant xylose-responsive promoter activities (Fig. S3.2). Next, we examined whether *xutFGH* expression is xylose inducible. To this end, a promoterless *lacZ* reporter gene was inserted into the coding region of *xutF*. This was achieved by cloning the same 700 bp *xutA-xutF* DNA fragment into the suicide plasmid vector pUIC3, followed by integration into the *xut* locus via homologous recombination. Results of β-galactosidase assay showed that xylose caused a 32-fold increase of *xutF* expression (Fig. S3.2). The fact that *xutF* is xylose-inducible but no xylose-responsive promoter was detected between *xutA* and *xutF* strongly suggests that *xutFGH* and *xutA* are co-transcribed as a single unit under the control of the P_A promoter (Fig. S3.2).

3.3.3 Determining transcriptional start sites of the *xut* operons

The intergenic region between *xutR* and *xutA* is only 139 bp long. However, data presented above indicated that it contains two divergent promoters: P_A is xylose-inducible whereas P_R is constitutively active. It is thus important to know how the two promoters are precisely organized. To this end, 5'-RACE was employed to identify the 5'-end sequence of each transcript using mRNAs prepared from cells grown on minimal medium with xylose as the sole carbon source

(Fig. 3.4). A sequence (TCGGCA N_{16} TAGTAT) similar to the δ^{70}-promoter consensus sequence (TTGACA N_{16-18} TATAAT) was identified immediately upstream of the *xutA* transcriptional start site. A putative δ^{70} binding site (GTGCGA N_{17} TAGTCT) was also detected upstream of the defined transcriptional start site of *xutR*. Notably, the two -35 elements of P_A and P_R are separated by only 22-bp; the XutR operator site required for P_A activity is thus likely located in the P_R region. This raises the question as to how XutR mediates xylose-induced *xutA* transcription without blocking expression of *xutR* itself (Fig. 3.3).

The XutR regulator is of 391 amino acids in length, showing 47% sequence identity with the well-characterized *E. coli* XylR. Both proteins share a similar domain structure typical of AraC family members: a N-terminal substrate-binding domain and two C-terminal HTH domains. Surprisingly, the *xutA* promoter region does not contain the previously identified consensus sequence of $XylR_{E.coli}$ "---gaAa-a--a-AAT---gaAa-a--a-AAT" (Song & Park, 1997). Furthermore, there is a significant difference between the genetic organization of structural genes in *E. coli* and in *P. fluorescens* (Fig. 3.1B). In *E. coli*, the two XylR-regulated operons (*xylAB* and *xylFGH*) are divergently transcribed. Divergent promoter organization is crucial for the current model of XylR-mediated regulation, which posits that transcription is activated by simultaneous binding of XylR to both P_{xylAB} and P_{xylFGH} via DNA looping (Ni et al., 2013). Together, the evidence available shows that the XylR regulatory model established in *E. coli* does not hold for XutR in *Pseudomonas*.

3.3.4 Mapping the xylose-inducible P_A promoter

Functional characterization of XutR started by defining the minimal DNA sequence required for XutR-mediated P_A promoter activity. To this end, four transcriptional *lacZ* fusions were made in wild-type SBW25 by cloning P_A DNA fragments with the same 3'-end (+48) but variable 5'-end into the mini-Tn7 vector (Fig. 3.4). Results of β-galactosidase assay showed that the three large DNA regions starting from -215, -129 or -79, respectively, remained xylose-inducible, whereas the smallest segment (-61 to +48, P_A4) lost xylose-inducible promoter activity. The 18 nt sequence from -79 to -61 is therefore crucial for XutR-mediated activation of the P_A promoter (Fig. 3.4). A close examination of this sequence and its vicinity revealed the presence of two imperfect inverted repeat sequences, designated P_A-I and P_A-II, which are likely the target sites of XutR (see details in Fig. 3.4). The loss of *xutA* transcription in the smallest P_A4 segment is

caused by the absence of an intact P_A-I sequence. The P_A-II repeat overlaps the -35 element of the P_A promoter; this kind of promoter organization is commonly found for activators belonging to the AraC family (Reeder & Schleif, 1993, Gallegos et al., 1997).

Figure 3.4. Genetic identification of the P_R and P_A promoters. **(A)** The DNA sequence of intergenic region between the first codons of *xutR* and *xutA*. Transcriptional start sites determined by 5'-RACE experiment are indicated by bent arrows and the related -10 and -35 elements are shown in box. The two inverted repeat sequences (P_A-I and P_A-II) required for P_A promoter activity are highlighted with underlined letters. **(B)** Results of P_A promoter mapping. The four P_A variants (P_A1 to P_A4) were cloned separately into pUC18-mini-Tn7T-*lacZ* and the resultant fusion strains were assayed for β-galactosidase activity. Of note, the -79 and -61 residues at the 5' end of P_A3 and P_A4, respectively, are marked with asterisks. Expression levels were compared between cells grown in the two media, and "s" in parenthesis denotes significant difference between means as revealed by the Student's t-test ($P < 0.05$).

3.3.5 Determining the *in vitro* molecular interactions between XutR and the P_A promoter

The DNA-binding properties of XutR were first examined using electrophoretic mobility shift assays (EMSA). Histidine-tagged fusion protein $XutR_{His6}$ was expressed in *E. coli* and subjected to purification using cobalt affinity chromatography. The specific DNA probe, a 205-bp DNA fragment corresponding to the P_A promoter region from -157 to +48, was amplified by PCR using a biotin-labelled primer (Table S3.1). As shown in Figure 3.5A, a significant shift of labelled DNA was observed in the presence of increasing concentrations of $XutR_{His6}$ (lanes 2 – 7). DNA retardation was abolished by addition of the same but unlabelled probe DNA (lane 8). Moreover, an unrelated control protein did not cause a shift of the P_A probe (lane 9). Thus, the data indicate that XutR is capable of specifically binding the P_A promoter.

The migration distance of the free probe and that of the protein-DNA complex were used to calculate the molecular weight of $XutR_{His6}$ (Bading, 1988). The DNA-bound $XutR_{His6}$ was estimated to be 102 kDa. Given that the predicted molecular weight of $XutR_{His6}$ monomer is 44 kDa, the data thus suggests that XutR forms a dimer when bound to the DNA target site.

We then tested the possible effects of xylose on XutR-binding. EMSA analysis was performed using the same 205-bp biotin-labelled P_A probe. There was no significant effects on protein-DNA binding affinities: the XutR dissociation constant (Kd) was calculated to be 107 ± 29.6 nM and 122.4 ± 31.3 nM in the presence and absence of xylose, respectively (Fig. 3.5B). This result is generally consistent with the functional role of XutR as a transcriptional activator, which can bind to the target site in the absence of the substrate (i.e. xylose).

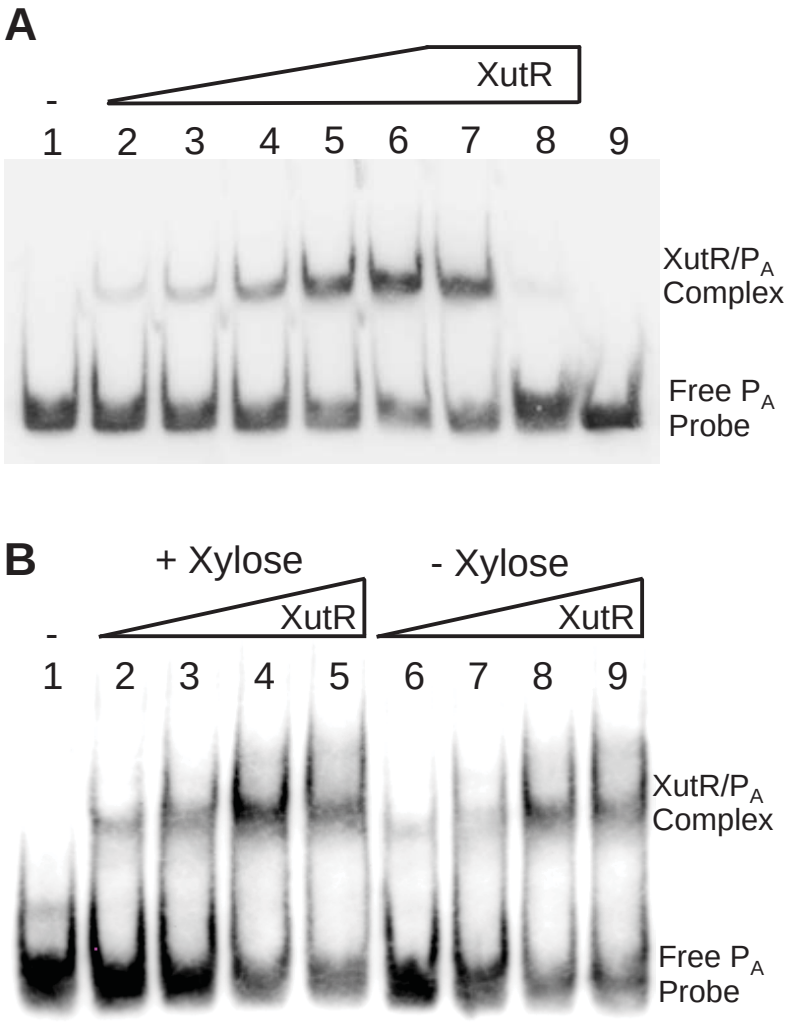

Figure 3.5. EMSA experiments showing specific binding of XutR to the P_A promoter (A) and the effects of xylose on XutR-P_A binding in vitro. EMSA was performed using biotin-labeled 205-bp DNA fragment corresponding to P_A region from -157 to +48 (Fig. 3.4). **(A)** Purified $XutR_{His6}$ was added at the concentration of 0, 25, 50, 100, 200, 400, 500 and 500 nM in lanes 1 to 8, respectively. A 200-fold molar excess of unlabelled probe (competitor DNA) was added in lane 8, and the EMSA assay in lane 9 was performed using the control protein OctA instead of XutR. **(B)** An increasing amount of $XutR_{His6}$ was added in lane 2-5 and lane 6-9 from 50, 100, 200 to 400 nM, and no $XutR_{His6}$ added in lane 1. Reactions in lane 2-5 contained 20 mM of xylose.

3.3.6 Analysis of the XutR binding sequences

To identify the precise XutR binding site, DNase I footprinting analysis was performed using the purified $XutR_{His6}$ protein and the biotin-labeled P_A promoter as the DNA probe. A representative gel image is shown in Figure 3.6. The data clearly show that XutR can protect a 49-bp DNA region from DNase I digestion. Significantly, the functional requirement of this XutR-protected region has been demonstrated by promoter mapping described above. An alignment of P_A homologues from nine *Pseudomonas* genomes revealed conserved residues in the XutR operator sites (AAAATC-N15-GATTTT) (Fig. S3.3A). Each of the two inverted repeat sequences (P_A-I and P_A-II) is of 17-bp in length, and it is predicted to possess two major grooves where monomeric XutR is most likely to make contact (Fig. S3.3B).

Although the data presented so far indicate XutR forms a dimer, with each monomer binding to a repeat sequence in the P_A promoter (or P_A-site), it is unclear how the molecular interactions between XutR and the repeat elements (P_A-I and P_A-II) cause activation of the promoter. We constructed two P_A variants (P_A1-1 and P_A1-2), each carrying a mutant allele of either P_A-I or P_A-II (Fig. 3.6B). Specifically, a conserved part of the repeat region in P_A-I or P_A-II was substituted with a 10-bp random sequence (shown in 5' to 3' orientation): P_A1-1 has the P_A-I element eliminated from TCAAAATCGC to GTCGCTGGTA; P_A1-2 possesses an altered P_A-II from GTGATTTTCA to TACCAGCGAC. Next, the two P_A variants were subjected to assays for promoter activity in vivo and EMSA analysis for XutR binding in vitro (Fig. 3.6B and 6C, respectively). β-galactosidase activities were measured using the related mini-Tn7 *lacZ* reporter gene fusions in wild-type SBW25. Disruption of either P_A-I or P_A-II completely abolished xylose-induced P_A promoter activity (Fig. 3.6B). Neither P_A variants were able to bind to the XutR regulatory protein (Fig. 3.6C). Together, the data led us to conclude that XutR functions by simultaneously binding to the two half-sites of P_A-I and P_A-II.

Close examination of the DNase I footprinting profiles reveals a significant difference of XutR binding affinities between the two repeat elements (Fig. 3.6A): XutR can bind to the P_A-I site with high affinity because the DNA region was well protected in the presence of XutR. However, the P_A-II site was weakly protected even when XutR was added at the highest concentration of 400 nM (Fig. 3.6A, lane 6), suggesting a low affinity binding between XutR and P_A-II.

Taking all data together, we propose that XutR functions as a dimer, with one monomer binding to one half-site of the P_A promoter. In the absence of xylose the XutR / P_A-II interaction is not strong enough to activate the P_A promoter. The role of the xylose inducer is most likely to enhance XutR / P_A-II binding affinity and cause activation of the P_A promoter in a xylose-dependent manner (Fig. 3.7). Interestingly, the P_A-I half-site is located at the P_R promoter region (Fig. 3.4). Thus, XutR likely represses its own expression when bound to the P_A promoter. Indeed, deletion of *xutR* resulted in a ~70% increase of P_R activity (Fig. S3.1). Given that *xutR* transcription is not responsive to xylose, it is likely that XutR can occasionally fall off the P_A operator site in both the presence and absence of xylose, enabling constant *xutR* transcription at low levels (Fig. 3.7).

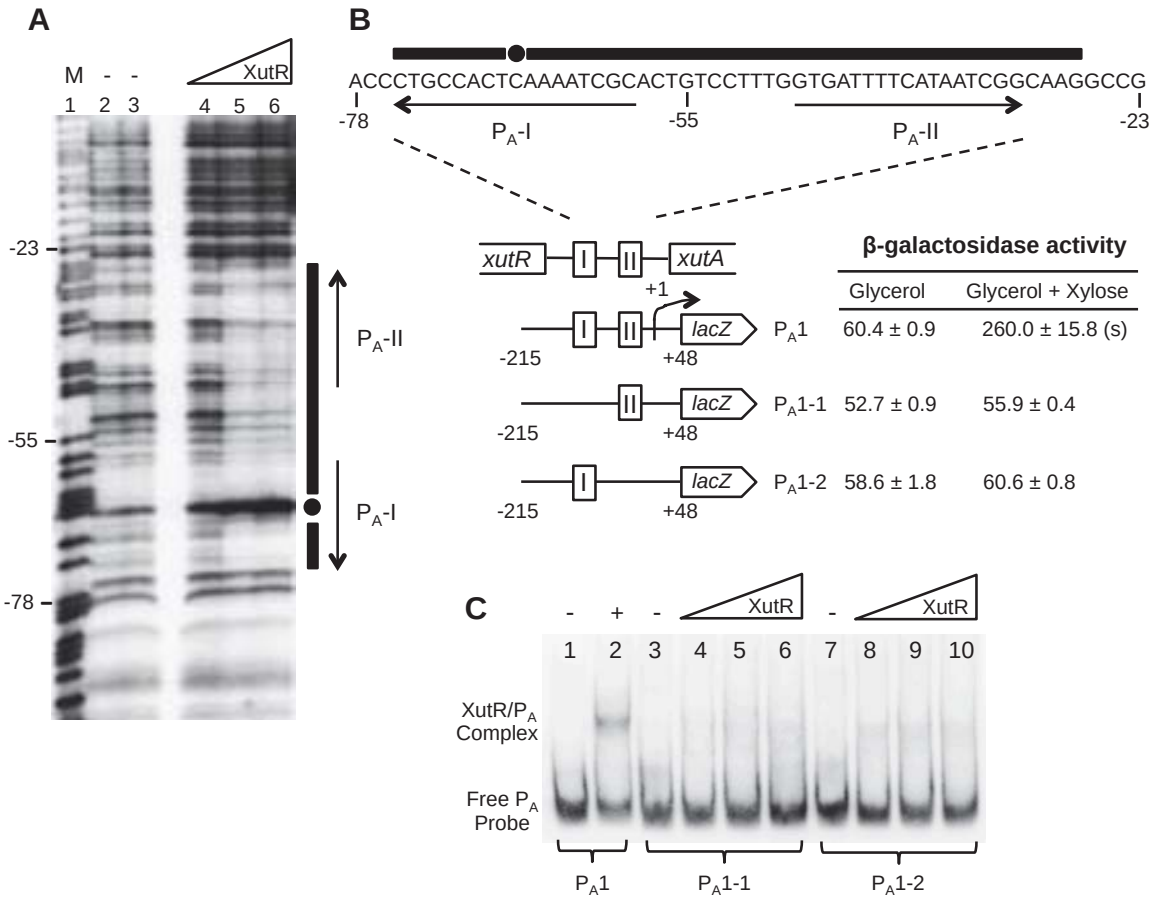

Figure 3.6. Functional analysis of XutR and its targeting P_A promoter. **(A)** DNase I footprinting was performed using purified $XutR_{His6}$ and a 205-bp biotin-labeled DNA probe containing the P_A promoter region from -157 to +48. Lane 1, G+A marker; Lanes 2 & 3, no XutR; Lanes 4-6, XutR added at 50, 200 and 400 nM respectively. Of note, the XutR-binding made one DNA residue to be hypersensitive to DNase I cleavage. **(B)** The XutR protected region is indicated by black bars with the internal hypersensitive site being marked with a filled circle. B-galactosidase activity was measured for *lacZ*

fusions to wild-type P_A promoter (P_A1) and its derived mutants P_A1-1 and P_A1-2 carrying mutations of the P_A-I and P_A-II repeats, respectively. Expression levels were compared between cells grown in the two media, and "s" in parenthesis denotes significant difference between means as revealed by the Student's t-test ($P < 0.05$). **(C)** EMSA was performed using 205-bp biotin-labeled DNA probes containing the wild-type (P_A1) or mutant alleles (P_A1-1 or P_A1-2). Lane 1, 3 and 7: no XutR; Lanes 4 to 6 and lanes 8 to 10, XutR added at 50, 100 and 200 nM, respectively.

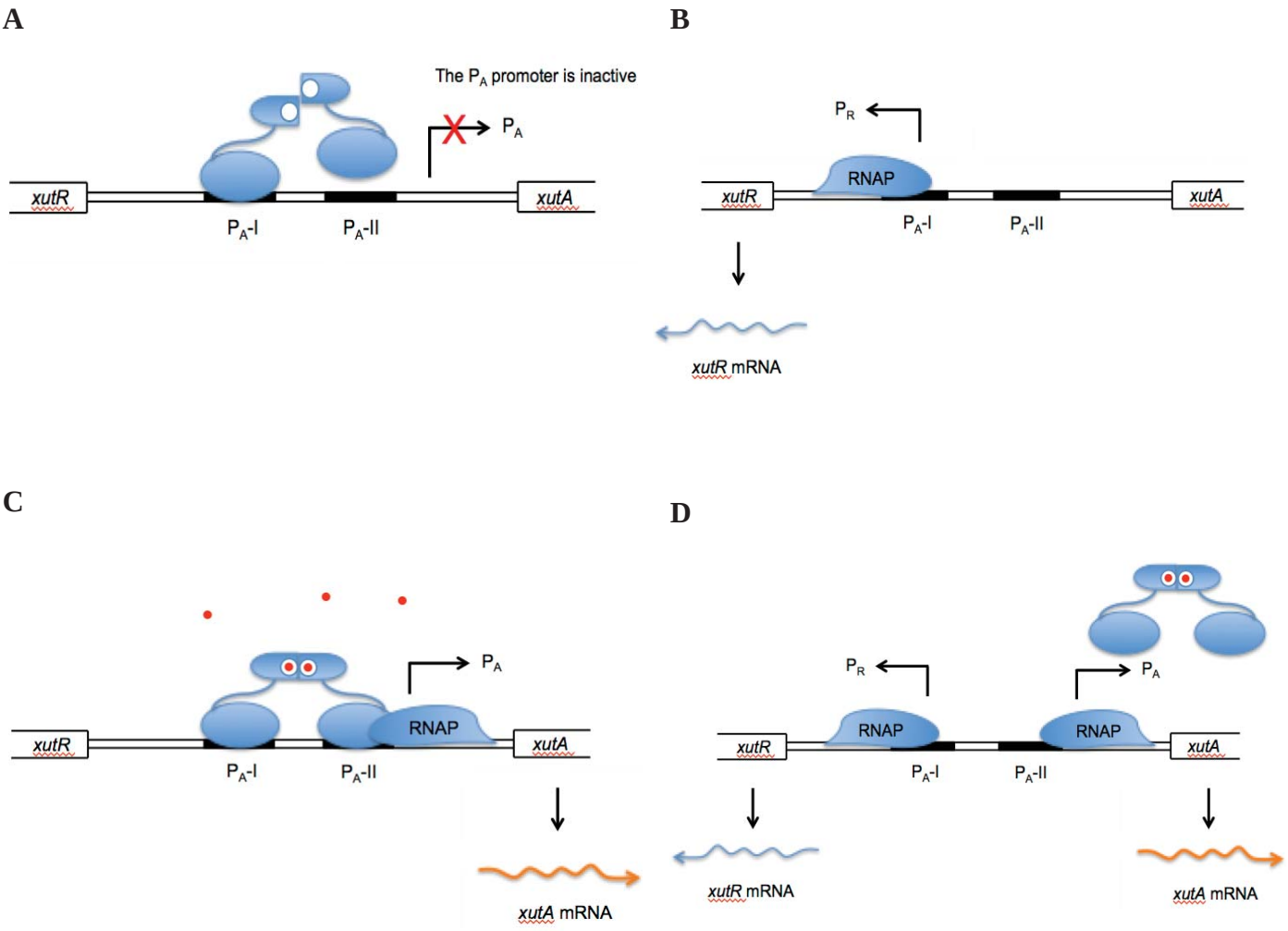

Figure 3.7. Model of XutR action in *P. fluorescens* SBW25. (A) In the absence of xylose, expression of *xutA* is not induced. Dimeric XutR is capable of contacting two half-sites of the P_A promoter. The binding of XutR to the P_A-II site is relatively weak. (B) When XutR occasionally falls from DNA, the P_R promoter region is exposed, resulting in low levels of *xutR* expression. (C) In the presence of xylose, the complex of XutR/xylose binds to P_A-I and P_A-II sites tightly, causing activation of the P_A promoter. (D) The complex of XutR/xylose may fall from DNA even in the presence of xylose. Thus, low level of *xutR* transcription is maintained.

3.3.7 Genetic analysis of the xylulokinase-encoding genes

Armed with the knowledge of XutR-mediated regulation of the *xutAFGH* operon, we proceeded to identify the missing *xutB* gene(s) encoding xylulokinase, an essential enzyme required for the second step of xylose degradation (Fig. 3.1A). A BLASTp search identified five homologues located outside of the *xut* locus (specifically, Pflu3115, Pflu2740, Pflu3929, Pflu3723 and Pflu1142). The genetic structure of two similar sequences (Pflu3115 and Pflu2740) with the highest sequence identity (>35%) is shown in Figure 3.1C. *pflu2740* was predicted to be one part of an operon responsible for the utilization of mannitol, sorbitol and arabitol (Brunker *et al.*, 1998). These three sugars are recognized by the same dehydrogenase MtlD, and the breakdown of arabitol requires xylulokinase activity (Fig. 3.1A). Also present at the same locus are four genes encoding an ABC-type transporter (*mtlEFGK*). Expression of the *mtl* structural genes is likely regulated by the preceding *mtlR*, which encodes an AraC-type transcriptional activator and shares a similar domain structure with XutR. Similarly, *pflu3115* is predicted to be co-transcribed together with a transcriptional regulator and an ABC-type transporter system for the utilization of yet-unknown substrate(s) (Fig. 3.1C).

To examine the possible involvement of *pflu2740* and *pflu3115* in xylose utilization, three isogenic mutants devoid of *pflu2740* and/or *pflu3115* were constructed and compared with wild-type SBW25 for their ability to grow on xylose. The deletion of either *pflu2740* or *pflu3115* resulted in a significant decrease of xylose utilization (Fig. S3.4A). *pflu2740* and *pflu3115* were thus designated *xutB1* and *xutB2*, respectively, to reflect their requirement for xylose utilization. Significantly, the double deletion mutant (MU47-6, Δ*xutB1* Δ*xutB2*) also showed a reduced but not abolished growth on xylose, hinting at the existence of other proteins with xylulokinase activity.

The genetic organization of *xutB1* and *xutB2* (specifically, their coexistence with other regulator and transporter genes) suggests that xylose utilization is not their primary physiological function (Fig. 3.1C). We hypothesized that the expression of *xutB1* and *xutB2* is not induced by xylose, rather, the xylulokinase activity required for xylose breakdown is provided by the products of multiple *xutB* genes that are expressed at basal levels. To test this hypothesis, two chromosomally integrated *lacZ* fusions were constructed to *xutB1* and *xutB2* in the genetic backgrounds of wild-type SBW25 and the *xutR* deletion mutant. Results of β-galactosidase assay are shown in Figure

S3.4B. Consistent with expectation, expression of *xutB2* was not responsive to the presence of xylose. Surprisingly, xylose caused a 14-fold increase of *xutB1* transcription and xylose-induced *xutB1* expression was abolished in the Δ*xutR* background (Fig. S3.4B). The observed xylose- and XutR-dependent *xutB1* transcription ran contrary to our expectations, and prompted further investigation into functionality of the *xutB1* promoter, with a specific focus on the roles of both XutR and MtlR regulators.

3.3.8 Defining the regulatory roles of XutR and MtlR in xylose-induced *xutB1* expression

We found that the xylose-responsive promoter for *xutB1* expression is located in the intergenic region between *mtlR* and *mtlE* (Fig. 3.1C). When this region (227 bp) was fused to the *lacZ* reporter gene at the mini-Tn7 integration site, xylose-induced expression was observed (Fig. S3.5). This functional promoter is denoted P_E. In contrast, the 473 bp region preceding *xutB1* did not have any detectable xylose-induced promoter activity (Fig. S3.5). Thus, the data support the prediction that *xutB1* is organized as an operon together with other *mtl* structural genes.

Next, we focused our characterization on the P_E promoter (Fig. 3.8). To test the requirement of MtlR and XutR for P_E activity, levels of the P_E-*lacZ* expression were compared in three genetic backgrounds (wild type, Δ*mtlR* and Δ*xutR*) with bacterial cells grown on glycerol, glycerol + xylose, or glycerol + mannitol as the carbon source(s). Mannitol was capable of activating the P_E promoter, and this activation required MtlR but not XutR (Fig. 3.8B). Surprisingly, deletion of either *mtlR* or *xutR* abolished the xylose-induced P_E expression (Fig. 3.8B). XutR can potentially activate P_E through binding to a specific operator site, as it does for the *xutA* operon. This begs the question as to why MtlR is additionally required for xylose-induced activation of P_E.

Interrogation of the P_E sequence revealed the presence of a putative activator-binding site, which comprises two direct repeats (P_E-I and P_E-II) with the P_E-II region overlapping the putative -35 element (Fig. 3.8A). Indeed, a P_E variant devoid of P_E-I showed no mannitol- or xylose-induced promoter activity (Fig. 3.8C). However, the P_E operator site only shows partial sequence similarity with the XutR-binding site. The DNA-binding sequence for MtlR has so far not been determined in *Pseudomonas* and other closely related bacteria. It is possible that either XutR or MtlR can bind to the same DNA region causing activation of P_E in the presence of xylose.

However, even if this is the case, it does not explain why both XutR and MtlR are required for the xylose-induced P_E activity.

We hypothesized that xylulose rather than xylose is the direct inducer molecule for MtlR. When bacteria are grown on xylose, MtlR directs expression of the *mtlE* operon containing *xutB1*, thus requiring XutR; however, activation is induced by xylulose, the enzymatic substrate of XutB1. If true, XutR is also required for *xutB1* expression, because without XutR, XutA - the enzyme that converts xylose to xylulose - is not expressed. To test this hypothesis, we monitored ability of xylulose to activate expression of the P_E-*lacZ* fusion in three genetic backgrounds (wild type, Δ*mtlR* and Δ*xutR*). Consistent with our expectation, xylulose caused a 1.5-fold increase of P_E activity; more importantly, induction remained unchanged in the Δ*xutR* background, but it was abolished in the Δ*mtlR* mutant background (Fig. 3.8D). Furthermore, we also showed that xylose was unable to induce P_E-*lacZ* expression in the Δ*xutA* background (Fig. 3.8E). Together, the data consistently indicate that activation of the *xutB1* operon is mediated by MtlR only, with xylulose rather than xylose being the inducing molecule.

The finding that xylulose acts as the direct inducer of the MtlR activator led us to consider the possibility that the same may hold for XutR. That means that the xylose-induced P_A activities are mediated by XutR via molecular interaction with xylulose, thus requiring functional XutA. To test this prediction, we first showed that *P. fluorescens* SBW25 was capable of growing on xylulose as the sole carbon source, and as expected, growth was independent of *xutA* (Fig. S3.6A). Next, we compared activities of the P_A promoter in response to xylulose between wild type and the Δ*xutR* mutant. Results shown in Figure S3.6B showed that xylulose is capable of inducing P_A activation and indeed, induction was dependent on XutR. Finally, we measured the xylose-induced P_A-*lacZ* expression in the *xutA* deletion background (Δ*xutA*). Contrary to our expectation, significant xylose-induced P_A-*lacZ* expression was observed in the Δ*xutA* mutant (Fig. S3.6C). The expression level was significantly higher in Δ*xutA* mutant than in wild type, likely due to relatively higher levels of intracellular xylose accumulated as a result of *xutA* deletion. Together, the data led us to conclude that both xylose and xylulose can directly activate XutR-mediated expression of the *xutAFGH* operon.

After elucidating the substrate specificity of XutR and MtlR in response to xylose, xylulose and mannitol, we extended our investigation to three other structurally similar carbon substrates

(fructose, sorbitol and ribose). The growth phenotypes of SBW25 and its derived mutants on these six carbon sources were also examined. The results are summarized in Figure S3.7 and Table 3.2, respectively. Deletion of *mtlZ* caused no growth on fructose and sorbitol (Table 3.2), which is consistent with the predicted role of MtlZ in the breakdown of sorbitol and fructose (Fig. 3.1C). However, both deletion analysis and assays for P_E promoter activity indicate that MtlR plays no role in bacterial utilization of sorbitol or fructose (Table 3.2, Fig. S3.7). Although sorbitol was able to activate P_E promoter, activation was independent of MtlR, indicating involvement of a yet-unidentified regulator (Fig. S3.7). It is interesting to note that ribose was capable of inducing expression of the *xutAFGH* operon; just like xylose and xylulose, induction was also dependent on XutR. However, the Δ*xutA* mutant and the Δ*xutFGH* mutant grew normally on ribose (Table 3.2). The SBW25 genome contains the *rbs* genes for ribose utilization (Fig. 3.1C). Deletion of *rbsK* resulted in no growth on ribose (Table 3.2). Expression of a chromosomally integrated *rbsK-lacZ* fusion was induced by ribose only (Fig. S3.8). Therefore, XutR plays no detectable role in ribose utilization despite its responsiveness to this sugar. Together, our data indicate complex overlapping responses to these structurally similar carbon substrates.

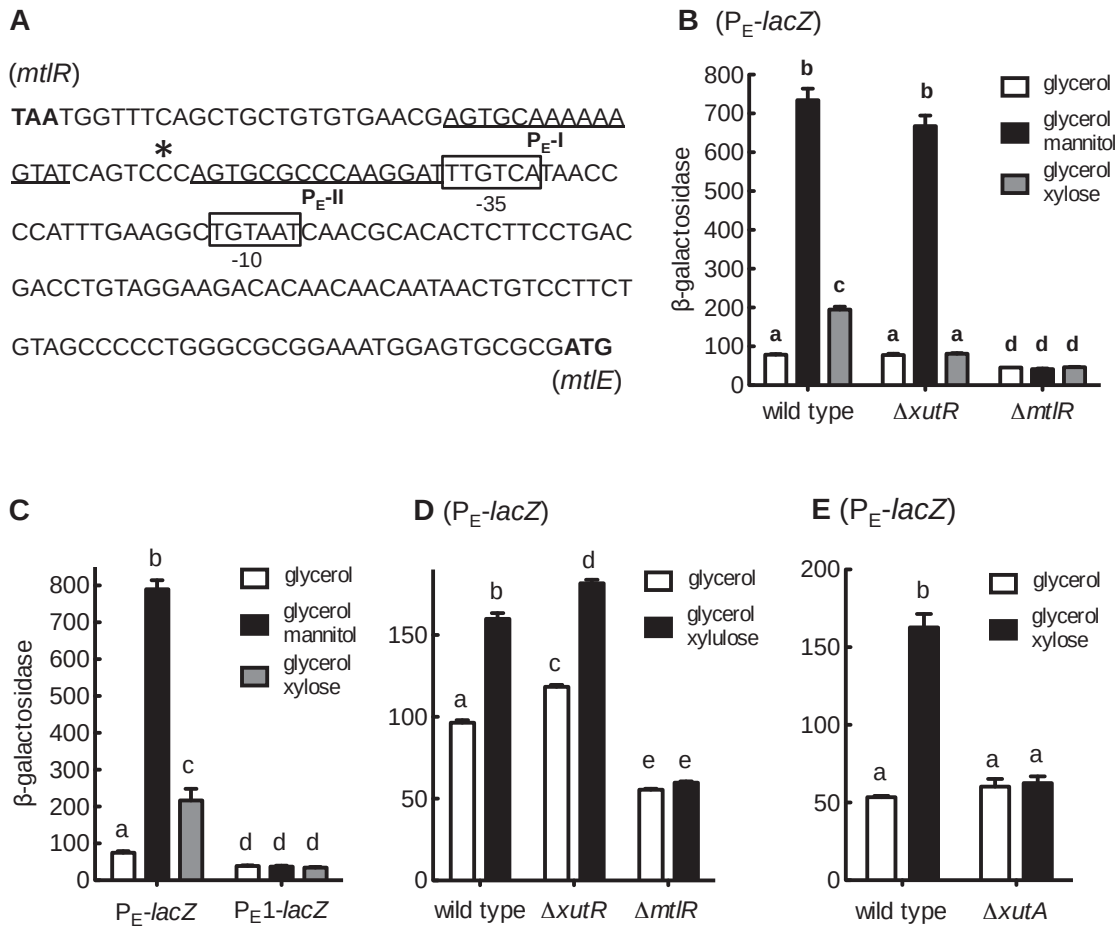

Figure 3.8. Genetic characterization of the P_E promoter and regulatory roles of XutR and MtlR. **(A)** DNA sequence of the intergenic region between the stop codon of *mtlR* and the first codon of *mtlE*. The two direct repeats (P_E-I and P_E-II) required for P_E promoter activity are highlighted with underlined letters, and the predicted -10 and -35 elements are boxed. The asterisk denotes 5'-end of the P_E1 promoter variant. **(B)** Expression of the P_E-*lacZ* fusion in wild-type SBW25 and its derived Δ*xutR* and Δ*mtlR* mutants in response to mannitol and xylose. **(C)** Promoter activities of P_E and a P_E variant (P_E1) lacking the P_E-I element in wild-type SBW25. **(D)** Responses of the P_E-*lacZ* fusion to the presence of xylulose in the genetic background wild type, Δ*xutR* and Δ*mtlR*. **(E)** Effects of *xutA* deletion on xylose-induced expression of P_E-*lacZ* fusions. Data are means and standard errors of three independent cultures. Bars that are not connected by the same letter (shown above each) are significantly different ($P < 0.05$) by Tukey's HSD test.

Table 3.2. Growth phenotypes of *P. fluorescens* SBW25 and its derived mutants on xylose and five other related sugars as the sole source of carbon and energy

Strain	Genotype	Xylose	Xylulose	Mannitol	Sorbitol	Fructose	Ribose
SBW25	Wild type	++	++	++	++	++	++
MU47-1	Δ*xutA*	-	++	++	++	++	++
MU47-2	Δ*xutR*	-	N/T	++	++	++	++
MU47-3	Δ*xutFGH*	+	N/T	++	++	++	++
MU47-4	Δ*xutB1*	+	+	++	++	+	++
MU47-5	Δ*xutB2*	+	N/T	++	++	++	++
MU47-6	Δ*xutB1* Δ*xutB2*	+	N/T	++	++	+	++
MU47-7	Δ*mtlR*::Km^r	+	N/T	-	++	++	++
MU47-8	Δ*mtlZ*::Km^r	++	N/T	-	-	-	++
MU47-9	Δ*xutB1* Δ*mtlZ*::Km^r	+	N/T	-	-	-	++
MU47-10	Δ*rbsK*::Km^r	++	N/T	++	++	++	-

a. Substrate utilization ability was measured in minimal salt medium supplemented with the related carbon substrate at the final concentration of 20 mM. ++ and – denote the ability of growth (OD_{600} > 0.4) and non-growth (OD_{600} < 0.2) after incubation at 28^{o}C for 48 hrs. + Indicates a reduced growth (OD_{600}, 0.2 - 0.4). N/T stands for "not tested".

3.3.9 The ecological significance of xylose utilization for bacterial colonization *in planta*

Finally, we took advantage of the Xut$^-$ mutant constructed in this work and asked whether xylose plays a significant role in bacterial colonization *in planta*. To do this we examined the ability of mutant MU47-1 (Δ*xutA*, Xut$^-$) to colonize sugar beet seedlings while in direct competition with the wild-type strain. Briefly, the Δ*xutA* mutant was mixed 1:1 with a *lacZ*-marked strain of SBW25 and the mixed bacteria were inoculated to sugar beet seeds. Two weeks after inoculation, bacteria recovered from the shoot and rhizosphere were enumerated on M9 plates containing X-Gal. Fitness of the mutant relative to the wild-type competitor was expressed as the selection rate constant (SRC), resulting in a fitness value of zero when the two strains were equally fit (Zhang & Rainey, 2007b). Results show that the calculated SRC values are -0.36 ± 0.1 in the shoot and -0.26 ± 0.14 in the rhizosphere, which are significantly different from zero ($P < 0.05$). Thus, the data indicate that the Δ*xutA* mutant is less competitive than the wild-type strain both in the shoot and the rhizosphere.

3.4 Discussion

In the present study, we characterized the catabolic genes and their regulators that are involved in the utilization of xylose in *P. fluorescens* SBW25. Our data revealed significant roles of two regulatory proteins XutR and MtlR; both are AraC-type activators and possesses a characteristic 100-residue region with two helix-turn-helix (HTH) DNA-binding motifs (Gallegos et al., 1997). Proteins in the AraC family can be categorised into three major functional groups, which are involved in the regulation of cellular carbon catabolism, stress response and pathogenicity respectively. The AraC-type stress response regulators such as Rob, MarA and SoxS function as monomers, and the two HTH motifs interact with a ~20 bp DNA region, which is composed of two major groves separated by one minor groove (Rhee *et al.*, 1998, Kwon *et al.*, 2000). In contrast, the AraC-type regulators of catabolic genes typically form a dimer (Gallegos et al., 1997). Dimerization permits the insertion of four HTH motifs onto the targeting DNA, which is believed to further enhance DNA-binding specificity (Ni et al., 2013). The *E. coli* AraC and XylR are the two well-studied examples of AraC-type activators in this functional category, and they are involved in the utilization of arabinose and xylose, respectively.

DNA looping plays an important role in the function of both activators for different physiological reasons. Schleif and colleagues proposed a light-switch mechanism for AraC, whereby DNA looping is involved to prevent expression of *ara* genes in the absence of arabinose (Seabold & Schleif, 1998, Schleif, 2003). In the case of the XylR regulator, DNA looping permits the simultaneous activation of two divergently organised ~37bp promoters consisting of two direct repeat sequences, each of which is responsible for transcription of *xylAB* and *xylFGH* (Song & Park, 1998, Song & Park, 1997, Ni et al., 2013).

In this work, we defined a new model of XutR activation in *Pseudomonas*. Although there are two divergent promoters located in the intergenic region between *xutR* and *xutAFGH* operons, only the P_A promoter is subject to XutR-mediated regulation. XutR forms a dimer and each monomer recognizes one of the two inverted repeat sequences at the operator site (P_A-I and P_A-II). However, XutR-binding to the P_A-II element is very weak, and requires effector molecules such as xylose for activation. Importantly, a similar mechanism likely applies to other AraC-type activators. For example, our work shows that the *P. fluorescens* SBW25 MtlR regulator recognizes two direct repeats, and no evidence suggests that DNA-looping is involved in MtlR-mediated regulation.

It is not uncommon for the first intermediate of a catabolic pathway to act as the physiological inducer that directly interacts with the regulatory protein. For example, the LacI repressor uses allolactose (as opposed to lactose) as the direct inducer of *lac* genes (Wheatley *et al.*, 2013). Similarly, urocanate but not histidine is the direct inducer of the HutC repressor, which mediates the expression of *hut* genes for the utilization of histidine and urocanate (Zhang & Rainey, 2007a). One advantage of such a regulatory organization is that it allows a set of catabolic genes to be shared for utilization of two related substrates, i.e. histidine and urocanate in the case of HutC (Zhang *et al.*, 2014b). In this work, we found that SBW25 is capable of growing on both xylose and xylulose as the sole source of carbon, and moreover, XutR is required for xylose- and xylulose-induced expression of *xutAFGH*. Although *xutA* is not required for xylulose utilization, the XutFGH transport system is partially responsible for the uptake of xylulose (Table 3.2). These initial findings led us to hypothesize that xylulose rather than xylose is the direct inducer molecule of XutR, similarly for the lacI and HutC regulators. However, our results have shown that both xylose and xylulose act as the direct inducer molecules of XutR. This represents an alternative strategy to enable the same set of catabolic genes for the utilization of a nutritional substrate and its derivatives.

XutR and MtlR display a similar domain structure and their activities are modulated by the related ligand-binding domains at the N-terminus. An interesting finding from this work is that XutR and MtlR have different substrate specificities but share a similar response to xylulose. Our transcriptional data clearly show that XutR can recognize three carbon substrates (xylose, xylulose and ribose), whereas MtlR is activated by mannitol and xylulose. Strikingly, XutR plays no apparent role in ribose utilization (Fig. S3.7), and ribose utilization (*rbs*) genes are subject to regulation by RbsR in response to ribose only (Fig. S3.8). RbsR is a repressor protein with a N-terminal HTH DNA-binding domain and a C-terminal ligand-binding domain (Mauzy & Hermodson, 1992). An overlapping response between xylose and ribose was previously reported in *E. coli* (Song & Park, 1998). The xylose-specific transporter XylFGH conferred the ability of mutant defective in the high-affinity ribose transporter (RbsABC) to grow on ribose. If the XutFGH system in *Pseudomonas* plays a similar role in ribose uptake, this may explain the responsiveness of XutR to ribose. Nevertheless, a future comparative structural analysis of XutR, MtlR and RbsR will provide insights into the mechanisms that determine the substrate specificities of these regulatory proteins.

Growth on xylose is an important feature for the classification of bacterial species belonging to the genus of *Pseudomonas* (Palleroni, 2005). Currently, there are a total of 46 genome sequences deposited in the *Pseudomonas* Genome Database (http://www.pseudomonas.com). Searching the functionally identified XutA sequence of *P. fluorescens* SBW25 indicate a clear pattern of phylogenetic distribution of xylose utilization among different species of *Pseudomonas* (Table S3.2). None of the 13 *P. aeruginosa* strains and 11 *P. putida* strains harbour a XutA homologue, suggesting that they are not able to use xylose. *P. aeruginosa* consists of opportunistic pathogens for humans and animals, whereas *P. putida* strains are commonly found in the soil. All the plant-associated *P. fluorescens* and *P. syringae* strains possess XutA. It is interesting to note that, in *P. syringae* pv. *phaseolicola* 1448A, the predicted xylose transporter gene (*xutF*) harbours several nonsense mutations. This suggests that this plant pathogenic bacterium has lost the capability of growing on xylose, as well as many other catabolic pathways as previously revealed (Rico & Preston, 2008). Significantly, for all *Pseudomonas* strains that can potentially grow on xylose, the *xutR* and *xutAFGH* genes are organized in the same order as in *P. fluorescens* SBW25, with no specific xylulokinase-like gene at the *xut* locus. This suggests that plant-associated *Pseudomonas* may have acquired the xylose utilization genes by horizontal gene transfer and lost the xylulokinase-encoding gene owing to intrinsic xylulokinase activities from other catabolic pathways.

Xylose exists in monomers in various natural environments, such as soil and the digestive tract of higher animals (Shallom & Shoham, 2003). Naturally occurring monomeric xylose is derived from the enzymatic hydrolysis of xylan, and the reactions are catalysed by xylanases, a group of extracellular hydrolytic enzymes produced by microorganisms (bacteria and fungi) (Juturu & Wu, 2014, Uffen, 1997). Therefore, xylanase-producing microflora play crucial roles in the decomposition of plant residues in the soil, and also in the process of nutrient extraction from dietary fibre for mammals (Hong *et al.*, 2014, Wang *et al.*, 2010, Zhang *et al.*, 2014a). The resultant xylose monosaccharide is water-soluble. It can be taken up and metabolized by many microbial species as a source of carbon and energy (Palleroni, 2005, Desai & Rao, 2010, Lokman *et al.*, 1991, Dahl et al., 1994). However, little is known about the sources and biological significance of monomeric xylose on the surfaces of living plant tissues.

In the present study, we showed that *P. fluorescens* mutants defective in xylose utilization was compromised in competitive colonization of sugar beet seedlings. This result supports findings from previous studies that xylose is a main constituent of root exudates and it can potentially

serve as a valuable nutrient for plant colonising microflora. Of particular note is that Lugtenberg and colleagues quantitatively analyzed the chemical composition of seed, seedling and root exudates in three crops (tomato, cucumber and sweet pepper). Results of high-performance liquid chromatography (HPLC) analysis consistently showed that xylose was one of the major sugars present in the exudates; and moreover, the relative abundance of xylose to other plant-derived sugars varied greatly at different stages of the early plant development (Kamilova *et al.*, 2006, Lugtenberg *et al.*, 1999). Significantly, when plants were grown in stone wool, xylose comprised nearly half (45.8%) of the total sugar in the exudates of tomato seedlings (Kamilova et al., 2006). Interestingly, xylose was also identified in the nectar of *Protea* and *Faurea* (two closely related genera commonly found in Africa), and represented 1 – 39% of the total nectar sugars by weight (Nicolson & Van Wyk, 1998). While there is abundant evidence for surface accumulation of xylose *in planta*, the underlying physiological reasons remain generally unknown. Some plant pathogens carry xylanase-encoding genes (Buttner & Bonas, 2010), but it seems very unlikely that xylose accumulation is caused by xylanase produced by plant colonizing microbes. In the case of nectar sugar, plants may have evolved to secret xylose as a mechanism to alter the behavior of insect or bird pollinators (Jackson & Nicolson, 2002).

Finally, it should be noted that xylose can only support slow bacterial growth, and thus, it is not the sugar of choice in the presence of other preferred carbon and energy sources such as succinate, glucose and arabinose. The means of discernment depends on carbon catabolite repression (CCR). CCR has been well studied in *E. coli*, where it is mainly mediated by the catabolite-activation protein CAP charged with cAMP (Görke & Stülke, 2008), but it still remains elusive for non-enteric bacteria such as *Pseudomonas* (Rojo, 2010). Our work on *xut* genes and their regulation has establish a foundation for further investigation into the mechanism of CCR on xylose utilization, which occurs at the post-transcriptional level under the control of the previously identified two-component signal transduction system CbrAB (Zhang *et al.*, 2010). Details of CCR regulation of the *xut* genes in *P. fluorescens* SBW25 will be published separately.

In conclusion, data presented here show that xylose utilization is an important trait for *P. fluorescens* SBW25 and *xut* genes contribute to the competitiveness of this bacterium in the plant environments; moreover, our results of genetic and biochemical analysis have revealed novel mechanisms of xylose utilization in terms of not only the metabolic genes but also the modes of regulation. Although xylose is broken down through the two-enzyme pathway established in bacteria, SBW25 does not carry a xylulokinase gene specific for xylose utilization. We have

functionally identified two xylulokinase-encoding genes *xutB1* and *xutB2*. Both contribute to bacterial growth on xylose, but their primary roles are the utilization of mannitol, arabitol and some other as-yet-unknown carbon substrates. Intriguingly, expression of *xutB1* is induced by xylose, but the induction is mediated by the mannitol-responsive activator MtlR with xylulose as the inducing molecule. Xylulose is a common intermediate of catabolic pathways for xylose and arabitol, and it can also be present in natural environments as SBW25 is capable of growth on xylulose as the sole source of carbon and nitrogen. Our data indicate a complex overlapping cellular responses to xylose and other structurally similar sugars such as manitol, sorbitol, fructose as well as ribose. With respect to regulation of xylose utilization genes, we have showed that the xylose catabolism of *P. fluorescens* SBW25 is controlled by two AraC-type activators (XutR and MtlR) instead of only one in other bacteria, such as XylR in *E. coli*. The molecular data presented here allow us to propose an unconventional mechanism of XutR action that does not involve DNA-looping.

3.5 Experimental procedures

3.5.1 Bacterial strains and growth conditions

The *E. coli* strain DH5αλ_{pir} was routinely used for gene cloning and conjugation into *P. fluorescens*. For cloning PCR products, the One Shot Top10 chemical competent cells were used in conjunction with the pCR8/GW/TOPO vector purchased from Invitrogen (Auckland). Other bacterial strains used in this work are listed in Table 3.1. *P. fluorescens* and *E. coli* strains were grown in Luria-Bertani (LB) medium at 28°C and 37°C, respectively. When *P. fluorescens* was grown in the minimal M9 salt medium (Sambrook *et al.*, 1989), each carbon source was supplemented at the final concentration of 20 mM except where indicated. Xylose and all other sugars involved in this work were D-isomers, which were of analytical grade, purchased from Sigma-Aldrich. When necessary, antibiotics were added at the following final concentrations (μg ml^{-1}): tetracycline (Tc), 10; ampicillin (Ap), 100; spectinomycin (Sp), 100; kanamycin (Km), 50, gentamycin (Gm), 25; and nitrofurantoin, 100. Growth kinetics of *P. fluorescens* SBW25 and its derived mutants were assessed in a 96-well plate using a Synergy 2 plate reader equipped with the Gen5 software (BioTek Instruments). Inoculant cells were prepared as previously described (Zhang & Rainey, 2007a), and absorbance at wavelength of 450 nm was determined every 5 min over a period of either 48 or 72 hrs.

Table 3.1. Bacterial strains and plasmids used in this work

Strain or plasmid	Genotypes and relevant characteristics	Reference
P. fluorescens		
SBW25	Wild-type strain isolated from phyllosphere of sugar beet	Bailey *et al.* (1995)
MU47-1	Δ*xutA*, SBW25 devoid of *pflu2301*	This work
MU47-2	Δ*xutR*, SBW25 devoid of *pflu2302*	This work
MU47-3	Δ*xutFGH*, SBW25 with deletion of the *pflu2298* - *pflu2300* DNA region	This work
MU47-4	Δ*xutB1*, SBW25 with deletion *pflu2740*	This work
MU47-5	Δ*xutB2*, SBW25 with deletion *pflu3115*	This work
MU47-6	Δ*xutB1* Δ*xutB2*, SBW25 with deletion *pflu2740* and *pflu3115*	This work
MU47-7	*ΔmtlR*::Km^r, SBW25 with *pflu2746* being replaced with a Km^r cassette from pUC4K	This work
MU47-8	*ΔmtlZ*::Km^r, SBW25 with *pflu2739* being replaced with a Km^r cassette from pUC4K	This work
MU47-9	Δ*xutB1* Δ*mtlZ*::Km^r, derived from MU47-4 with *pflu2739* being replaced with a Km^r cassette from pUC4K	This work
MU47-10	*ΔrbsK*::Km^r, SBW25 with *pflu4156* being replaced with a Km^r cassette from pUC4K	This work
Plasmid		
pCR8/GW/TOPO	Cloning vector, Sp^r	Invitrogen
pUC4K	Donor of Km^r gene cassette, Km^r, Ap^r	Taylor and Rose (1988)
pRK2013	Helper plasmid, Tra^+, Km^r	Ditta *et al.* (1980)
pUC18-mini-Tn7T-LAC	Mini-Tn7 vector, Ap^r, Gm^r	Choi *et al.* (2005)
pUC18-mini-Tn7T-Gm-*lacZ*	Mini-Tn7 vector for transcriptional fusion to promoterless *lacZ*, Ap^r, Gm^r	Choi *et al.* (2005)
pUX-BF13	Helper plasmid for transposition of mini-Tn7 element, Ap^r	Bao *et al.* (1991)
pXY6-*xutR*	pUC18-mini-Tn7T-LAC containing *xutR* for complementation	This work
pXY6-*xutA*	pUC18-mini-Tn7T-LAC containing *xutA* for complementation	This work
pXY7-P_R	pUC18-mini-Tn7T-*lacZ* containing *lacZ* fusion to P_R promoter for *xutR*	This work
pXY7-P_A	pUC18-mini-Tn7T-*lacZ* containing *lacZ* fusion to P_A promoter for *xutA* (-416 to +48)	This work
pXY7-P_A1	pUC18-mini-Tn7T-*lacZ* containing *lacZ* fusion to P_A1 (-215 to +48)	This work
pXY7-P_A2	pUC18-mini-Tn7T-*lacZ* containing *lacZ* fusion to P_A1 (-129 to +48)	This work
pXY7-P_A3	pUC18-mini-Tn7T-*lacZ* containing *lacZ* fusion to P_A1 (-79 to +48)	This work

pXY7-P_A4	pUC18-mini-Tn7T-*lacZ* containing *lacZ* fusion to P_A1 (-61 to +48)	This work
pXY7-P_A1-1	pUC18-mini-Tn7T-*lacZ* containing *lacZ* fusion to P_A1-1, a derivative of P_A1 without the P_A-I half-site	This work
pXY7-P_A1-2	pUC18-mini-Tn7T-*lacZ* containing *lacZ* fusion to P_A1-2, a derivative of P_A1 without the P_A-II half-site	This work
pXY7-P_E	pUC18-mini-Tn7T-*lacZ* containing a 227-bp P_E promoter region fused to *lacZ* reporter.	This work
pXY7-P_E1	pUC18-mini-Tn7T-*lacZ* containing a 151-bp P_E promoter region fused to *lacZ* reporter.	This work
pXY7-P_{xutF}	pUC18-mini-Tn7T-*lacZ* containing *lacZ* fusion to putative promoter for *xutFGH*	This work
pXY7-P_{xutB1}	pUC18-mini-Tn7T-*lacZ* containing *lacZ* fusion to a 473 bp DNA fragment preceding *xutB1*	This work
pCR8-mtlR::Km	Recombinant plasmid for the deletion of *mtlR*	This work
pCR8-mtlZ::Km	Recombinant plasmid for the deletion of *mtlZ*	This work
pCR8-rbsK::Km	Recombinant plasmid for the deletion of *rbsK*	This work
pUIC3	Suicide vector with promoterless '*lacZ*, Mob^+, Tc^r	Rainey (1999)
pUIC3-148	pUIC3 containing *xutF-lacZ* fusion, Tc^r	This work
pUIC3-149	pUIC3 containing *xutB1-lacZ* fusion, Tc^r	This work
pUIC3-150	pUIC3 containing *xutB2-lacZ* fusion, Tc^r	This work
pUIC3-151	pUIC3 containing *rbsK-lacZ* fusion, Tc^r	This work
pTrc99A	Protein expression vector, P_{tac} promoter, Ap^r	Amann *et al.* (1988)
pTrc99A-*xutR*	pTrc99A carrying $XutR_{His6}$, Ap^r	This work

3.5.2 Recombinant DNA techniques

Standard protocols were used for the preparation of plasmid DNAs, restriction endonuclease digestion and ligation (Sambrook et al., 1989). PCR was performed using DNA polymerase from Invitrogen (Auckland, New Zealand). A summary of oligonucleotide primers used in this work is provided in Table S3.2. For the purpose of gene cloning from the genomic DNA of *P. fluorescens* SBW25, PCR product was first cloned into pCR8/GW/TOPO by using the TA cloning kit from Invitrogen (Auckland), and then subjected to DNA sequencing (Macrogen Inc., South Korea). Next, the error-free DNA fragments were subcloned into another destination vector such as pUIC3 or directly integrated into the chromosome of SBW25 through electroporation.

3.5.3 Strains construction

Site-directed mutagenesis of *xut* genes was performed using a combination of SOE-PCR (splicing by overlapping extension using the polymerase chain reaction, (Horton *et al.*, 1989)) and a two-step allelic-exchange strategy with the suicide-integration vector pUIC3 as previously described (Zhang & Rainey, 2007a). Briefly, two pairs of primers were designed to amplify two DNA fragments of similar length (~1.0 Kb) that flank the gene to be deleted. The resultant PCR products were then gel-purified and used as the DNA templates in the second round of PCR whereby the two DNA fragments were joined together. Next, pUIC3 plasmid carrying DNA fragment with the desired mutation was mobilized into *P. fluorescens* through conjugation with the help of pRK2013. Integration of the recombinant plasmid into chromosome was selected on LB agar plates supplemented with nitrofurantoin (to counter select *E. coli*) and tetracycline. Allelic exchange mutants were selected following a previously described procedure of D-cycloserine enrichment (Zhang & Rainey, 2007a).

Deletion of *mtl* and *rbs* genes was achieved by replacing the deleted region with a kanamycin-resistant cassette derived from pUC4K (Taylor & Rose, 1988). Similarly as above, gene deletion fragment obtained by SOE-PCR was cloned into pCR8/GW/TOPO. The DNA insert contains a *Bam*H1 restriction site in the middle, which allows insertion of the 1.0 kb BglII fragment of kanamycin resistance. The resultant recombinant plasmid was then introduced into *P. fluorescens* by electroporation. Allelic exchange mutants, which are Km^R and Sp^S, were directly selected on LB agar plates supplemented with kanamycin followed by replica plating on agar plates containing 200 μg ml^{-1} of spectinomycin. All gene deletion mutants have been subjected to PCR verification using appropriate primers.

Two plasmid vectors (pUIC3 and pUC18-mini-Tn7T-Gm-*lacZ*) were used for the construction of transcriptional fusions to the promoterless *lacZ* reporter gene. The pUIC3 fusion plasmids were introduced into *P. fluorescens* through conjugation with the help of pRK2013, and the *lacZ* gene was integrated into the chromosome via homologous recombination of the cloned DNA fragment. Thus, the resultant fusion strains are suitable for monitoring gene transcription *in situ*. In the contrast, *lacZ* reporter fusions cloned in pUC18-mini-Tn7T-Gm-*lacZ* were integrated into a separate site located downstream of *glmS* (Liu et al., 2014). Consequently, they were used for studying functionalities of the promoter cloned into the mini-Tn7 element. Gene

complementation was performed using the mini-Tn7 vector pUC18-mini-TnT7-LAC, which contains an IPTG-inducible P_{tac} promoter (Choi *et al.*, 2005).

3.5.4 Assays for β-galactosidase and plant colonization

β-Galactosidase activity was measured using bacterial cells grown in minimal medium 6 hrs after the inoculation except where indicated. The assay was performed a using a standard protocol with 4-methylumbelliferyl-β-D- galactoside (4MUG) as the enzymatic substrate. The fluorescent product, 7-hydroxy-4-methylcoumarin (4MU), was detected at 460 nm after excision at 365 nm using a Synergy 2 plate reader (BioTek Instruments). *β*-Galactosidase activity was calculated as the amount of 4MU (μM) produced per minute and per cell (OD_{600}). Competitive plant colonization was performed using the neutrally-marked strain of SBW25-lacZ according to the previously described protocol (Zhang & Rainey, 2007b).

3.5.5 Rapid amplification of cDNA 5'-ends

The 5'-RACE system purchased from Invitrogen (Auckland, New Zealand) was used to determine the transcriptional start sites of the *xut* operons. *P. fluorescens* SBW25 was grown in minimal medium with xylose as the sole carbon source, and cells at late log phase were harvested for total RNA preparation using TRIzol® Max™ bacterial RNA isolation kit (Invitrogen). Following the manufacturer's recommendation, three nested primers were designed to synthesize the specific cDNA fragments (Table S3.2). The final 5'-RACE products were gel-purified and cloned into pCR8/GW/TOPO (Invitrogen). At least 6 clones were subjected to DNA sequencing for each promoter.

3.5.6 Electrophoretic mobility shift assays

The coding region of XutR was amplified by PCR from the genomic DNA of SBW25 and was subsequently cloned into the protein expression vector pTrc99A (Amann *et al.*, 1988). The forward primer was designed to allow an integration of six histidine residues at the N-terminal (Table S3.2). The recombinant plasmid pTrc99A-*xutR* was then transformed into *E. coli* BL21(DE3). To induce expression of $XutR_{His6}$, IPTG was added at the final concentration of 1 mM to *E. coli* culture at min-log phase (OD600, ~0.6), which was further incubated overnight at

25°C. Cells were harvested and lysed by sonication using the Sonicator S-4000 (Misonix, Inc) in a buffer containing 20 mM HEPES pH 7.5, 500 mM NaCl and 10 mM imidazole. Next, the His6-tagged XutR was purified by using the TALON metal affinity resin (Clontech Laboratories Inc.) according to the manufacturer's protocol. Concentration of the purified $XutR_{His6}$ was determined by the Bradford method (Bradford, 1976).

DNA probes for EMSA analysis was prepared by PCR with a biotin-labelled primer xutA-DNaseF1 (Table S3.2). The protein and DNA interaction was then assessed using 0.1 μM of probe and varying concentrations of $XutR_{His6}$ ranging from zero to 500 nM, in reactions of 20 μl containing 20 mM HEPES (pH 7.5), 50 mM KCl, 1 mM DTT and 1 μg poly(dI-dC)). After incubation at room temperature for 30 min, the DNA probes were separated through a 7% nondenaturing polyacrylamide gel in 0.5X TBE buffer at 4°C (Sambrook et al., 1989). Next, the DNA in gel was transferred by electroblotting to positively charged Whatman® Nytran™ SuPerCharge nylon membranes (Sigma-Aldrich Co.), and were subsequently immobilized by baking the membrane at 80°C for 30 min. Finally, the biotin-labelled DNA was detected using the Pierce's LightShift™ chemiluminescent EMSA kit purchased from Thermo Fisher Scientific Inc. (Auckland) and the image was visualized using the Luminescent Image Analyzer LAS-4000 system equipped with the Image Reader LAS-4000 software (Fujifilm).

3.5.7 DNase I footprinting

$XutR_{His6}$ binding with the same biotin-labelled DNA probe was performed under the same condition described for EMSA but in a larger volume of 50 μl. Each reaction was mixed with 50 μl cofactor solution (5 mM $CaCl_2$ and 10 mM $MgCl_2$), and then treated with 0.03 unit of DNase I (Invitrogen) for 5 min at room temperature. After the reaction was stopped with 100 μl of stop buffer (200 mM NaCl, 20 mM EDTA and 1% SDS), DNA was extracted with an equal volume of phenol:chloroform (1:1) and precipitated with of 1 μl of glycogen (20 mg/ml, Fermentas), 1/10th volume of 3 M sodium acetate (pH 5.2) and three volumes of absolute ethanol at -20ºC for at least 1 hour. Precipitated DNA was collected by centrifugation and then dissolved with 8 μl of loading buffer (95% formamide, 0.05% bromophenol blue and 20 mM EDTA). After denaturing at 95ºC for 10 minutes the DNA samples were subject to electrophoresis with a 5% denaturing urea-polyacrylamide gel (21 x 40 cm) using the Sequi-Gen GT electrophoresis system (Bio-Rad Laboratories Pty Ltd). The DNA in gel was then transferred to nylon membrane using the classic

method of contact blotting (Petersen *et al.*, 1996), and detected using the similar methods described above in EMSA analysis. A DNA sequence ladder obtained by the G+A chemical sequencing reaction with the same biotin-labelled probe was included in the gel to help determine the protein-protected DNA region (Maxam & Gilbert, 1980).

3.6 Acknowledgements

We thank Honour McCann for critical reading of the manuscript.

3.7 References

Amann, E., B. Ochs & K. J. Abel, (1988) Tightly regulated tac promoter vectors useful for the expression of unfused and fused proteins in *Escherichia coli*. *Gene* **69**: 301-315.

Bading, H., (1988) Determination of the molecular weight of DNA-bound protein(s) responsible for gel electrophoretic mobility shift of linear DNA fragments examplified with purified viral myb protein. *Nucleic acids research* **16**: 5241-5248.

Bailey, M. J., A. K. Lilley, I. P. Thompson, P. B. Rainey & R. J. Ellis, (1995) Site directed chromosomal marking of a fluorescent pseudomonad isolated from the phytosphere of sugar beet; stability and potential for marker gene transfer. *Mol Ecol* **4**: 755-763.

Beg, Q. K., M. Kapoor, L. Mahajan & G. S. Hoondal, (2001) Microbial xylanases and their industrial applications: a review. *Appl Microbiol Biotechnol* **56**: 326-338.

Bhuvaneswari, K. & N. S. Subba-Rao, (1959) Root excretions in relation to the rhizosphere effect. *Plant Soil* **11**: 53-64.

Binder, J. B., J. J. Blank, A. V. Cefali & R. T. Raines, (2010) Synthesis of furfural from xylose and xylan. *ChemSusChem* **3**: 1268-1272.

Bradford, M. M., (1976) A rapid and sensitive method for the quantitation of microgram quantities of protein utilizing the principle of protein-dye binding. *Analytical biochemistry* **72**: 248-254.

Brunker, P., J. Altenbuchner & R. Mattes, (1998) Structure and function of the genes involved in mannitol, arabitol and glucitol utilization from *Pseudomonas fluorescens* DSM50106. *Gene* **206**: 117-126.

Buttner, D. & U. Bonas, (2010) Regulation and secretion of *Xanthomonas* virulence factors. *FEMS Microbiol Rev* **34**: 107-133.

Choi, K. H., J. B. Gaynor, K. G. White, C. Lopez, C. M. Bosio, R. R. Karkhoff-Schweizer & H. P. Schweizer, (2005) A Tn7-based broad-range bacterial cloning and expression system. *Nature methods* **2**: 443-448.

Dahl, M. K., J. Degenkolb & W. Hillen, (1994) Transcription of the xyl operon is controlled in *Bacillus subtilis* by tandem overlapping operators spaced by four base-pairs. *Journal of molecular biology* **243**: 413-424.

Dakora, F. D. & D. A. Phillips, (2002) Root exudates as mediators of mineral acquisition in low-nutrient environments. *Plant Soil* **245**: 35-47.

de Las Heras, A., S. Fraile & V. de Lorenzo, (2012) Increasing signal specificity of the TOL network of *Pseudomonas putida* mt-2 by rewiring the connectivity of the master regulator XylR. *PLoS Genet* **8**: e1002963.

Desai, T. A. & C. V. Rao, (2010) Regulation of arabinose and xylose metabolism in *Escherichia coli*. *Applied and environmental microbiology* **76**: 1524-1532.

Ellis, R. J., T. M. Timms-Wilson & M. J. Bailey, (2000) Identification of conserved traits in fluorescent pseudomonads with antifungal activity. *Environ Microbiol* **2**: 274-284.

Gal, M., G. M. Preston, R. C. Massey, A. J. Spiers & P. B. Rainey, (2003) Genes encoding a cellulosic polymer contribute toward the ecological success of *Pseudomonas fluorescens* SBW25 on plant surfaces. *Molecular ecology* **12**: 3109-3121.

Gallegos, M. T., R. Schleif, A. Bairoch, K. Hofmann & J. L. Ramos, (1997) Arac/XylS family of transcriptional regulators. *Microbiology and molecular biology reviews : MMBR* **61**: 393-410.

Gärtner, D., J. Degenkolb, J. A. Ripperger, R. Allmansberger & W. Hillen, (1992) Regulation of the *Bacillus subtilis* W23 xylose utilization operon: interaction of the Xyl repressor with the xyl operator and the inducer xylose. *Molecular & general genetics : MGG* **232**: 415-422.

Giddens, S. R., R. W. Jackson, C. D. Moon, M. A. Jacobs, X. X. Zhang, S. M. Gehrig & P. B. Rainey, (2007) Mutational activation of niche-specific genes provides insight into regulatory networks and bacterial function in a complex environment. *Proceedings of the National Academy of Sciences of the United States of America* **104**: 18247-18252.

Görke, B. & J. Stülke, (2008) Carbon catabolite repression in bacteria: many ways to make the most out of nutrients. *Nature reviews. Microbiology* **6**: 613-624.

Hasona, A., Y. Kim, F. G. Healy, L. O. Ingram & K. T. Shanmugam, (2004) Pyruvate formate lyase and acetate kinase are essential for anaerobic growth of *Escherichia coli* on xylose. *J Bacteriol* **186**: 7593-7600.

Hong, P. Y., M. Iakiviak, D. Dodd, M. Zhang, R. I. Mackie & I. Cann, (2014) Two new xylanases with different substrate specificities from the human gut bacterium *Bacteroides intestinalis* DSM 17393. *Appl Environ Microbiol* **80**: 2084-2093.

Horton, R. M., H. D. Hunt, S. N. Ho, J. K. Pullen & L. R. Pease, (1989) Engineering hybrid genes without the use of restriction enzymes: gene splicing by overlap extension. *Gene* **77**: 61-68.

Humphris, S. N., A. G. Bengough, B. S. Griffiths, K. Kilham, S. Rodger, V. Stubbs, T. A. Valentine & I. M. Young, (2005) Root cap influences root colonisation by *Pseudomonas fluorescens* SBW25 on maize. *FEMS Microbiol Ecol* **54**: 123-130.

Jackson, S. & S. W. Nicolson, (2002) Xylose as a nectar sugar: from biochemistry to ecology. *Comp Biochem Physiol B Biochem Mol Biol* **131**: 613-620.

Jaderlund, L., M. Hellman, I. Sundh, M. J. Bailey & J. K. Jansson, (2008) Use of a novel nonantibiotic triple marker gene cassette to monitor high survival of *Pseudomonas fluorescens* SBW25 on winter wheat in the field. *FEMS Microbiol Ecol* **63**: 156-168.

Jeffries, T. & N.-Q. Shi, (1999) Genetic engineering for improved xylose fermentation by yeasts. In: Recent Progress in Bioconversion of Lignocellulosics. Berlin/Heidelberg: Springer, pp. 117-161.

Juturu, V. & J. C. Wu, (2014) Microbial exo-xylanases: a mini review. *Appl Biochem Biotechnol*.

Kamilova, F., L. V. Kravchenko, A. I. Shaposhnikov, T. Azarova, N. Makarova & B. Lugtenberg, (2006) Organic acids, sugars, and L-tryptophane in exudates of vegetables growing on stonewool and their effects on activities of rhizosphere bacteria. *Mol Plant Microbe Interact* **19**: 250-256.

Kwon, H. J., M. H. Bennik, B. Demple & T. Ellenberger, (2000) Crystal structure of the *Escherichia coli* Rob transcription factor in complex with DNA. *Nature structural biology* **7**: 424-430.

Lawlis, V. B., M. S. Dennis, E. Y. Chen, D. H. Smith & D. J. Henner, (1984) Cloning and sequencing of the xylose isomerase and xylulose kinase genes of *Escherichia coli*. *Applied and environmental microbiology* **47**: 15-21.

Liu, Y., P. B. Rainey & X. X. Zhang, (2014) Mini-Tn7 vectors for studying post-transcriptional gene expression in *Pseudomonas*. *J Microbiol Methods* **107**: 182-185.

Lokman, B. C., M. Heerikhuisen, R. J. Leer, A. van den Broek, Y. Borsboom, S. Chaillou, P. W. Postma & P. H. Pouwels, (1997) Regulation of expression of the *Lactobacillus pentosus xylAB* operon. *J Bacteriol* **179**: 5391-5397.

Lokman, B. C., R. J. Leer, R. van Sorge & P. H. Pouwels, (1994) Promoter analysis and transcriptional regulation of *Lactobacillus pentosus* genes involved in xylose catabolism. *Molecular & general genetics : MGG* **245**: 117-125.

Lokman, B. C., P. van Santen, J. C. Verdoes, J. Kruse, R. J. Leer, M. Posno & P. H. Pouwels, (1991) Organization and characterization of three genes involved in D-xylose catabolism in *Lactobacillus pentosus*. *Molecular & general genetics : MGG* **230**: 161-169.

Lugtenberg, B. J., L. V. Kravchenko & M. Simons, (1999) Tomato seed and root exudate sugars: composition, utilization by Pseudomonas biocontrol strains and role in rhizosphere colonization. *Environmental microbiology* **1**: 439-446.

Mauzy, C. A. & M. A. Hermodson, (1992) Structural and functional analyses of the repressor, RbsR, of the ribose operon of *Escherichia coli*. *Protein science : a publication of the Protein Society* **1**: 831-842.

Maxam, A. M. & W. Gilbert, (1980) Sequencing end-labeled DNA with base-specific chemical cleavages. *Methods Enzymol* **65**: 499-560.

Ni, L., N. K. Tonthat, N. Chinnam & M. A. Schumacher, (2013) Structures of the *Escherichia coli* transcription activator and regulator of diauxie, XylR: an AraC DNA-binding family member with a LacI/GalR ligand-binding domain. *Nucleic acids research* **41**: 1998-2008.

Nicolson, S. W. & B.-E. Van Wyk, (1998) Nectar sugars in *Proteaceae*: patterns and processes. *Aust J Bot* **46**: 489-504.

Palleroni, N. J., (2005) Genus I. *Pseudomonas*. In: Bergey's Manual of Systematic Bacteriology. D. J. Brenner, N. R. Krieg, J. T. Staley & G. M. Garrity (eds). New York: Springer, pp. 323-379.

Petersen, I., M. B. Reichel & M. Dietel, (1996) Use of non-radioactive detection in SSCP, direct DNA sequencing and LOH analysis. *Clinical molecular pathology* **49**: M118-121.

Rainey, P. B., (1999) Adaptation of *Pseudomonas fluorescens* to the plant rhizosphere. *Environmental microbiology* **1**: 243-257.

Reeder, T. & R. Schleif, (1993) AraC protein can activate transcription from only one position and when pointed in only one direction. *Journal of molecular biology* **231**: 205-218.

Rennie, E. A. & H. V. Scheller, (2014) Xylan biosynthesis. *Curr Opin Biotechnol* **26**: 100-107.

Rhee, S., R. G. Martin, J. L. Rosner & D. R. Davies, (1998) A novel DNA-binding motif in MarA: the first structure for an AraC family transcriptional activator. *Proc Natl Acad Sci U S A* **95**: 10413-10418.

Rico, A. & G. M. Preston, (2008) *Pseudomonas syringae* pv. *tomato* DC3000 uses constitutive and apoplast-induced nutrient assimilation pathways to catabolize nutrients that are abundant in the tomato apoplast. *Mol Plant Microbe Interact* **21**: 269-282.

Rojo, F., (2010) Carbon catabolite repression in *Pseudomonas* : optimizing metabolic versatility and interactions with the environment. *FEMS Microbiol Rev* **34**: 658-684.

Sambrook, J., E. F. Fritsch & T. Maniatis, (1989) *Molecular Cloning: A Laboratory Manual*. Cold Spring Harbor Laboratory Press, New York, USA.

Schleif, R., (2003) AraC protein: a love-hate relationship. *Bioessays* **25**: 274-282.

Seabold, R. R. & R. F. Schleif, (1998) Apo-AraC actively seeks to loop. *J Mol Biol* **278**: 529-538.

Shallom, D. & Y. Shoham, (2003) Microbial hemicellulases. *Current opinion in microbiology* **6**: 219-228.

Silby, M. W., A. M. Cerdeno-Tarraga, G. S. Vernikos, S. R. Giddens, R. W. Jackson, G. M. Preston, X. X. Zhang, C. D. Moon, S. M. Gehrig, S. A. Godfrey, C. G. Knight, J. G. Malone, Z. Robinson, A. J. Spiers, S. Harris, G. L. Challis, A. M. Yaxley, D. Harris, K. Seeger, L. Murphy, S. Rutter, R. Squares, M. A. Quail, E. Saunders, K. Mavromatis, T. S. Brettin, S. D. Bentley, J. Hothersall, E. Stephens, C. M. Thomas, J. Parkhill, S. B. Levy, P. B. Rainey & N. R. Thomson, (2009) Genomic and genetic analyses of diversity and plant interactions of *Pseudomonas fluorescens*. *Genome biology* **10**: R51.

Song, S. & C. Park, (1997) Organization and regulation of the D-xylose operons in *Escherichia coli* K-12: XylR acts as a transcriptional activator. *J Bacteriol* **179**: 7025-7032.

Song, S. & C. Park, (1998) Utilization of D-ribose through D-xylose transporter. *FEMS microbiology letters* **163**: 255-261.

Taylor, L. A. & R. E. Rose, (1988) A correction in the nucleotide sequence of the Tn903 kanamycin resistance determinant in pUC4K. *Nucleic acids research* **16**: 358.

Uffen, R. L., (1997) Xylan degradation: a glimpse at microbial diversity. *J. Ind. Microbiol. Biotechnol.* **19**: 1-6.

Wang, G., Y. Wang, P. Yang, H. Luo, H. Huang, P. Shi, K. Meng & B. Yao, (2010) Molecular detection and diversity of xylanase genes in alpine tundra soil. *Appl Microbiol Biotechnol* **87**: 1383-1393.

Wheatley, R. W., S. Lo, L. J. Jancewicz, M. L. Dugdale & R. E. Huber, (2013) Structural explanation for allolactose (lac operon inducer) synthesis by lacZ beta-galactosidase and the evolutionary relationship between allolactose synthesis and the lac repressor. *J Biol Chem* **288**: 12993-13005.

Wohlbach, D. J., A. Kuo, T. K. Sato, K. M. Potts, A. A. Salamov, K. M. Labutti, H. Sun, A. Clum, J. L. Pangilinan, E. A. Lindquist, S. Lucas, A. Lapidus, M. Jin, C. Gunawan, V. Balan, B. E. Dale, T. W. Jeffries, R. Zinkel, K. W. Barry, I. V. Grigoriev & A. P. Gasch, (2011) Comparative genomics of xylose-fermenting fungi for enhanced biofuel production. *Proc Natl Acad Sci U S A* **108**: 13212-13217.

Zhang, M., J. R. Chekan, D. Dodd, P. Y. Hong, L. Radlinski, V. Revindran, S. K. Nair, R. I. Mackie & I. Cann, (2014a) Xylan utilization in human gut commensal bacteria is orchestrated by unique modular organization of polysaccharide-degrading enzymes. *Proc Natl Acad Sci U S A*.

Zhang, X. X., Y. H. Liu & P. B. Rainey, (2010) CbrAB-dependent regulation of pcnB, a poly(A) polymerase gene involved in polyadenylation of RNA in *Pseudomonas fluorescens*. *Environmental microbiology* **12**: 1674-1683.

Zhang, X. X. & P. B. Rainey, (2007a) Genetic analysis of the histidine utilization (hut) genes in *Pseudomonas fluorescens* SBW25. *Genetics* **176**: 2165-2176.

Zhang, X. X. & P. B. Rainey, (2007b) Construction and validation of a neutrally-marked strain of *Pseudomonas fluorescens* SBW25. *Journal of microbiological methods* **71**: 78-81.

Zhang, X. X. & P. B. Rainey, (2008) Dual involvement of CbrAB and NtrBC in the regulation of histidine utilization in *Pseudomonas fluorescens* SBW25. *Genetics* **178**: 185-195.

Zhang, X. X., S. R. Ritchie & P. B. Rainey, (2014b) Urocanate as a potential signaling molecule for bacterial recognition of eukaryotic hosts. *Cellular and molecular life sciences : CMLS* **71**: 541-547.

3.8 Supplementary data

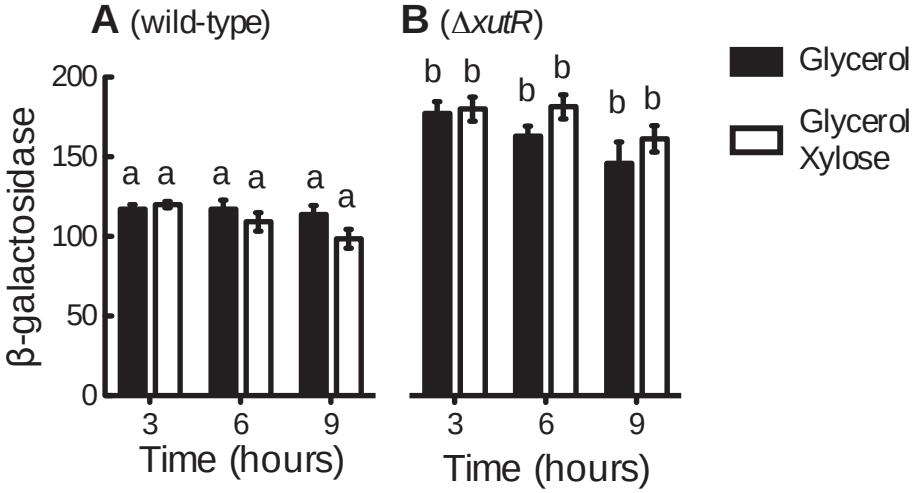

Figure S3.1. Responses of the P_{xutR} promoter to xylose in wild-type *P. fluorescens* SBW25 and the derived *xutR* deletion mutant.

β-galactosidase activities (μM 4MU min^{-1} OD_{600}^{-1}) were measured for cells grown in minimal salts medium supplemented with glycerol or glycerol plus xylose at 3, 6 or 9 hrs after inoculation. Values are means and standard errors of three biological repeats. Three-way ANOVA revealed a significant interaction between genotype and medium [$F_{(1,24)} = 4.97$, $P < 0.05$]. Bars that are not connected by the same letter (shown above each) are significantly different ($P < 0.05$) by Tukey's HSD test.

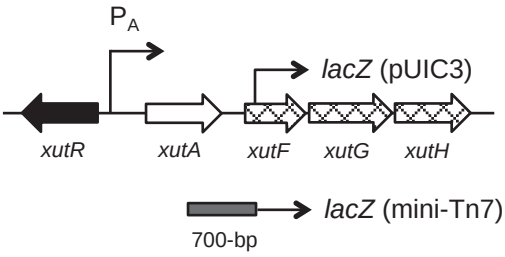

	β-galactosidase activity of *xutF-lacZ*	
	In the *glmS* locus via mini-Tn7	In the *xut* locus via pUIC3
Glycerol	104.2 ± 2.9	46.4 ± 8.9
Glycerol Xylose	114.9 ± 3.4	1482.9 ± 70.3 (s)

Figure S3.2. Co-transcription of *xutA* and *xutFGH* in *P. fluorescens* SBW25.

The putative *xutF* promoter (700-bp) was fused to promoterless *lacZ* carried in plasmid pUC18-mini-Tn7T-Gm-lacZ, and the resulting *hutF-lacZ* was integrated at the unique mini-Tn7 insertion site located downstream of *glmS*. As a control for xylose-induced expression of *xutF*, the promoterless *lacZ* was placed at the original *xut* locus via cloning into the integrative plasmid pUIC3. β-galactosidase activity (μM 4MU min^{-1} OD_{600}^{-1}) was measured for cells grown on minimal medium with either glycerol or glycerol plus xylose as carbon sources. Data are means and standard errors of three independent cultures. Expression levels were compared between cells grown in the two media, and "s" in parenthesis denotes significant difference between means as revealed by the Student's t-test ($P < 0.05$).

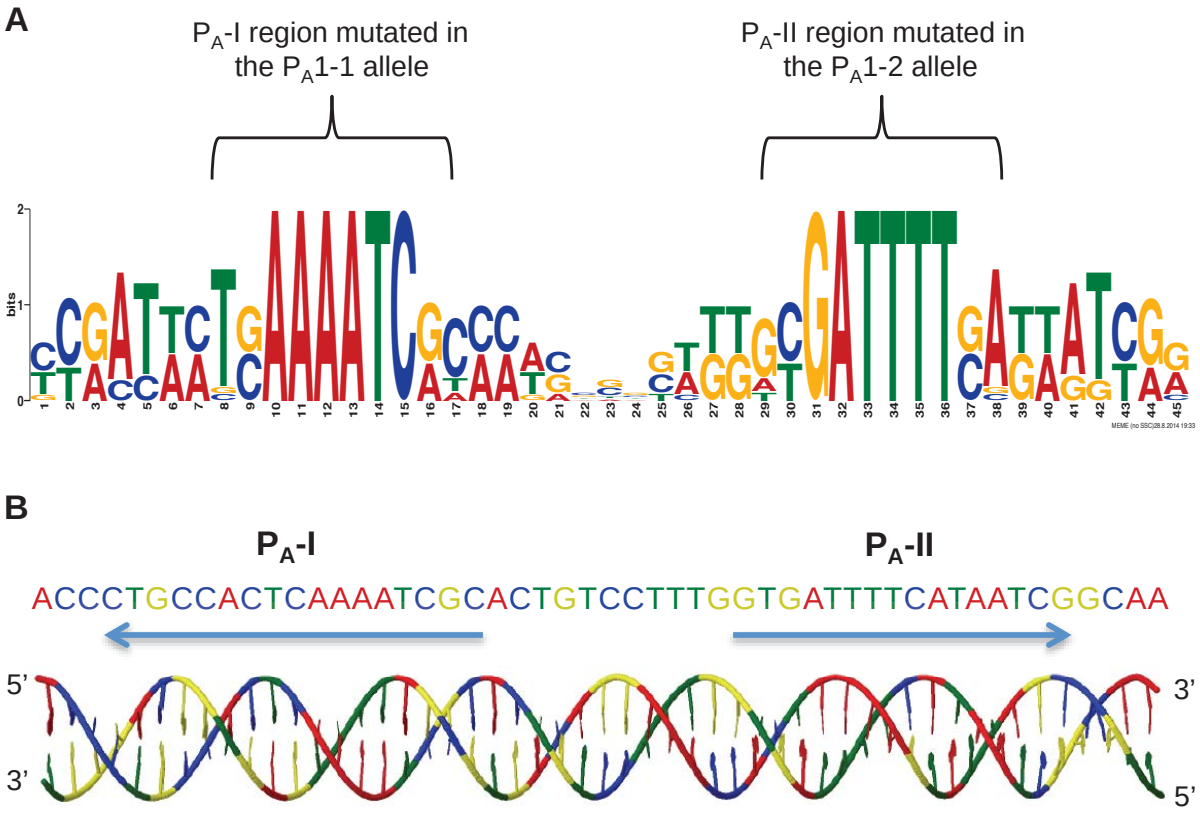

Figure S3.3. Consensus sequence of the XutR binding sites in *Pseudomonas* (A) and the predicted DNA structure of XutR operator in *P. fluorescens* SBW25 (B).

(**A**) The consensus sequence was generated using the WebLogo 3 online server (http://weblogo.threeplusone.com/create.cgi) based on alignment of homologous sequences from nine *Pseudomonas* genomes that are currently deposited in the *Pseudomonas* database (http://www.pseudomonas.com/search.jsp). The marked highly conserved regions of the P_A-I and P_A-II elements were subjected to site-directed mutagenesis.

(B) The DNA structure of the XutR operator was predicted using the w3DNA web server (http://w3dna.rutgers.edu). The P_A-I and P_A-II elements are marked with arrow lines.

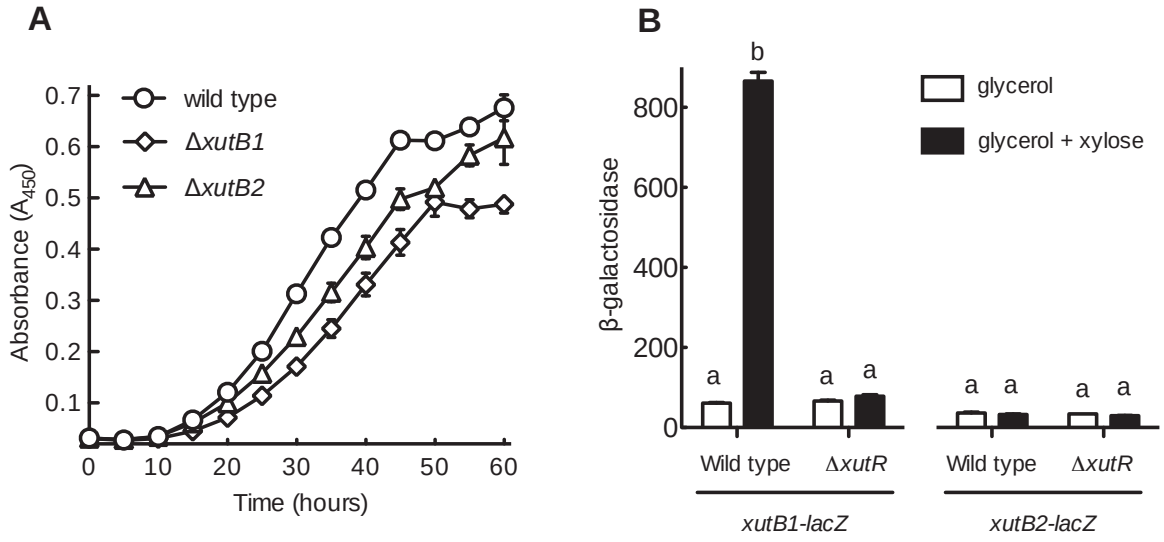

Figure S3.4. Functional analysis of the two putative xylulokinase genes *xutB1* and *xutB2*.

(**A**) Growth properties of wild-type SBW25 and its derived mutants of Δ*xutB1*and Δ*xutB2*. Growth curve of the double deletion mutant (Δ*xutB1* Δ*xutB2*) was similar with the Δ*xutB1* mutant, and data are shown for clarity. Bacterial cells were grown in minimum salts medium supplemented with xylose (20 mM). Data are means and standard errors of six independent cultures.

(**B**) Responses of *xutB1* and *xutB2* expression to the presence of xylose in the growth medium. Levels of *xutB1* and *xutB2* transcription were monitored using chromosomally integrated *lacZ* fusions carried on suicide plasmid pUIC3. β-galactosidase activities (μM 4MU min^{-1} OD_{600}^{-1}) were measured for cells grown in minimal salts medium supplemented with glycerol or glycerol plus xylose. Values are means and standard errors of three biological repeats. Bars that are not connected by the same letter (shown above each) are significantly different ($P < 0.05$) by Tukey's HSD test.

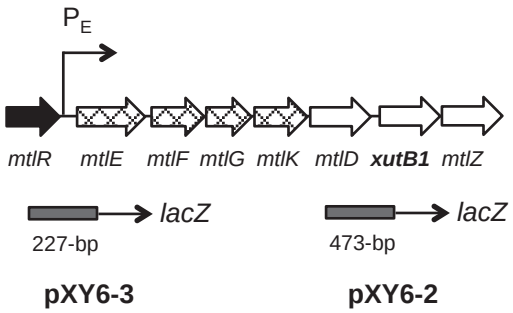

	β-galactosidase activity (μM 4MU min^{-1} OD_{600}^{-1})	
	pXY6-2	**pXY6-3**
Glycerol	81.8 ± 1.4	79.0 ± 1.2
Glycerol Xylose	78.0 ± 0.3	195.2 ± 7.4 (s)

Figure S3.5. Localization of the xylose-responsive promoter for *xutB1* expression.

The intergenic region of *mtlD* - *xutB1* and *mtlR* – *mtlE* were cloned into the mini-Tn7 vector pUC18-mini-Tn7T-Gm-LacZ, and *lacZ* fusions in the resultant plasmids pXY6-2 and pXY6-3 were then integrated into SBW25 genome at the mini-Tn7 insertion site. β-galactosidase activity was measured for cells grown on minimal salt medium supplemented with glycerol or glycerol plus xylose. Data are means and standard errors of three independent cultures. Expression levels were compared between cells grown in the two media, and "s" in parenthesis denotes significant difference between means as revealed by the Student's t-test ($P < 0.05$).

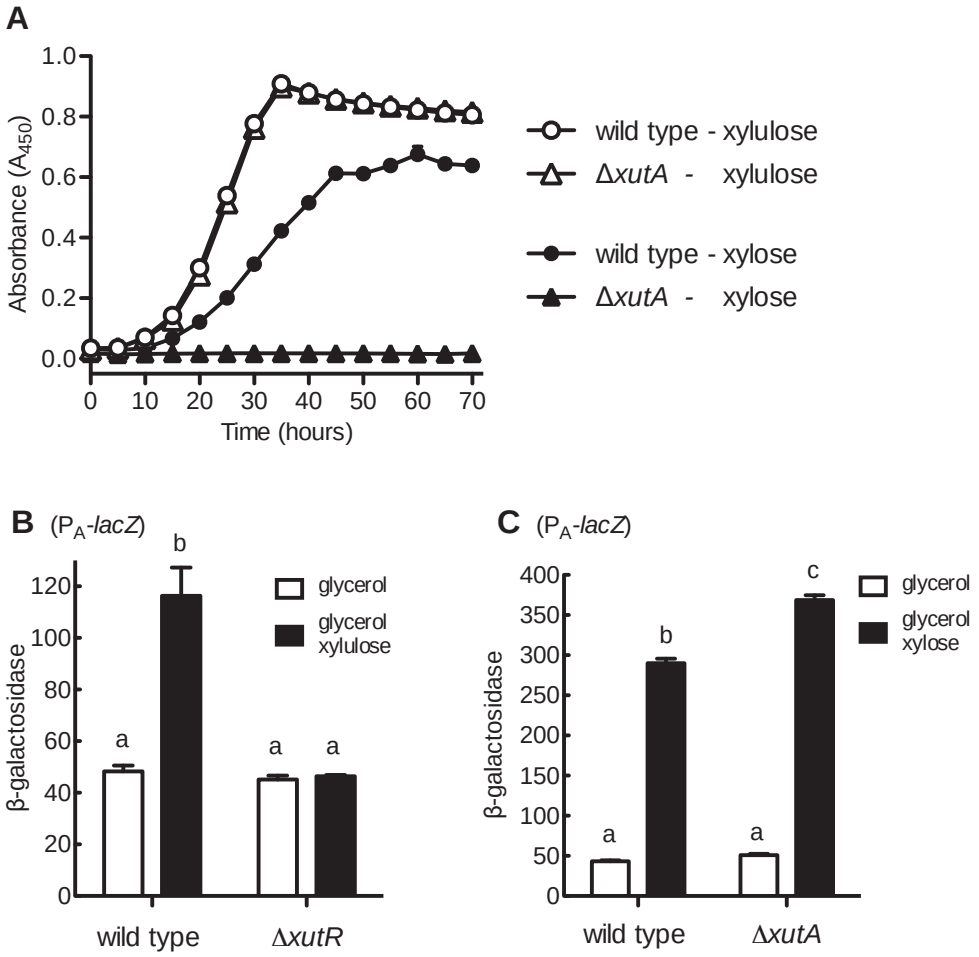

Figure S3.6. Xylulose-induced expression of the *xutAFGH* operon.

(A) Growth kinetics of wild-type SBW25 and the Δ*xutA* mutant in minimal salt medium using xylose and xylulose as the sole carbon sources. Data are means and standard errors of 3 independent cultures. (B) and (C) show the responses of P_A-*lacZ* fusion in the genetic background of Δ*xutR* and Δ*xutA* to xylulose and xylose, respectively. β-galactosidase activity (μM 4MU min^{-1} OD_{600}^{-1}) was measured for cells grown on minimal salt medium supplemented with glycerol or glycerol plus xylose or xylulose. Data are means and standard errors of three independent cultures. Bars that are not connected by the same letter (shown above each) are significantly different ($P < 0.05$) by Tukey's HSD test.

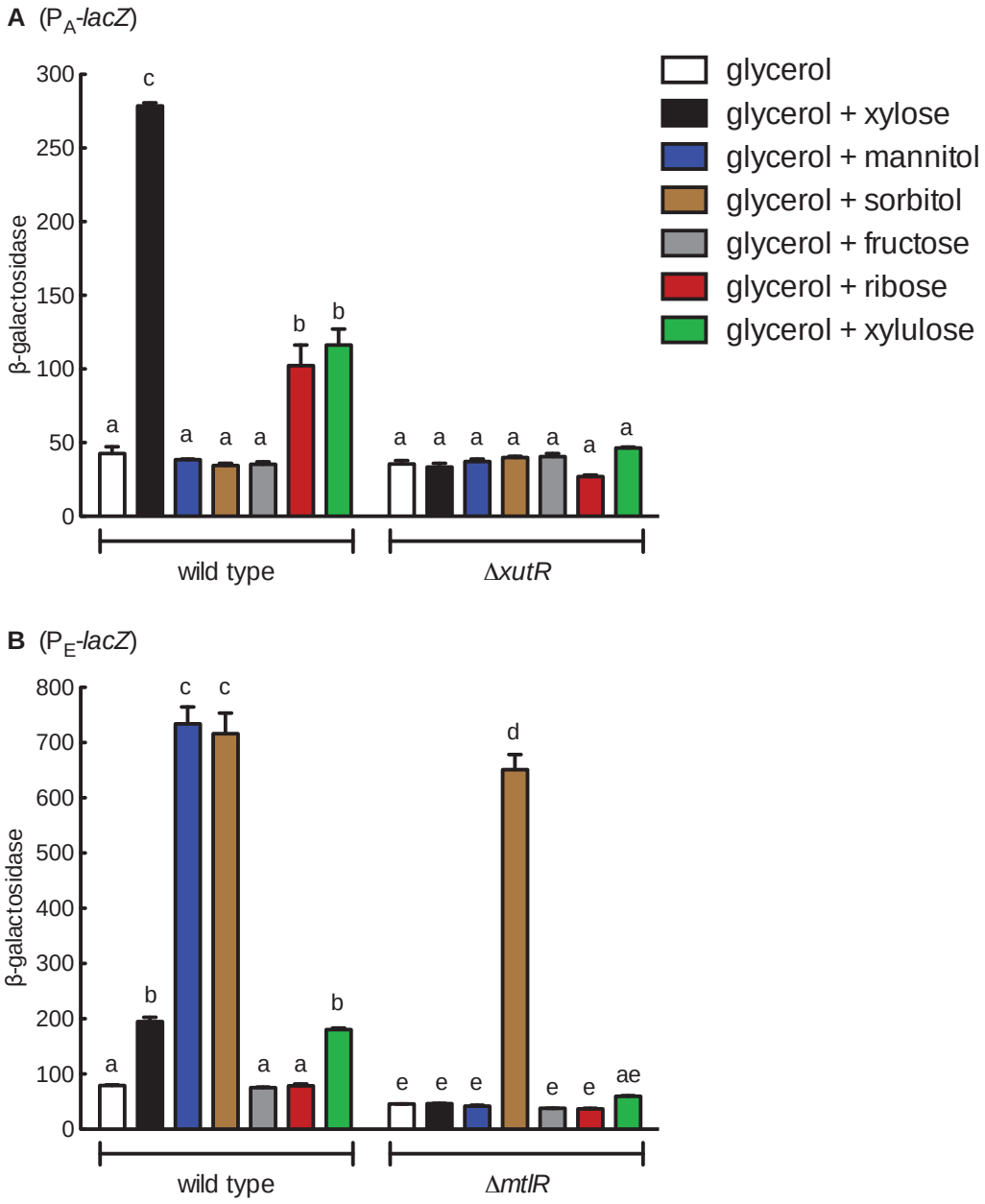

Figure S3.7. Responses of the P_A and P_E promoters to a panel of six structurally similar carbon substrates.

Comparison was made between wild type and Δ*xutR* for P_A promoter (A), and between wild type and Δ*mtlR* for P_E promoter (B). β-galactosidase activity (μM 4MU min^{-1} OD_{600}^{-1}) was measured for cells grown on minimal salt medium supplemented with the related sugar at 20 mM, except xylulose (5 mM). Data are means and standard errors of three independent cultures. Bars that are not connected by the same letter (shown above each) are significantly different ($P < 0.05$) by Tukey's HSD test.

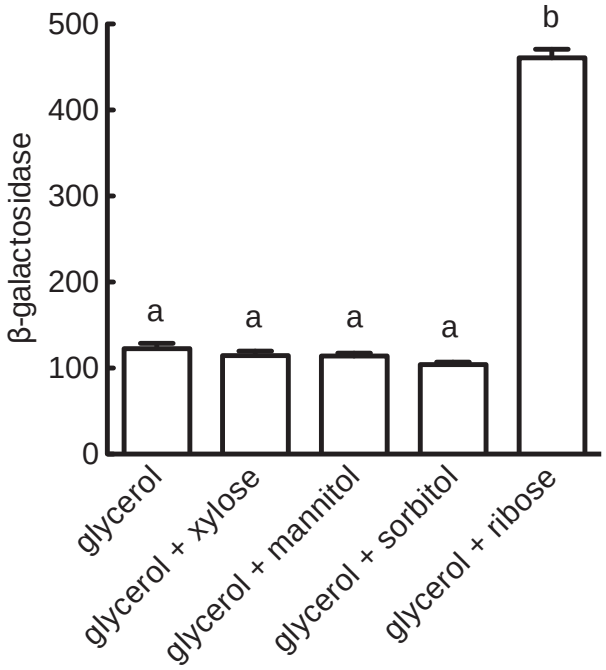

Figure S3.8. Responses of the chromosomally integrated *rbsK-lacZ* fusion to for different carbon substrates.

β-galactosidase activity (μM 4MU min^{-1} OD_{600}^{-1}) was measured for cells grown on minimal salt medium supplemented with the related sugars at 20 mM. Data are means and standard errors of three independent cultures. Bars that are not connected by the same letter (shown above each) are significantly different ($P < 0.05$) by Tukey's HSD test.

Table S3.1. Oligonucleotides used in this work

Primer	**Sequence (5' - 3')**[a]	**Application**
xutA1	gagatctGATGATACCGATGGGCTTGG	*xutA* deletion
xutA2	tccgtcaacggatccgcatgctgCATGGCGTTTTCCTTATTGT	
xutA3	cagcatgcggatccgttgacggaCTGATAGGGGTAAACACTGGC	
xutA4	gagatctCACCTTGGCGTTGTTATCGG	
xutR-1	gagatCTTCACGGCCACCCCACAGCAC	*xutR* deletion
xutR-2	cagcatgcggatccgttgacggaTTTCATTGTTGTTGTCCTGG	
xutR-3	tccgtcaacggatccgcatgctgTAGGGCCTCGTATTCAGACTG	
xutR-4	gagatCTGGGCGCACGGGTCAAATACGAC	
xutA-lacZF	gactagtCATAAGGAATGCCCTTGGGGT	P_A transcriptional fusion to *lacZ*
xutA-lacZR	gaagcttGACACCGGGGAAGTACGGCATGGC	
xutR-lacZF	gactagtTAGTAGTCGATGCCCAGTTTG	P_R transcriptional fusion to promoterless *lacZ*
xutR-lacZR	gaagcttCACGGGCGGTAGGGTTTTCATTGT	
xutR-compF	gactagtggAGGACAACAACAATGAAAACCC	*xutR* complementation
xutR-compR	gaagcttTGAATACGAGGCCCTAGGCC	
xutA-compF	gactagtggAGGAAAACGCCATGCCGTAC	*xutA* complementation
xutA-compR	gaagcttCAGTGTTTACCCCTATCAGGT	
xutA-pmF1	ggactagtCGCACTGTCCTTTGGTGATT	Forward primer for *xutA* promoter mapping, with "xutA-lacZR" as the reverse primer
xutA-pmF2	ggactagtGGCGGTAGGGTTTTCATTGT	
xutA-pmF3	ggactagtGACCCTGCCACTCAAAATCG	
xutA-pmF4	ggactagtAAGTCGGCGATGATGCCGTC	
xutA-pmF5	ggactagtTGCTGCTCAGGTAGTTGCCGA	
xutR-ProF	aaatttggaattccatcatcatcatcatcatAAAACCCTACCGCCCGTGCAC	XutR protein expression
xutR-ProR	aaatttgaagcttTGAATACGAGGCCCTAGGCC	
xutR-RACE3	CCGCTTCGATCAAATGTTCG (+361 nt from the ATG start)	*xutR* 5'-RACE analysis
xutR-RACE4	AGGCGACAGAGAAAGTCCTC (+152 nt from the ATG start)	
xutA-RACE1	AGTAGTCGATGCCCAGTTTG (+289 nt from the ATG start)	*xutA* 5'-RACE analysis
xutA-RACE2	TTGAAGGTGCCTACACCGAA (+194 nt from the ATG start)	
xutFGH-1	gagatctTATCTTCGGCAGCATCGACG	*xutFGH* deletion
xutFGH-2	cagcatgcggatccgttgacggaCATGGTGGTGCGTCCTTTTA	
xutFGH-3	tccgtcaacggatccgcatgctgCGCTGAATCCACGCCAACGA	

xutFGH-4	gagatctGCAAACTGGCGGTGTAGAGAA	
xutF-lacZF	gactagtTATCTTCGGCAGCATCGACG	Cloning the *xutFGH* putative promoter
xutF-lacZR	gaagcttGGTACGTTTGAATGACTTCATGGT	
xutA-DNaseF1	GTTGAAGAGCAAGGCAATGCG (biotin labelled)	Forward primer for cloning P_A for XutR binding assays, with "xutA-lacZR" as the reverse primer
xutR-BSmut1	TAGACCCTGCCACgtcgctggtaACTGTCCTTTGGTGATTTTCAT	Mutagenizing XylR binding site I (P_A-I)
xutR-BSmut2	ACCAAAGGACAGTtaccagcgacGTGGCAGGGTCTAGTCTGTGGC	
xutR-BSmut3	GCACTGTCCTTTGtaccagcgacTAATCGGCAAGGCCGATGCCGT	Mutagenizing XylR binding site II (P_A-II)
xutR-BSmut4	GCCTTGCCGATTAgtcgctggtaCAAAGGACAGTGCGATTTTGAG	
xutB1-1	gagatctTCGTGCACGAGACCATGAAC	*xutB1* deletion *xutB1-lacZ* fusion in plasmid vector pUIC3
xutB1-2	cagcatgcggatccgttgacggaCATGAGGGTGTGCTCAGCAGT	
xutB1-3	tccgtcaacggatccgcatgctgACCCTTTAAGAGCGAACGAC	
xutB1-4	gagatctTAGAGCAGGTGCAGGTCTTC	
2739-1	ggagatCTGTTCGACCTCGACCTGGCC	*mtlZ* deletion
2739-2	cagcatgcggatccgttgacggaCAGATACATAGTCGTTCGCTC	
2739-3	tccgtcaacggatccgcatgctgGGATGAAGGTTTTGTCAGCCAG	
2739-4	ggagatctACACTCCACACCCACAGCAGC	
4156-1	ggagatCTGGTGCGTATCGATCACGAG	*rbsK* deletion *rbsK-lacZ* fusion in plasmid vector pUIC3
4156-2	cagcatgcggatccgttgacggaTGGCATACATCAGTACTCATC	
4156-3	tccgtcaacggatccgcatgctgCCCTCATGAAAAAGACACCTC	
4156-4	ggagatctATCGCGAACAGCAACGCCACC	
3115-1	ggagatctAACGAAATTCCCGCTGTGCTG	*xutB2* deletion *xutB2-lacZ* fusion in plasmid vector pUIC3
3115-2	cagcatgcggatccgttgacggaCATATGCAGGTCTTCCAATCA	
3115-3	tccgtcaacggatccgcatgctgATGGAGGCTACAGGGGCTTCG	
3115-4	gagatctGACAGGTATTCTAGGGACGTA	
xutB1-lacZF	gactagtGACGGTTCGTCGAAGTTTCC	Amplify the 473 bp DNA fragment for the construction of *xutB1-lacZ* in mini-Tn7
xutB1-lacZR	gaagcttGTACAGGTTTTGCTGGGTCATGAG	

mtlR-1	ggagatctAAGGCCACGGCCTTACACAACC	*mtlR* deletion
mtlR-2	cagcatgcggatccgttgacggaGGTCATGCTGCCGTCGCTTTAT	
mtlR-3	tccgtcaacggatccgcatgctgTTGGCTTAATGGTTTCAGCTGC	
mtlR-4	ggagatctAACCCTTGACTGACAAACCGTC	
mtlE-pmF1	ggactaGTGCAGCGCTTGACCGAGCAGA	Forward primer for pXY7-P_E
mtlE-pmF2	ggactagtCCAGTGCGCCCAAGGATTTGTC	Forward primer for pXY7-P_E1
mtlE-lacZR	ggaagcttTGCTGTGAACTTCATCGCGCAC	Reverse primer for pXY7- P_E and pXY7-P_E1

[a] Artificial sequences integrated into the primers are shown in lowercase whereas with restriction sites underlined.

Table S3.2. Presence or absence of XutA homologue in the genome-sequenced Pseudomonas

Species	**Strain(s)**	**XutA homologue**
P. aeruginosa	2192, 39016, B136-33, C3719, DK2, LESB58, M18, NCGM2.S1, PA7, PACS2, PAO1, RP73, PA14	None
P. brassicacearum	NFM421	Yes
P. denitrificans	ATCC 13867	None
P. entomophila	L48	None
P. fulva	12-X	None
P. mendocina	NK-01, ymp	None
P. protegens	CHA0, Pf-5	None
P. putida	BIRD-1, DOT-T1E, F1, GB-1H8234, HB3267, KT2440, NBRC 14164, ND6, S16, W619	None
P. resinovorans	NBRC 106553	None
Pseudomonas sp.	UW4	None
P. stutzeri	A1501, ATCC 17588, CCUG 29243, DSM 10701, DSM 4166, RCH2	None
P. syringae	DC3000, B728a, 1448A*	Yes
P. fluorescens	SBW25, A506, F113 and Pf0-1	Yes
P. poae	RE*1-1-14	Yes

Chapter 4

Mini-Tn7 vectors for studying post-transcriptional gene expression in *Pseudomonas*

Molecular mechanisms of carbon catabolic repression (CCR) has been well studied in enteric bacteria, which is mediated by the CRP regulator charged with cAMP. However, CCR in *Pseudomonas* is poorly understood, and it does not occur at the level of gene transcription. Instead, it occurs at post-transcriptional levels involving a RNA-binding protein Crc. Our previous work has showed that non-coding RNAs are also involved in the CCR of *P. fluorescens* SBW25. It is thus necessary to monitor the levels of gene expression at the post-transcriptional levels, not only for protein-encoding genes but also for non-coding small regulatory RNA genes. To fill in this technology gap and facilitate our own study on CCR of xylose utilization in *Pseudomonas*, we successfully constructed five mini-Tn7 vectors and validated their use for studying post-transcriptional gene expression.

This work has been published in the *Journal of Microbiological Methods* (2014), Vol. 107: 182-185

(The published version is available in Appendix I)

Mini-Tn7 vectors for studying post-transcriptional gene expression in *Pseudomonas*

Yunhao Liu[1,2], Paul B. Rainey[2,3] and Xue-Xian Zhang[1]*

[1]Institute of Natural and Mathematical Sciences, Massey University at Albany, Auckland 0745, New Zealand

[2]NZ Institute for Advanced Study, Massey University at Albany, Auckland 0745, New Zealand

[3]Max Planck Institute for Evolutionary Biology, August Thienemann Strasse 2, 24306 Plön, Germany

***Author for correspondence:** Xue-Xian Zhang

Phone: +64 (9) 414 0800

Fax: +64 (9) 441 8142

E-mail: x.x.zhang1@massey.ac.nz

4.1 Abstract

We describe the construction and validation of five mini-Tn7 vectors for analysis of post-transcriptional gene expression in *Pseudomonas*. Four vectors allow construction of translational fusions to β-galactosidase (*lacZ*), while the fifth is designed for functional analysis of noncoding RNA genes. Translational fusions can be constructed without a functional promoter in the vector or from an inducible promoter of either P_{tac} or P_{dctA}. We show that promoterless fusions have value for determining levels of translation, whereas fusions to inducible promoters have utility in the analysis of mRNA-binding factors.

Key words: gene regulation, LacZ, noncoding RNAs, translational fusion, mini-Tn7, *Pseudomonas*

The mini-Tn7 transposon system is a useful tool for studying gene regulation in bacteria because of its ability to deliver reporter gene fusions into the chromosome in a site- and orientation-specific manner (Bao et al., 1991, Lambertsen et al., 2004, Schweizer, 2008). Unlike classical plasmid vectors, mini-Tn*7* allows cloned genes to be integrated into the chromosome at a single highly conserved position (*attTn7*) located downstream of *glmS*. Moreover, cloned genes are stably maintained in the absence of antibiotic selection at the same copy number as the chromosome (Parks and Peters, 2009, Peters and Craig, 2001). Accordingly, cloning systems based upon mini-Tn7 are versatile genetic tools for a wide range of bacterial species and applications (Choi et al., 2006, Damron et al., 2013).

In 2005, Schweizer and colleagues constructed a panel of mini-Tn7 delivery vectors, which included two plasmids: one containing a transcriptional fusion to β-galactosidase (*lacZ*) and the other a transcriptional fusion to bioluminescence (*lux*) reporter genes (Choi et al., 2005). Also included was the vector pUC18-mini-Tn7T-LAC suitable for genetic complementation.

Gene regulation is effected not only at the level of transcription but also at the level of translation, with the involvement of RNA-binding proteins or non-protein coding RNAs (ncRNAs) (Babitzke et al., 2009, Rojo, 2010, Sonnleitner and Haas, 2011). To facilitate their analysis we constructed five additional mini-Tn7 vectors (designated pXY1 to pXY5, Fig. 4.1), which have been successfully used in genetic analysis of the model bacterium *Pseudomonas fluorescens* SBW25 (Bailey et al., 1995, Silby et al., 2009).

The *lacZ* gene from *E. coli* is one of the most commonly used reporters (Casadaban et al., 1983). It is suitable for making translational fusions because the first ~30 amino acid codons of *lacZ* can be eliminated or altered without affecting the encoded β-galactosidase enzymatic activity (Simons et al., 1987). To construct a mini-Tn7 translational fusion vector to *lacZ*, a pair of primers was designed to amplify the *lacZ* gene from plasmid pUC18-mini-Tn7T-Gm-*lacZ*, with the *lacZ* segment beginning at the 9th codon of *lacZ* (Table S4.1). To facilitate gene cloning, restriction sites *Spe*I-*Pst*I-*Bam*HI-*Hin*dIII and *Kpn*I were incorporated into the forward primer lacZF-MCS and reverse primer lacZR, respectively. The 3-kb PCR product was first cloned into pCR8/GW/TOPO by using the TA cloning kit from Invitrogen^{TM} (Auckland). After sequence identity was confirmed by DNA sequencing, the *lacZ* fragment was retrieved by *Spe*I / *Kpn*I digestion and cloned into the corresponding sites of vector pUC18R6K- mini-Tn7T-Gm. The resultant fusion protein vector was designated pXY1 (Fig. 4.1A).

The multiple cloning site (MCS) of pXY1 contains 4 unique restriction sites for promoter cloning (*Nsi*I, *Spe*I, *Pst*I and *Bam*HI). However, the more desirable *Hin*dIII site couldn't be used for fusion protein construction, because there is a second *Hin*dIII site in the R6K origin of replication (ori_{R6K}). To eliminate this additional *Hin*dIII site and construct a plasmid vector with a ColE1 replication origin (*ori*), we removed the 2-kb *Sac*I fragment from pXY1 containing the MCS and the 5' portion of *lacZ*, and used this fragment to replace the corresponding region of pUC18-mini-Tn7T-Gm-*lacZ* (Fig. 4.1A). The resultant fusion protein plasmid pXY2 differs from the transcriptional fusion plasmid pUC18-mini-Tn7T-Gm-*lacZ* only in the 5' end of the *lacZ* reporter gene.

Next, pXY2 was validated for use in the translational analysis of *hut* genes for histidine utilization (Zhang and Rainey, 2007b). To do this, a 500 bp DNA fragment containing the transcription and translation initiation region of *hut* genes (P_{hutU}) was obtained by PCR amplification from the genomic DNA of *P. fluorescens* SBW25 and directionally cloned into the *Spe*I and *Hin*dIII sites of pXY2. Details of oligonucleotide primers used in this work are provided in Table S4.1. The resulting P_{hutU}-*lacZ* translational fusion was then introduced into *P. fluorescens* SBW25 by electroporation along with the pUX-BF13 helper (Bao, et al., 1991). Integration of the Tn7 element carrying the P_{hutU}-*lacZ* fusion into the unique chromosomal site was confirmed by PCR using primers SBW25-glmS and Tn7R109 (Table S4.1). β-galactosidase assays were performed using cells grown on either M9 broth or M9 broth supplemented with histidine (10 mM). Consistent with expectation, a 5-fold increase of *hut* gene expression was observed in response to the presence of histidine in the medium (mean μM 4MU/OD600/min ± standard error): 12.31 ± 0. 29 in M9 versus 63.52 ± 1.21 in M9 plus histidine.

Standard translational vectors, including pXY1 and pXY2 described above, encode a fusion protein whose transcription is regulated by native promoter(s) of the gene under investigation. Thus, they report a combined effect of regulatory factors involved in the entire process of gene transcription and translation. For demonstrating the regulatory roles of RNA-binding proteins or ncRNAs *in vivo*, it is important to separate the predicted post-transcriptional effects from those of transcriptional regulation. To this end, we designed a translational fusion to *lacZ* under the transcriptional control of an independent promoter (e.g., P_{tac}), and then compared expression levels of the same *lacZ* reporter gene between wild type and a mutant devoid of the regulatory gene of interest. Though transcription of the target gene (i.e., the *lacZ* fusion reporter) is expected

to be maintained at similar levels between mutant and wild-type, an increase of β-galactosidase activity is expected for mutant over the wild-type if a RNA-binding protein or ncRNA plays a significant role in repressing translation. The opposite is expected for an mRNA-interacting activator.

Two mini-Tn7 vectors, pXY3 and pXY4, were constructed for the assessment of post-transcriptional gene regulation (outlined in Fig. 4.1A). pXY3 contains a translational fusion to *lacZ* under the control of the P_{tac} promoter. It was made by cloning the ~ 3 kb *Spe*I / *Kpn*I *lacZ* fragment derived from pCR8/GW/TOPO-lacZ7 into vector pUC18-mini-Tn7T-LAC (Choi, et al., 2005). The DNA region corresponding to the 5'-end transcript of a given target gene can be inserted into the MCS of pXY3, and expression of the resultant *lacZ* translational fusion transcriptionally induced by using a non-metabolizible inducer molecule such as IPTG (Isopropyl β-D-1-thiogalactopyranoside). The availability of a non-metabolizible inducer for P_{tac} makes it possible to manipulate levels of the target mRNA by adding different concentrations of IPTG in the growth medium. However, the transcriptional start site of the P_{tac} promoter is located at the beginning of the operator site for LacI binding (de Boer et al., 1983). Consequently, ~50 nt is incorporated into the 5'-end of the mRNA transcript. This extra sequence can potentially alter the mRNA secondary structure and affect interactions of some mRNAs with their putative mRNA binding factors.

To overcome the above-mentioned shortcoming for pXY3, vector pXY4 was designed to ensure that transcription starts precisely from the previously determined transcriptional start site of the target gene. pXY4 harbours a *lacZ* translational fusion under the transcriptional control of the *dctA* promoter (P_{dctA}) from *P. fluorescens* SBW25 (Liang, 2014). In the presence of succinate, fumarate or malate, P_{dctA} activates *dctA* transcription in a σ^{54}-dependent manner; activation is mediated by the DctBD two-component regulatory system (Kleefeld et al., 2009, Yarosh et al., 1989). In unrelated work, we have determined the transcriptional start site of *dctA* using the rapid amplification of cDNA 5' ends (5'-RACE) system purchased from Invitrogen (Auckland). Transcription starts at the 13th nucleotide downstream from the conserved cysteine residue of the predicted σ^{54}-binding site (data not shown). Armed with this knowledge, a pair of primers was designed to amplify P_{dctA}: forward primer dctA-NsiI and reverse primer dctA-TSS with transcription starting at the *Hin*dIII site (Table S4.1). The resulting 490 bp PCR product was first cloned into pCR8/GW/TOPO and its sequence identity was verified by DNA sequencing

(Macrogen Inc., South Korea). Next, pXY4 was generated by directionally cloning the P_{dctA} fragment into the *Nsi*I and *Hin*dIII sites of pXY2 (Fig. 4.1A).

To demonstrate the functionality of the above-described vectors pXY3 and pXY4, we tested the role of the well-characterized Crc regulator in repressing expression of *xylA* gene for D-xylose utilization, which occurs at post-transcription level (Rojo, 2010, Zhang and Rainey, 2008). The DNA region corresponding to the 5' end of the *xylA* transcript was amplified from the genomic DNA of *P. fluorescens* SBW25 by PCR and cloned into pXY3 and pXY4, respectively (Table S4.1). The resultant P_{tac}-*xylA*-*lacZ* fusion in pXY3 and P_{dctA}-*xylA*-*lacZ* fusion in pXY4 were introduced into *P. fluorescens* SBW25 and its derived mutant MU12-58 (Δ*crc*), and their transcription was induced by growth of cells in minimal medium with the addition of IPTG (0.05 mM) and succinate (20 mM), respectively. β-galactosidase activities were assayed using a standard protocol with 4-methylumbelliferyl-b-D- galactoside (4MUG) as the enzymatic substrate (Zhang and Rainey, 2007a). The fluorescent product, 7-hydroxy-4-methylcoumarin (4MU), was detected at 460-nm after excision at 365-nm using a Synergy 2 plate reader (BioTek Instruments). The results are shown in Fig. 4.1B and 4.1C. For each fusion strain, addition of the related inducer compound resulted in a significant increase in β-galactosidase activity, indicating that the encoded P_{tac} and P_{dctA} promoters are functional. Moreover, for the induced cells (i.e. those treated with IPTG or succinate), the levels of β-galactosidase activity were significantly higher in the mutant (Δ*crc*) than in the wild-type background (Fig. 4.1B, 4.1C). This result is consistent with the known role of Crc in repressing *xylA* expression via molecular interactions with the 5' end of the *xylA* transcript (Rojo, 2010). Furthermore, as shown in Fig. S4.1, the 5'-transcript end of the P_{dctA}-*xylA*-*lacZ* fusion in pXY4 was confirmed in succinate-induced cells by using the method of 5'-RACE analysis. Together, the data consistently indicate that both pXY3 and pXY4 can be used to investigate post-transcriptional gene regulation mediated by the mRNA-binding protein. Our data also show that the ~50 additional nucleotides incorporated into the 5'-transcript end of *xylA* in pXY3 did not produce any detectable effects on Crc-mediated regulation.

The successful application of the P_{dctA} promoter in vector pXY4 prompted further construction of the fifth mini-Tn7 vector, namely pXY5, wherein P_{dctA} was employed to drive the expression of a noncoding RNA gene for functional characterization. To accomplish this, a new reverse primer dctAR-SpeI (Table S4.1) was designed and it was used in conjunction with the forward primer

dctA-NsiI to amplify a 490-bp P_{dctA} fragment from the genomic DNA of *P. fluorescens* SBW25. Next, the pXY5 vector was generated by cloning the P_{dctA} fragment into vector pUC18R6K-mini-Tn7T-Gm at the *Nsi*I and *Spe*I sites, following the similar procedures described above for pXY4 construction (Fig. 4.1A). Expression of ncRNA gene cloned into pXY5 can be induced with the addition of succinate, fumarate or malate. Several nonmetabolizible succinate analogues were reported in different bacterial species, but their abilities to activate P_{dctA} in *Pseudomonas* were not investigated in this work (Reid et al., 1996). Notably, P_{dctA} is constitutively active in the genetic background of *dctA* deletion (Kleefeld, et al., 2009, Yarosh, et al., 1989).

To validate pXY5 in the functional analysis of ncRNA genes, the previously characterized *crcZ* gene was amplified by PCR using primers crcZ-EV1 and crcZ-EV3 (Table S4.1) and cloned into pXY5 at the *Spe*I site (Zhang et al., 2010). The resulting plasmid pXY5-*crcZ* was then introduced into mutant MU45-70 (Δ*cbrB*, Δ*dctA*). CbrB is a response regulator required for the expression of *crcZ*; when the CrcZ is expressed, it functions as a ncRNA and sequesters the mRNA-binding protein Crc, causing de-repression of many catabolic genes including *xylA* for D-xylose utilization (Liu, 2014, Rojo, 2010, Zhang, et al., 2010). Therefore, when pXY5-*crcZ* was introduced into mutant MU45-70 (Δ*cbrB*, Δ*dctA*; Xyl^-), the CrcZ ncRNA will be produced in the absence of a P_{dctA} inducer compound, and confer ability of the mutant cell to grow on D-xylose. Results shown in Fig. 4.1D indicate that mutant MU45-71 (Δ*cbrB*, Δ*dctA*, with the mini-Tn7-*crcZ*) grew well on D-xylose, whereas the mutant MU45-72 (Δ*cbrB*, Δ*dctA*, with the mini-Tn7 element only) could not grow on D-xylose. The data was consistent with our expectations and confirmed the suitability of pXY5 for functional analysis of ncRNA genes.

Finally, it is relevant to note that while Tn7 integrates at a single *attTn7* site, we observed integration at three different positions within the intergenic region between *glmS* and *pflu6112*. Details are provided in supplementary Fig. S4.2. Why mini-Tn7 should integrate at these three positions is unknown, but may be caused by the non-specific transposition system (TnsABC+E) carried on the helper plasmid pUX-BF13 (Bao, et al., 1991, Peters and Craig, 2001). For some studies, it maybe important to verify the precise mini-Tn7 integration site.

In summary, we have constructed five mini-Tn7 vectors and demonstrated their usefulness for studying gene regulation at post-transcriptional levels in *P. fluorescens* SBW25. These plasmids can be added to the growing list of mini-Tn7 vectors that have proven important genetic tools for

many bacterial species. DNA sequences of pXY1 to pXY5 are available at GenBank database under the accession numbers from KM201422 to KM201426.

4.2 Acknowledgements

We thank Hao Chang for technical assistance, Gayle Ferguson for critical reading of the manuscript and Herbert Schweizer for providing us the mini-Tn7 vectors that were further modified in this work. XXZ acknowledges support from Baode Biological Engineering Co. and the Auckland Medical Research Foundation (AMRF 4114009).

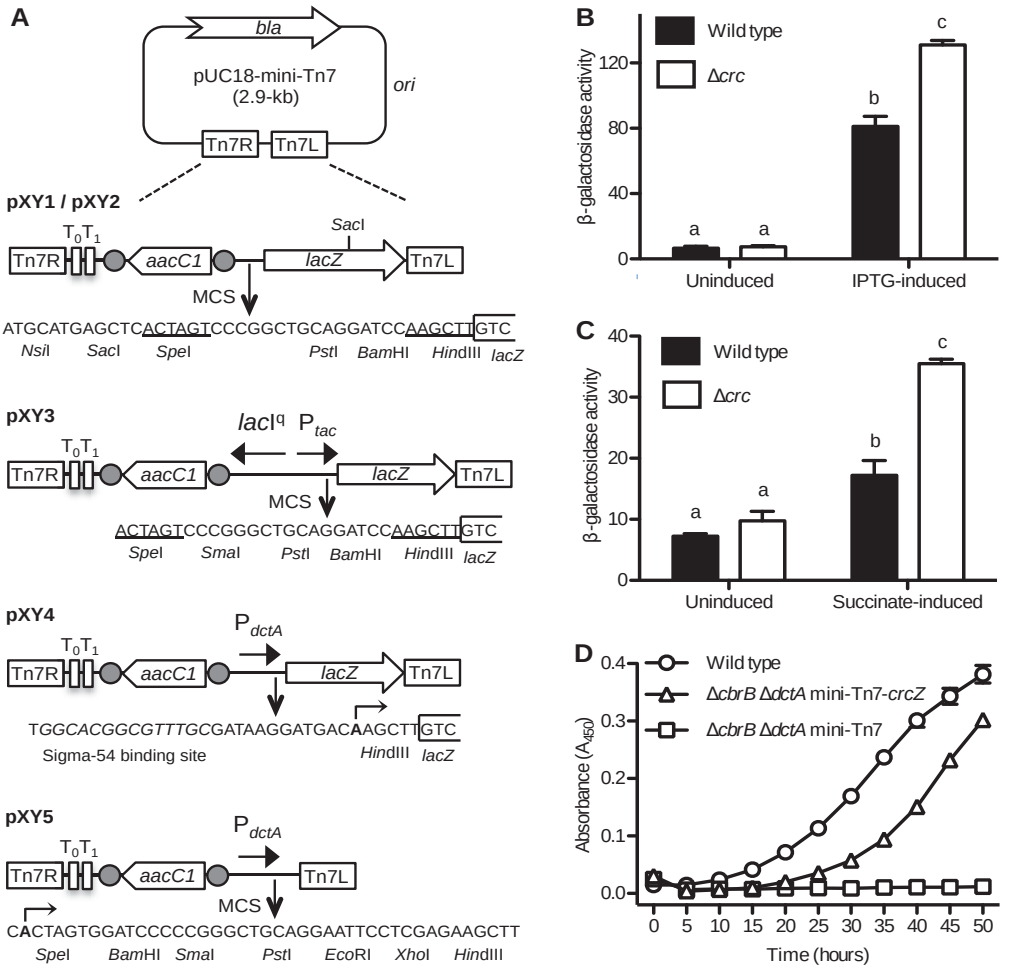

Fig. 4.1. Structure and validation of the mini-Tn7 vectors.

(A) The five pUC18-derived plasmids possess either a ColE1 origin of replication or the o*ri*$_{R6K}$ (Table S4.1). They contain the β-lactamase gene (*bla*) for resistance to ampicillin and two transcriptional terminators T_0 and T_1 from phage λ. The aminoglycoside-3-O-acetyltransferase-I gene (*aacC1*) is flanked by Flp recombinase target sites (denoted by circles); thus, it can be excised upon the introduction of the Flp recombinase gene (Choi et al., 2005). Transcriptional start sites are indicated by bent arrows, and codon 9 of the *lacZ* gene is shown together with DNA sequences of the multiple cloning site (MCS). Of note, a *Sac*I site located immediately upstream of the MCS for both plasmids, and another *Sac*I site in the *lacZ* coding region. **(B)** and **(C)** are results of β-galactosidase assays of the P_{tac}-*xylA*-*lacZ* (pXY3) fusion and P_{dctA}-*xylA*-*lacZ* (pXY4) fusion, respectively, in the genetic background of wild type SBW25 and its derived mutant (Δ*crc*). The enzymatic activity is expressed as μM 4MU/OD_{600}/min. Data are means and standard errors of three independent cultures. Bars with different letters (shown above each) are significantly different ($P < 0.05$) as revealed by two-way ANOVA analysis. **(D)** The growth kinetics of three strains were compared for cells growing in a 96-well microtitre plate using a Synergy 2 plate reader (BioTek Instruments): wild type SBW25 and its derived mutants (Δ*cbrB*, Δ*dctA*) with the mini-Tn7 element from the vector (as a negative control) or mini-Tn7-*crcZ*. Inoculant was prepared as previously described (Zhang and Rainey, 2008). Turbidity was measured at the wavelength of 450-nm every 5-min over a period of 50 hours. Data shown at 5-hour intervals are means and standard errors of 6 independent cultures.

4.3 References

Babitzke, P., Baker, C.S., Romeo, T., 2009. Regulation of translation initiation by RNA binding proteins. Annu Rev Microbiol. 63, 27-44.

Bailey, M.J., Lilley, A.K., Thompson, I.P., Rainey, P.B., Ellis, R.J., 1995. Site directed chromosomal marking of a fluorescent pseudomonad isolated from the phytosphere of sugar beet; stability and potential for marker gene transfer. Mol Ecol. 4, 755-763.

Bao, Y., Lies, D.P., Fu, H., Roberts, G.P., 1991. An improved Tn7-based system for the single-copy insertion of cloned genes into chromosomes of gram-negative bacteria. Gene. 109, 167-168.

Casadaban, M.J., Martinez-Arias, A., Shapira, S.K., Chou, J., 1983. Beta-galactosidase gene fusions for analyzing gene expression in *Escherichia coli* and yeast. Methods Enzymol. 100, 293-308.

Choi, K.H., DeShazer, D., Schweizer, H.P., 2006. mini-Tn7 insertion in bacteria with multiple glmS-linked attTn7 sites: example *Burkholderia mallei* ATCC 23344. Nat Protoc. 1, 162-169.

Choi, K.H., Gaynor, J.B., White, K.G., Lopez, C., Bosio, C.M., Karkhoff-Schweizer, R.R., Schweizer, H.P., 2005. A Tn7-based broad-range bacterial cloning and expression system. Nat Methods. 2, 443-448.

Damron, F.H., McKenney, E.S., Schweizer, H.P., Goldberg, J.B., 2013. Construction of a broad-host-range Tn7-based vector for single-copy P(BAD)-controlled gene expression in gram-negative bacteria. Appl Environ Microbiol. 79, 718-721.

de Boer, H.A., Comstock, L.J., Vasser, M., 1983. The *tac* promoter: a functional hybrid derived from the *trp* and *lac* promoters. Proc Natl Acad Sci U S A. 80, 21-25.

Kleefeld, A., Ackermann, B., Bauer, J., Kramer, J., Unden, G., 2009. The fumarate/succinate antiporter DcuB of *Escherichia coli* is a bifunctional protein with sites for regulation of DcuS-dependent gene expression. J Biol Chem. 284, 265-275.

Lambertsen, L., Sternberg, C., Molin, S., 2004. Mini-Tn7 transposons for site-specific tagging of bacteria with fluorescent proteins. Environ Microbiol. 6, 726-732.

Liang, Y., 2014. Genetic analysis of the succinate utilization genes in *Pseudomonas fluorescens* SBW25, Institute of Natural and Mathematical Sciences, Vol. Master thesis, Massey University, Auckland.

Liu, Y., 2014. Genetic analysis of D-xylose utilization and its catabolite control by succinate in *Pseudomonas fluorescens* SBW25, Institute of Natural and Mathematical Sciences, Vol. Ph.D. thesis, Massey University, Auckland.

Parks, A.R., Peters, J.E., 2009. Tn7 elements: engendering diversity from chromosomes to episomes. Plasmid. 61, 1-14.

Peters, J.E., Craig, N.L., 2001. Tn7: smarter than we thought. Nat Rev Mol Cell Biol. 2, 806-814.

Reid, C.J., Walshaw, D.L., Poole, P.S., 1996. Aspartate transport by the Dct system in *Rhizobium leguminosarum* negatively affects nitrogen-regulated operons. Microbiology. 142 (Pt 9), 2603-2612.

Rojo, F., 2010. Carbon catabolite repression in *Pseudomonas* : optimizing metabolic versatility and interactions with the environment. FEMS Microbiol Rev. 34, 658-684.

Schweizer, H., 2008. Bacterial genetics: past achievements, present state of the field, and future challenges. Biotechniques. 44, 633-634, 636-641.

Silby, M.W., Cerdeno-Tarraga, A.M., Vernikos, G.S., Giddens, S.R., Jackson, R.W., Preston, G.M., Zhang, X.X., Moon, C.D., Gehrig, S.M., Godfrey, S.A., Knight, C.G., Malone, J.G., Robinson, Z., Spiers, A.J., Harris, S., Challis, G.L., Yaxley, A.M., Harris, D., Seeger, K., Murphy, L., Rutter, S., Squares, R., Quail, M.A., Saunders, E., Mavromatis, K., Brettin, T.S., Bentley, S.D., Hothersall, J., Stephens, E., Thomas, C.M., Parkhill, J., Levy, S.B.,

Rainey, P.B., Thomson, N.R., 2009. Genomic and genetic analyses of diversity and plant interactions of *Pseudomonas fluorescens*. Genome Biol. 10, R51.

Simons, R.W., Houman, F., Kleckner, N., 1987. Improved single and multicopy lac-based cloning vectors for protein and operon fusions. Gene. 53, 85-96.

Sonnleitner, E., Haas, D., 2011. Small RNAs as regulators of primary and secondary metabolism in *Pseudomonas* species. Appl Microbiol Biotechnol. 91, 63-79.

Yarosh, O.K., Charles, T.C., Finan, T.M., 1989. Analysis of C4-dicarboxylate transport genes in *Rhizobium meliloti*. Mol Microbiol. 3, 813-823.

Zhang, X.X., Liu, Y.H., Rainey, P.B., 2010. CbrAB-dependent regulation of *pcnB*, a poly(A) polymerase gene involved in polyadenylation of RNA in *Pseudomonas fluorescens*. Environ Microbiol. 12, 1674-1683.

Zhang, X.X., Rainey, P.B., 2007a. Construction and validation of a neutrally-marked strain of *Pseudomonas fluorescens* SBW25. J Microbiol Methods. 71, 78-81.

Zhang, X.X., Rainey, P.B., 2007b. Genetic analysis of the histidine utilization (*hut*) genes in *Pseudomonas fluorescens* SBW25. Genetics. 176, 2165-2176.

Zhang, X.X., Rainey, P.B., 2008. Dual involvement of CbrAB and NtrBC in the regulation of histidine utilization in *Pseudomonas fluorescens* SBW25. Genetics. 178, 185-195.

4.4 Supplementary data

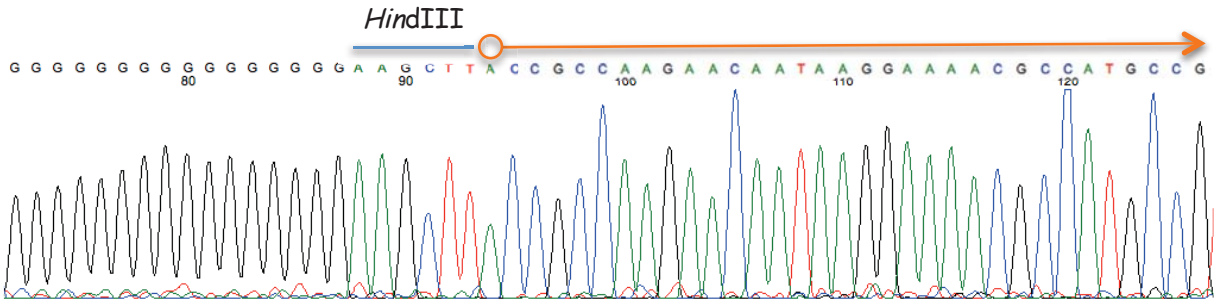

Fig. S4.1. Verification of the transcriptional start site of the P_{dctA}-*xylA*-*lacZ* translational fusion in *P. fluorescens* SBW25.

Fusion strain MU45-80 was grown in minimal M9 salt medium supplemented with histidine (10 mM) and succinate (20 mM). Total RNAs were prepared from cells in mid-log phase (OD_{600} 0.6) using the TRIzol RNA extraction reagent (Invitrogen, Auckland). The transcriptional start site was determined with the 5'-RACE system (Invitrogen, Auckland) following the manufacturer's recommendation. The first strand cDNA was amplified using primer lacZ7, specific for the *lacZ* reporter, and the following PCR was performed with primer 5'xylA-R, specific for the *xylA* fragment. The resulting PCR products were cloned into the TA cloning vector pCR8/GW/TOPO, and six colonies were randomly picked up for DNA sequencing. Results confirmed the predicted transcriptional start site of the P_{dctA} promoter (Fig. 4.1A), with a representative DNA sequencing profile shown here.

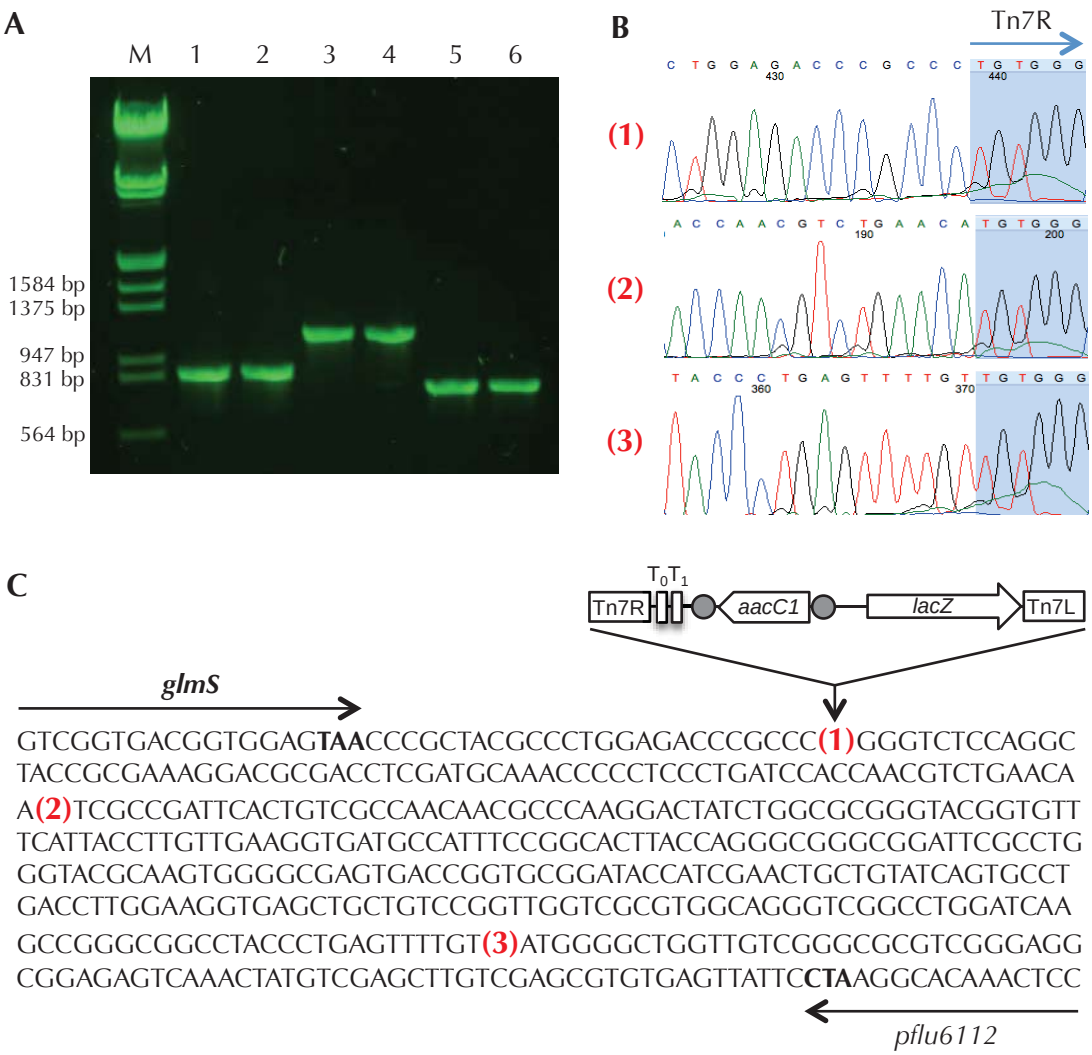

Fig. S4.2. Determination of chromosomal integration sites of mini-Tn7 in *P. fluorescens* SBW25.

(A) To verify integration of the pXY2 mini-Tn7 element into the unique sites located downstream of *glmS* gene. *P. fluorescens* SBW25 transconjugants were subjected to PCR amplification using the forward primer SBW25-glmS and the reverse primer Tn7R-109 (Table S4.1). The resulting PCR products were of three different sizes, and two representatives for each were visualized by agarose gel electrophoresis: M, lambda DNA *Eco*RI / *Hin*dIII marker from Thermo Scientific Ltd (Auckland). **(B)** The six PCR products were sequenced using primer Tn7R-109. **(C)** The three integration sites in the intergenic region of *glmS* and *pflu6112* are indicted by numbers in parentheses. Integration at site (1), (2) and (3) occurs at an approximate frequency of 70%, 20% and 10%, respectively.

Table S4.1. Bacterial strains, plasmids and oligonucleotide primers used in this work

Strain or plasmid	Genotypes and relevant characteristics	Reference or application
P. fluorescens		
SBW25	Wild-type strain isolated from phyllosphere of sugar beet	(Bailey, et al., 1995)
MU12-58	Δ*crc*, SBW25 carrying deletion of *pflu5989*	X.X. Zhang, unpublished
PBR810	Δ*cbrB*, SBW25 carrying deletion of *pflu5237*	(Zhang and Rainey, 2007b)
MU45-70	Δ*cbrB* Δ*dctA*, derivative of SBW25 with deletion of *pflu5237* and *pflu4717*	(Liu, 2014)
MU45-71	MU45-70 carrying mini-Tn7-*crcZ*, Δ*cbrB* Δ*dctA*, Gm^R	This work
MU45-72	MU45-70 carrying the mini-Tn7 element of vector pXY5, Δ*cbrB* Δ*dctA*, Gm^R	This work
MU45-83	Wild-type SBW25 containing the mini-Tn7 element of P_{tac}-*xylA*-*lacZ* from pXY3-*xylA*, Gm^R	This work
MU45-84	MU12-58 containing the mini-Tn7 element of P_{tac}-*xylA*-*lacZ* from pXY3-*xylA*, Gm^R	This work
MU45-80	Wild-type SBW25 containing the mini-Tn7 element of P_{dctA}-*xylA*-*lacZ* from pXY4-*xylA*, Gm^R	This work
MU45-73	MU12-58 containing the mini-Tn7 element of P_{dctA}-*xylA*-*lacZ* from pXY4-*xylA*, Gm^R	This work
Plasmid		
pUX-BF13	Helper plasmid for transposition of Tn7 element, Ap^R	(Bao, et al., 1991)
pUC18R6K-mini-Tn7T-Gm	Mini-Tn7 vector, Ap^R, Gm^R	(Choi, et al., 2005)
pUC18-mini-Tn7T-Gm-*lacZ*	Mini-Tn7 vector, Ap^R, Gm^R	(Choi, et al., 2005)
pCR8/GW/TOPO	TA cloning vector, Sp^R	Invitrogen (Auckland)
pUC18-mini-Tn7T-LAC	Mini-Tn7 vector, Ap^R, Gm^R	(Choi, et al., 2005)
pCR8/GW/TOPO -lacZ7	pCR8/GW/TOPO containing *lacZ* amplified using primers lacZF-MCS and lacZR. This *lacZ* fragment was used in the construction of pXY3	This work
pCR8/GW/TOPO -lacZ8	pCR8/GW/TOPO containing *lacZ* amplified using primers lacZF-MCS and lacZR. This *lacZ* fragment was used in the construction of pXY1 and pXY2. One nucleotide error located in the primer lacZF-MCS was initially overlooked and it eliminates the designed *Sma*I site in the MCS (Fig. 4.1).	This work
pXY1	pUC18R6K-mini-Tn7T-Gm containing a *lacZ* translational fusion, Ap^R, Gm^R (GenBank No. KM201422)	This work
pXY2	pUC18-mini-Tn7T-Gm containing a *lacZ* translational fusion, Ap^R, Gm^R (GenBank No. KM201423)	This work
pXY3	pUC18-mini-Tn7T-LAC containing a *lacZ* translational fusion, Ap^R, Gm^R (GenBank No. KM201424)	This work

pXY4	Derivative of pXY2 carrying P_{dctA}-*lacZ* fusion, Ap^R, Gm^R (GenBank No. KM201425)	This work
pXY5	pUC18R6K-mini-Tn7T-Gm with the P_{dctA} promoter, Ap^R, Gm^R (GenBank No. KM201426)	This work
pXY2-Phut	pXY2 containing the P_{hut}-*lacZ* protein fusion, Ap^R, Gm^R	This work
pXY3-xylA	pXY3 containing the P_{tac}-*xylA-lacZ* translational fusion, Ap^R, Gm^R	This work
pXY4-xylA	pXY4 containing the P_{dctA}-*xylA-lacZ* translational fusion, Ap^R, Gm^R	This work
pXY5-*crcZ*	pXY5 containing ncRNA gene *pflu5238*, Ap^R, Gm^R	This work
Primer[a]		
lacZF-MCS	A*ACTAGTCCCGGGCTGCAGGATCCAAGCTT*GTCGTTTTAC AACGTCGTGACTGG	*lacZ* amplification
lacZR-KpnI	A*GGTACC*ATAATGGATTTCCTTACGC	
lacZ1	AGGACAGTCGTTTGCCGTC	*lacZ* amplification
lacZ2	GGATTGAAAATGGTCTGCTGC	*lacZ* amplification
lacZ3	GGCTGTGCCGAAATGGTCCA	*lacZ* amplification
lacZ4	GCGTAGTGCAACCGAACGC	*lacZ* amplification
lacZ5	GATGTTGAAGTGGCGAGCG	*lacZ* amplification
InsertSeq-F	GGATCTTGAAGTTCCTATTCCG	Checking insert in pXY1 and pXY2
lacZ6	CTTTCCGGCACCGCTTCTGG	
PhutUAFwd	AAATTT*ACTAGT*GCCTGATCGAACTGACCCAG	P_{hutU} amplification
PhutUR-HindIII	GC*AAGCTT*GTTACCGTGGGCGGCACGGAT	
dctA-NsiI	GG*ATGCAT*GGATCAGCGCGTGGCACATCATGG	pXY4 and pXY5 construction
dctA-TSS	GG*AAGCTT***T**GTCATCCTTATCGCAAACGCCG	pXY4 construction
dctAR-SpeI	GG*ACTAGT***T**GTCATCCTTATCGCAAACGCCG	pXY5 construction
5'xylA-F	G*ACTAGT*ACCGCCAAGAACAATAAGG	Forward primer for cloning P_{xylA} into pXY3
xylA-Hind3	GG*AAGCTT*ACCGCCAAGAACAATAAGGAAAAC	Forward primer for cloning P_{xylA} into pXY4
5'xylA-R	G*AAGCTT*GTCGTAATGGCGAAAGGCGA	Reverse primer for cloning P_{xylA} into pXY3 and pXY4
crcZ-EV1	A*ACTAGT*ACAAAAACAATAACAAGCTTTG	*crcZ* amplification
crcZ-EV3	AACTAGTGCTGCGTTTGTGTTGCGTAC	
lacZ7	ATCTGCCAGTTTGAGGGGAC	Checking insert in pXY3
dctA-race1	ACGTTGACCACGATCAAGCCG	5'-RACE analysis of *dctA*
dctA-race2	GTAGCCGCCGGTTTTGCCGA	
SBW25-glmS	CACCAAAGCTTTCACCACCCAA	Determining the mini-Tn7 insertion in SBW25
Tn7R109	CAGCATAACTGGACTGATTTCAG	(Lambertsen, et al., 2004)

[a] Primer sequences are shown 5' to 3' orientation. Restriction sites incorporated into the primers are italicized and transcriptional start sites are shown in bold.

Chapter 5

Molecular mechanisms of succinate-mediated carbon catabolite repression of *xut* genes for xylose utilization

5.1 Introduction

Expression of catabolic enzymes is controlled by both specific induction (presence or absence of substrates) and general induction (mediated by global regulatory proteins that sense the physiological status of the cell). For the expression of *xut* genes for xylose utilization, data presented in Chapter 3 show the mechanism of specific induction of the *xutAFGH* operon by xylose, which is mediated by the AraC-type activator XutR. In a previous work, Zhang and Rainey (2008) showed that CbrAB is required by *P. fluorescens* SBW25 for growth on xylose as the sole carbon source. CbrAB is a two-component signal transduction system that plays a central role in the global regulation of carbon and nitrogen metabolism. These findings suggest that CbrAB is involved in the control of xylose utilization, but how CbrAB performs this function is unclear.

In the present study, we show that CbrAB plays an essential role in the repression of *xut* genes when xylose co-exists with other preferred carbon substrate(s), such as succinate, a phenomenon known as carbon catabolite repression (CCR) (Görke & Stülke, 2008). CCR allows bacteria to acclimate rapidly to preferred carbon and energy sources thereby maximizing growth rates. The molecular mechanism of CCR has been well studied in enteric bacteria.

E. coli cells preferentially utilize glucose over lactose when both carbon sources are present in the medium: transcription of lactose utilization (*lac*) genes is activated by the catabolite-activating protein (CAP) charged with cAMP, but the adenylate cyclase for cAMP synthesis (and lactose transporter) is inhibited in the presence of glucose. However, it is clear that this CCR model does not hold for non-enteric bacteria,

including *Pseudomonas* (Rojo, 2010). In *Pseudomonas*, succinate (an intermediate of the TCA cycle) is one of the most preferred carbon sources and its presence represses expression of many catabolic pathways, such as lactamide, fructose and glucose (Collier *et al.*, 1996). Repression is mediated by Crc, a potential RNA binding protein (Moreno *et al.*, 2007). This suggests that CCR in *Pseudomonas* occurs at the post-transcriptional level instead of the transcriptional level as in *E. coli*.

This work aims to elucidate the mechanism of CCR in *P. fluorescens* SBW25 using succinate-mediated repression of *xut* genes as a model system. Using a combination of random transposon mutagenesis and site-directed mutagenesis, I have successfully identified the major components that enable the CbrAB system to play its regulatory role in succinate-mediated repression of *xut* genes. These include two small non-coding RNAs genes *crcY* and *crcZ* whose expression is directly regulated by CbrAB; and two regulatory proteins (Crc and Hfq), which form a protein complex repressing expression of catabolic genes via binding to the 5'-end of their respective mRNA transcripts. The role of CrcY and CrcZ in CCR appears to be to sequester the Crc/Hfq complex, thereby relieving repression of the *xut* genes. The data obtained here allow me to propose a regulatory model, which explains how CCR is mediated in *P. fluorescens* SBW25.

5.2 Results

5.2.1 Suppressor analysis of the *cbrB* deletion mutant for xylose utilization

The two-component regulatory system CbrA / CbrB plays an important role in the coordinate expression of genes for nutrient utilization in *P. fluorescens* SBW25. A mutant devoid of *cbrB* was shown previously to be compromised in its ability to utilize a wide range of nutritional substrates, including xylose (Zhang & Rainey, 2008). However, data presented in Chapter 3 show that the *xutAFGH* operon for xylose utilization is regulated by an AraC-type activator (i.e. XutR) in a xylose-dependent manner. The *xutAFGH* promoter region (P_A) has been extensively characterized (see Chapter 3), showing no evidence of direct CbrB-binding to the P_A promoter. This indicates that the effects of CbrB on *xut* expression are mediated by an unidentified factor(s) in the CbrAB regulon.

To identify the predicted unknown activators, Dr. Xue-Xian Zhang has adopted a transposon mutagenesis strategy to select for mutants that have restored their ability to grow on xylose as the sole source of carbon and energy. The suppressor analysis was performed with the Δ*cbrB* mutant (Xut$^-$) using IS-Ω-Km/hah, which harbours an outward promoter at one end and thus can drive expression of cryptic activators (Giddens *et al.*, 2007). Twenty Xut$^+$ mutants were identified from selective agar plates of M9 salt medium supplemented with xylose and nitrofurantoin (to counter select *E. coli*) and Km. The genomic location of the transposon (IS-Ω-Km/hah) insertion was determined using an arbitrary-primed PCR (AP-PCR) strategy followed by DNA sequencing. A total of sixteen mutants were successfully mapped and no putative activator genes were identified: fourteen transposon insertions were mapped to the coding region of *crc*, and the remaining two mutants were located at the *hfq* locus (Figure 5.1). The IS-Ω-Km/hah insertions in *crc* were scattered throughout the entire coding region, clearly indicating that these are loss-of-function mutations. However, two insertions were found within *hfq*: one close to the 3'-end of the coding region and the other in the putative ribosomal binding site. Moreover, *hfq* and the downstream gene *hflX* are separated by only 14 bp. The location and orientation of the IS-Ω-Km/hah transposon suggest that the suppression might be caused by either a loss-of-function mutation in *hfq* or overexpression of *hfq* and / or *hflX*

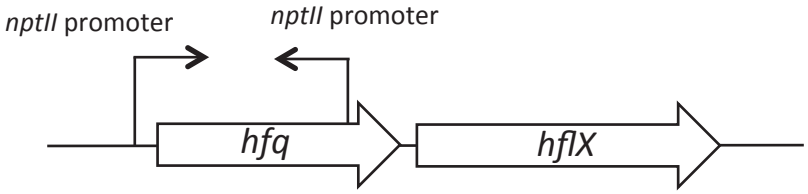

Figure 5.1. Location of transposon insertions at the *hfq* locus of *P. fluorescens* SBW25. Arrows denote the orientation of the *nptII* promoter carried in the transposon.

On the basis of these findings, I used site-directed mutagenesis to verify the results of the transposon mutagenesis. Double deletion mutants (Δ*cbrB*Δ*crc* and Δ*cbrB*Δ*hfq*) were constructed and their ability to grow on xylose was measured in minimal salt medium (MSM) supplemented with xylose as a sole carbon source. As shown in Figure 5.2, the Δ*cbrB* mutant showed no growth whereas the Δ*cbrB*Δ*crc* and Δ*cbrB*Δ*hfq* mutants restored the ability to grow on xylose and reached the similar cell density as the wild type. Together, the data indicate that CbrAB regulates expression of *xut* genes via effects mediated through Crc and Hfq.

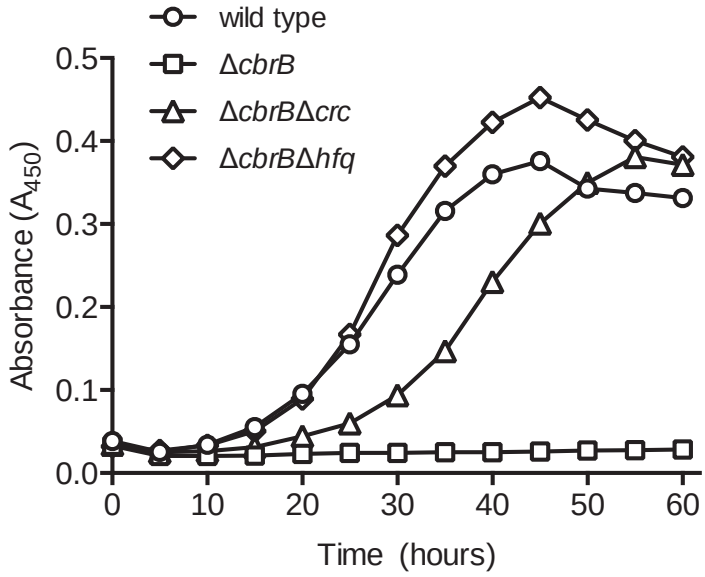

Figure 5.2. Growth dynamics of wild-type SBW25, Δ*cbrB*, Δ*cbrB*Δ*crc* and Δ*cbrB*Δ*hfq* mutants. Growth (OD_{450}) was measured for wild-type SBW25 (circles), the Δ*cbrB* mutant (squares), the Δ*cbrB*Δ*crc* mutant (triangles) and the Δ*cbrB*Δ*hfq* mutant (diamonds) in MSM supplemented with xylose (20 mM) as a sole carbon source. Data are means and standard deviations of six independent cultures. Data were collected at 5-min intervals.

5.2.2 Succinate-mediated CCR of *xut* genes for xylose utilization

Crc is a key regulator of CCR in *Pseudomonas* (Rojo, 2010). Hfq is a RNA chaperone protein required for the stabilization of RNA molecules (Vogel & Luisi, 2011). The finding that Crc is involved in CbrAB-mediated activation of *xut* genes suggests an important physiological role of CbrAB in CCR of *P. fluorescens* SBW25. Indeed, xylose is a non-preferred carbon source as it supports slow bacterial growth. Thus, utilization of xylose is likely to be repressed in the presence of preferred carbon

sources (such as succinate) that can support rapid growth. To elucidate the molecular mechanism of CCR in *P. fluorescens* SBW25, it was necessary to first establish growth and assay conditions suitable for the analysis of CCR and then to investigate the role of Crc in CCR control of the *xut* operons.

5.2.3 Evidence of succinate-mediated CCR of *xut* genes for xylose utilization

To monitor expression of the *xutAFGH* operon, a translational *xutA-lacZ* fusion was constructed by cloning a 460 bp DNA fragment (the promoter region plus 21 nt of the *xutA* coding sequence) into a mini-Tn7 vector pXY2 (Liu *et al.*, 2014). The resulting construct was introduced into wild-type SBW25 by electroporation with the helper plasmid pUX-BF13 (Bao *et al.*, 1991). The native chromosomal *xut* locus was not affected by this modification. β-galactosidase activity of *xutA-lacZ* translational fusions was measured in cells grown in MSM supplemented with xylose only, or succinate and xylose as carbon sources. As shown in Figure 5.3, levels of *xutA-lacZ* expression were 2~5 times lower for cells grown on succinate and xylose compared to those obtained with xylose only over a period of 8 hours after inoculation. However, xylose-grown cells were still in lag phase, showing no increase in cell density whereas cells in "succinate + xylose" entered into log phase (inset graph). The effect of stage of growth on gene expression is undesirable and I thus attempted to eliminate this potentially confounding effect.

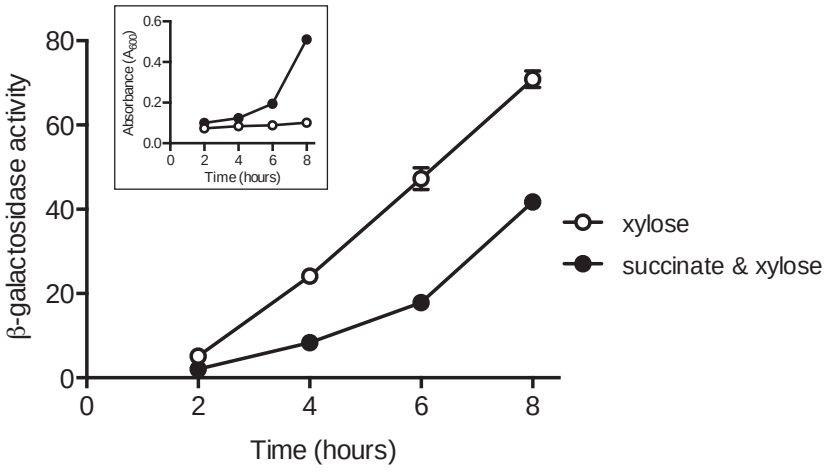

Figure 5.3. Expression of *xutA-lacZ* translational fusions in wild-type SBW25 grown in MSM supplemented with xylose only (open circles), or succinate and xylose (solid circles).

β-galactosidase activity (μM 4MU OD_{600}^{-1} min^{-1}) of the *xutA-lacZ* fusion was measured at different time-points. Data are means and standard errors of three independent cultures. Inset graph: growth dynamics of wild-type SBW25 in xylose only, or succinate and xylose.

Experimental search of a panel of carbon substrates identified glycerol as a carbon source that is capable of supporting rapid growth but producing no effects on xylose utilization. As shown in Figure 5.4, bacteria grew rapidly with the addition of glycerol (inset graph); however, levels of *xutA-lacZ* expression were similar when bacteria were grown in two media: xylose only vs. glycerol + xylose. Together, the data indicate that both succinate and glycerol can support rapid bacterial growth, but only succinate (but not glycerol) exerts CCR responses in *P. fluorescens* SBW25. Therefore, assays for CCR were subsequently performed by growing cells on succinate plus xylose (a "CCR-environment") or glycerol plus xylose (a "non-CCR environment"). In accord with my expectations, the expression level of the *xutA-lacZ* fusion was significantly reduced in cells grown on succinate and xylose compared to those obtained with glycerol and xylose (Figure 5.5). The data clearly indicate that expression of *xutA* is subjected to succinate-mediated CCR.

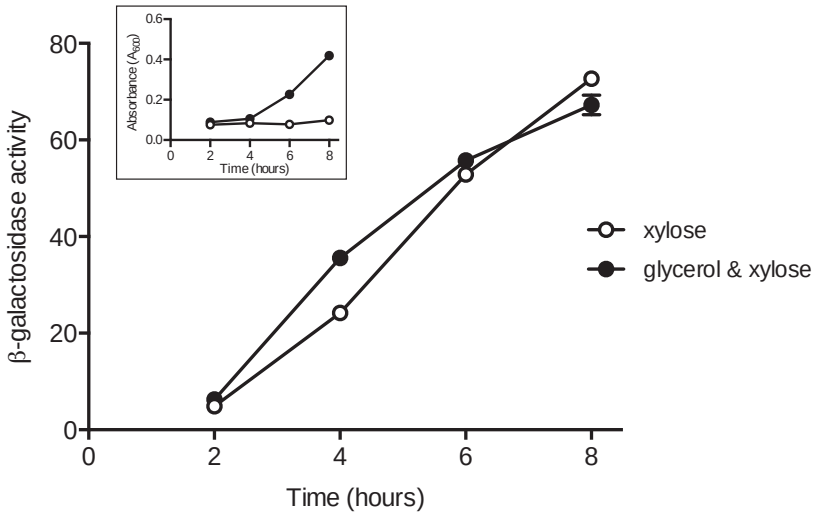

Figure 5.4. Expression of *xutA-lacZ* translational fusion in wild-type SBW25 grown in MSM supplemented with xylose only (open circles), or glycerol and xylose (solid circles). β-galactosidase activity (μM 4MU OD_{600}^{-1} min^{-1}) of the *xutA-lacZ* fusion was measured at different time-points. Data are means and standard errors of three independent cultures. Inset graph: growth dynamics of wild-type SBW25 in xylose only, or glycerol and xylose.

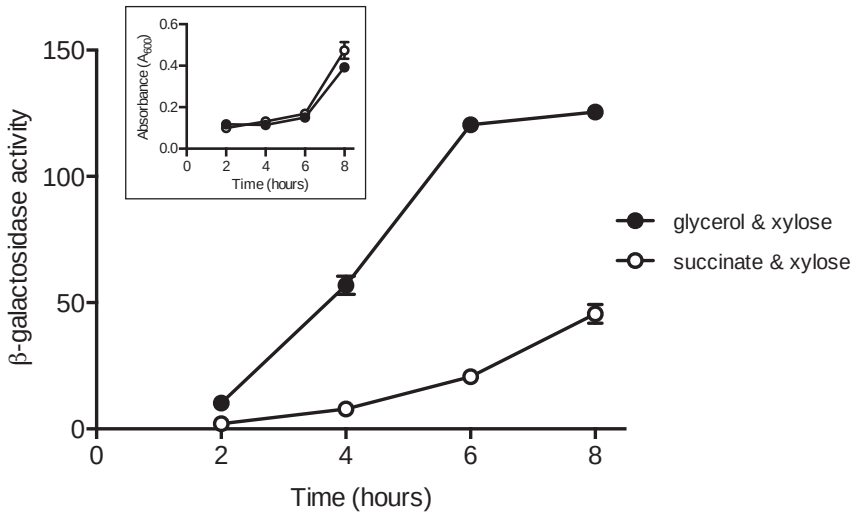

Figure 5.5. Expression of *xutA-lacZ* translational fusion in wild-type SBW25 grown in MSM supplemented with glycerol and xylose (solid circles), or succinate and xylose (open circles). β-galactosidase activity (μM 4MU OD_{600}^{-1} min^{-1}) of the *xutA-lacZ* fusion was measured at different time-points. Data are means and standard errors of three independent cultures. Inset graph: growth dynamics of wild-type SBW25 in glycerol and xylose, or succinate and xylose.

Next, I examined the effect of succinate on expression of *xutR*, a xylose-responsive activator of the *xutA* operon. A *xutR-lacZ* translational fusion was constructed by cloning the 450 bp promoter region with 21 nt of the *xutR* coding region into pXY2 (Liu *et al.*, 2014). The resulting construct was introduced into wild-type SBW25 by electroporation. β-galactosidase activity of the *xutR-lacZ* translational fusion was measured in cells grown in MSM supplemented with glycerol and xylose, or succinate and xylose as carbon sources. As shown in Figure 5.6, β-galactosidase activity of the *xutR-lacZ* fusion was about 1.5 times higher in glycerol medium than in succinate medium. These results indicate that expression of the XutR regulator is also subjected to succinate-mediated catabolite repression.

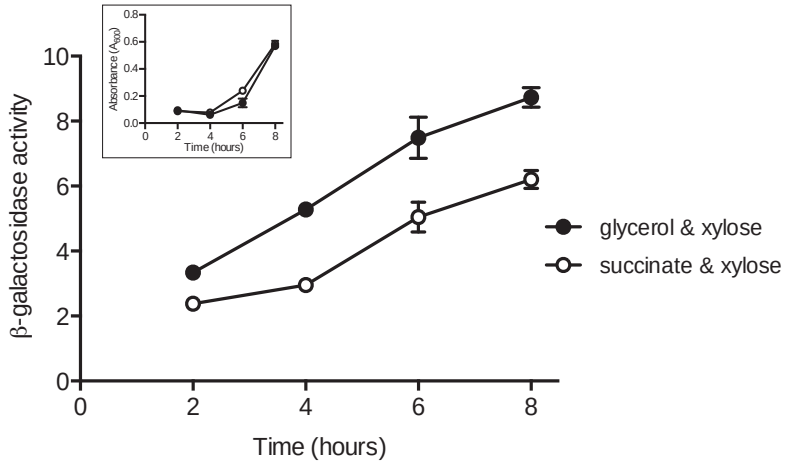

Figure 5.6. Expression of *xutR-lacZ* translational fusions in wild-type SBW25 grown in MSM supplemented with glycerol and xylose (solid circles), or succinate and xylose (open circles). β-galactosidase activity (μM 4MU OD_{600}^{-1} min^{-1}) of the *xutR-lacZ* fusion was measured at different time-points. Data are means and standard errors of three independent cultures. Inset graph: growth dynamics of wild-type SBW25 in glycerol and xylose, or succinate and xylose.

5.2.4 Role of Crc in the CCR control of *xutR* expression

Results of the transposon mutagenesis of the Δ*cbrB* mutant indicate that *xut* genes are negatively regulated by Crc. To confirm the predicted role of Crc in *xutR* expression, the *xutR-lacZ* translational fusion was introduced into wild-type SBW25 and the derived Δ*crc* mutant. β-galactosidase assays were performed in MSM supplemented with glycerol and xylose, or succinate and xylose as carbon sources. As shown in Figure 5.7A, in cells growing exponentially on succinate and xylose (CCR-conditions), *xutR* expression was ~1.5 times higher in the Δ*crc* mutant than wild-type SBW25. By contrast, no significant difference in the expression of *xutR* was observed between wild-type SBW25 and the Δ*crc* mutant when cells were grown on glycerol and xylose (non-CCR-conditions) (Figure 5.7B).

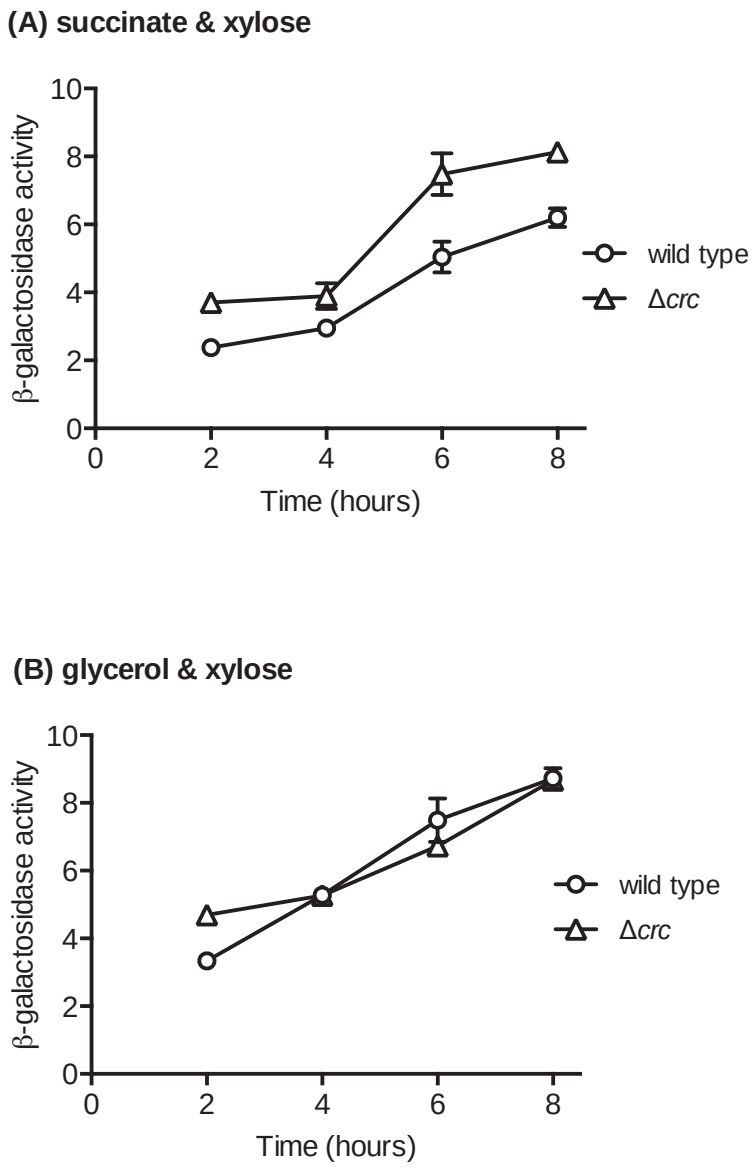

Figure 5.7. Effect of Crc on translation of *xutR*. (A) β-galactosidase activities (μM 4MU OD_{600}^{-1} min^{-1}) of *xutR-lacZ* translational fusions in wild-type SBW25 (circles) and the Δ*crc* mutant (triangles) were measured when cells were grown in MSM supplemented with succinate and xylose. (B) β-galactosidase activities of *xutR-lacZ* translational fusions were measured in wild-type SBW25 and the *Δcrc* mutant grown in MSM supplemented with glycerol and xylose. Data are means and standard errors of three independent cultures.

Next, to determine if repression of *xutR* occurred at the translational level or at the transcriptional level, a *xutR-lacZ* transcriptional fusion was constructed in the genetic background of wild-type SBW25 and the Δ*crc* mutant (see Materials and Methods). The resulting fusion strains were assayed for β-galactosidase activity under the same

CCR and non-CCR conditions. As shown in Figure 5.8, when cells were grown on media containing either succinate and xylose (Figure 5.8A) or glycerol and xylose (Figure 5.8B), *xutR-lacZ* was expressed at similar levels between wild-type SBW25 and the Δ*crc* mutant. The results indicate that Crc-mediated catabolite repression of *xutR* does not occur at the transcriptional level.

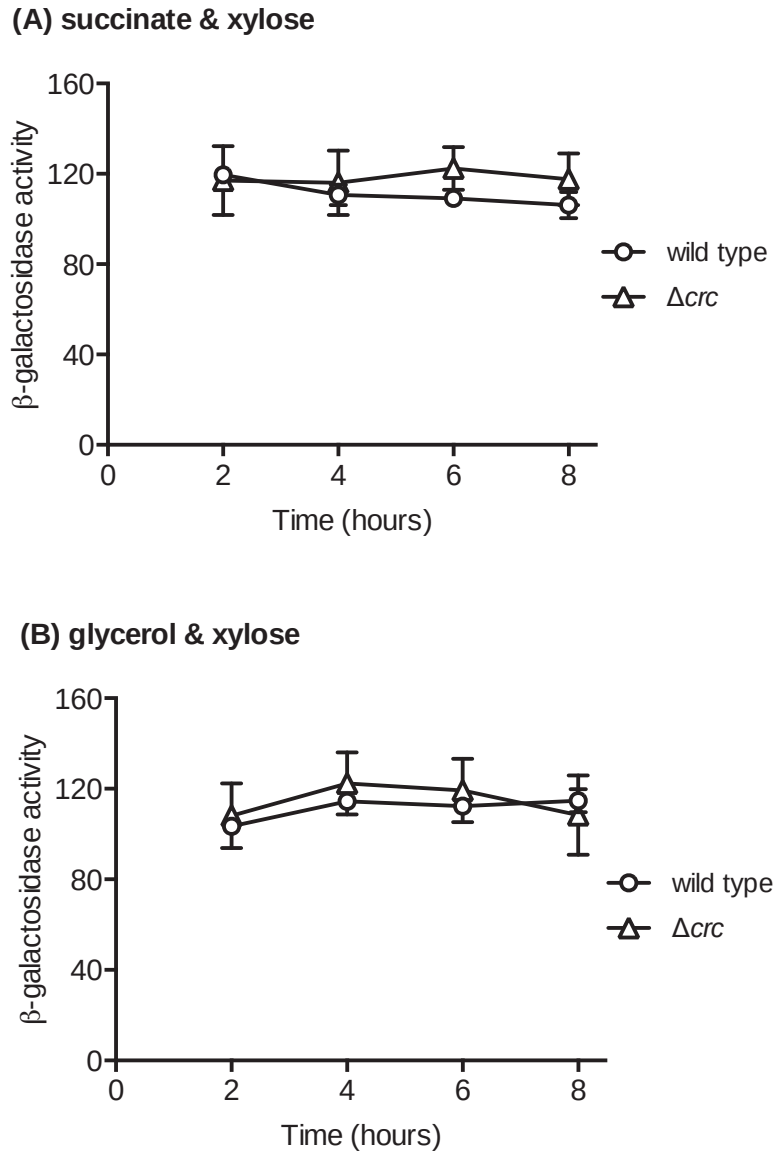

Figure 5.8. Effect of Crc on transcription of *xutR*. (A) β-galactosidase activities (μM 4MU OD_{600}^{-1} min^{-1}) of *xutR-lacZ* transcriptional fusions in wild-type SBW25 (circles) and the Δ*crc* mutant (triangles) were measured in cells grown in MSM supplemented with succinate and xylose. (B) β-galactosidase activities of *xutR-lacZ* transcriptional fusions were measured in wild-type SBW25 and the Δ*crc* mutant grown in MSM supplemented with glycerol and xylose. Data are means and standard errors of three independent cultures.

5.2.5 Role of Crc in the CCR control of *xutA* expression

To investigate the role of Crc in regulation of *xutA*, the *xutA-lacZ* translational fusion was introduced into wild-type SBW25 and the Δ*crc* mutant. Expression of the *xutA-lacZ* translational fusion was monitored by β-galactosidase assays in cells grown in MSM supplemented with succinate and xylose, or glycerol and xylose as carbon sources. As shown in Figure 5.9A, when cells were cultivated on succinate and xylose, *xutA-lacZ* expression in the Δ*crc* mutant was 2~3 times higher than those measured in wild-type SBW25. No significant difference in the expression of *xutA* was observed when bacteria were grown on non-CCR-conditions (i.e. glycerol and xylose; Figure 5.9B).

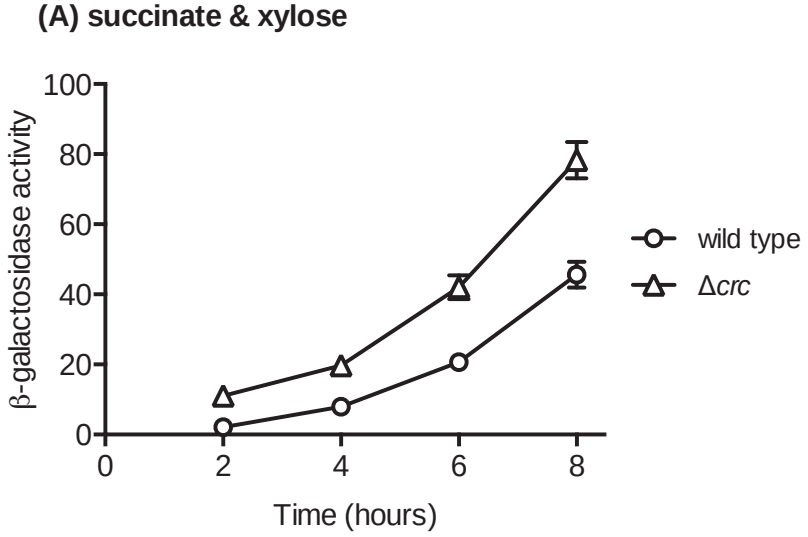

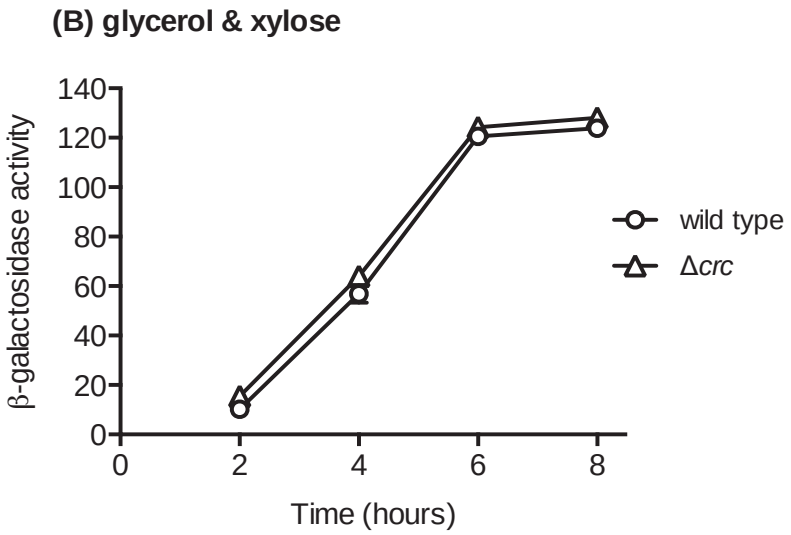

Figure 5.9. Effect of Crc on translation of *xutA*. (A) β-galactosidase activities (μM 4MU OD_{600}^{-1} min^{-1}) of the *xutA-lacZ* translational fusion in wild-type SBW25 (circles) and the Δ*crc* mutant (triangles) were measured when cells were grown in MSM supplemented with succinate and xylose. (B) β-galactosidase activities of the *xutA-lacZ* translational fusion were measured in wild-type SBW25 and the Δ*crc* mutant grown in MSM supplemented with glycerol and xylose. Data are means and standard errors of three independent cultures.

Similar for *xutR*, a *xutA-lacZ* transcriptional fusion was also constructed in the genetic background of wild-type SBW25 and the Δ*crc* mutant, and expression of *xutA* was assayed using cells grown in MSM supplemented with succinate and xylose, or glycerol and xylose as carbon sources. As shown in Figure 5.10A, expression of the *xutA-lacZ* transcriptional fusion was 1.5-2 times higher in the Δ*crc* mutant than wild-type SBW25 when cells were grown on succinate and xylose. On the other hand, there was no significant difference in *xutA-lacZ* expression between the Δ*crc* mutant and wild-type SBW25 when cells were grown on glycerol and xylose (Figure 5.10B). Taken together, these results show that both transcription and translation of *xutA* are repressed by Crc under CCR-conditions (i.e. in the presence of succinate and xylose). This makes sense as *xutA* transcription is regulated by XutR and XutR is subjected to CCR control.

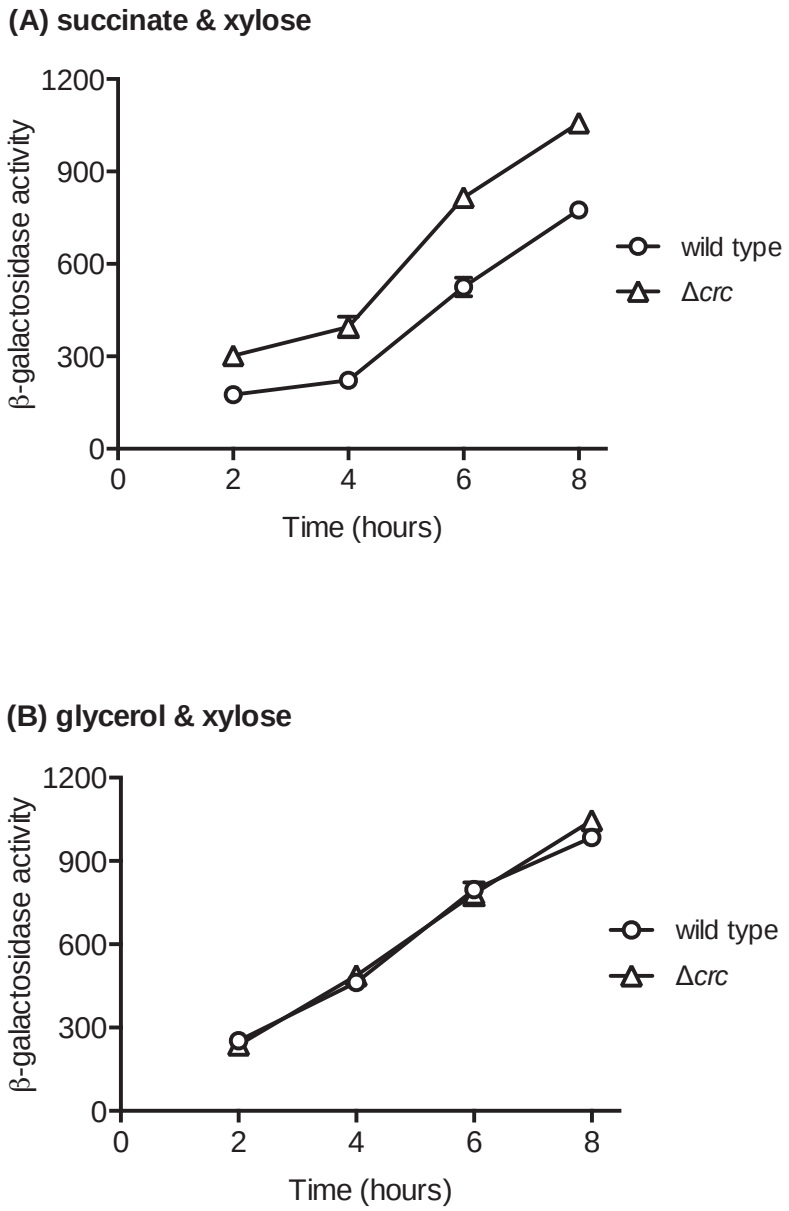

Figure 5.10. Effect of Crc on the transcription of *xutA*. (A) β-galactosidase activity (μM 4MU OD_{600}^{-1} min^{-1}) of the *xutA-lacZ* transcriptional fusion in wild-type SBW25 (circles) and the Δ*crc* mutant (triangles) was measured when cells were grown in MSM supplemented with succinate and xylose. (B) β-galactosidase activity of the *xutA-lacZ* transcriptional fusion was measured in wild-type SBW25 and the Δ*crc* mutant grown in MSM supplemented with glycerol and xylose. Data are means and standard errors of three independent cultures.

5.2.6 Demonstrating the role of Crc in post-transcriptional regulation of *xutA*

In silico analysis of *xutR* and *xutA* sequences showed that the 5'-ends of *xutA* and *xutR* transcripts contain putative Crc-binding sites also identified in other *Pseudomonas* species (Figure 5.11). This suggests that Crc likely represses *xutA* and *xutR* expression via binding to their mRNAs in response to the presence of succinate.

xutR

xutA

Figure 5.11. Nucleotide sequences of translation initiation regions of *xutR* and *xutA*. The transcription start sites of *xutR* and *xutA* are indicated by '+1' and arrowed lines. The translation start sites are marked with underlined letters in bold. The putative Crc-binding sites in *xutR* and *xutA* are boxed.

Data presented above showed that both transcription and translation of *xutA* are elevated in the Δ*crc* mutant under CCR-conditions. The inhibitory effect of Crc on *xutA* expression could be indirect due to Crc-mediated translational repression of the XutR regulator. However, a putative Crc-binding site is also present in the translation initiation region of *xutA*, suggesting that Crc directly inhibits expression of *xutA* by binding to its mRNA. To determine whether translation of *xutA* is directly or indirectly controlled by Crc, a *xutA-lacZ* translational fusion was made in a new mini-Tn7 vector pXY3 (Liu *et al.*, 2014). A 108 bp DNA fragment defined by the *xutA* transcription start site and the 81st nt of the *xutA* coding region was obtained by PCR amplification and cloned into pXY3, producing plasmid pXY3-*xutA*. The resultant *xutA-lacZ* fusion was transcribed under the control of IPTG-inducible P_{tac} promoter and transcription starts from the previously determined *xutA* transcriptional start site (Figure 5.12). Notably, the XutR-binding site is absent in pXY3-*xutA*, and transcription of the *xutA-lacZ* fusion is independent of the XutR regulator (and xylose

in the medium). Thus, pXY3-*xutA* is suitable for studying post-transcriptional regulation of the *xutA* operon

The fusion pXY3-*xutA* was introduced into wild-type SBW25 and the Δ*crc* mutant by electroporation. β-galactosidase activity of the *xutA-lacZ* translational fusion was measured in cells grown in MSM supplemented with succinate (20 mM) and IPTG (50 μM). As shown in Figure 5.13, β-galactosidase activity of the Δ*crc* mutant was 1.3-fold higher than that of wild-type SBW25. Given that the Δ*cbrB* mutant was unable to grow on xylose but the Δ*cbrB*Δ*crc* mutant restored growth ability (Figure 5.2), it is predicted that Crc is probably fully active in the Δ*cbrB* mutant, producing strong repression of *xut* genes. To test this, pXY3-*xutA* was introduced into the Δ*cbrB* and Δ*cbrB*Δ*crc* mutants, and monitored by β-galactosidase assays under the same growth conditions. As expected, expression of the *xutA-lacZ* fusion was 5~6 times lower in the Δ*cbrB* mutant than wild-type SBW25 (Figure 5.13). This suggests that Crc is fully active and inhibits translation of *xutA* in the Δ*cbrB* mutant. In addition, *xutA-lacZ* expression increased approximately 6-fold in the Δ*cbrB*Δ*crc* mutant compared to the Δ*cbrB* mutant. These results indicate that Crc directly represses translation of *xutA*.

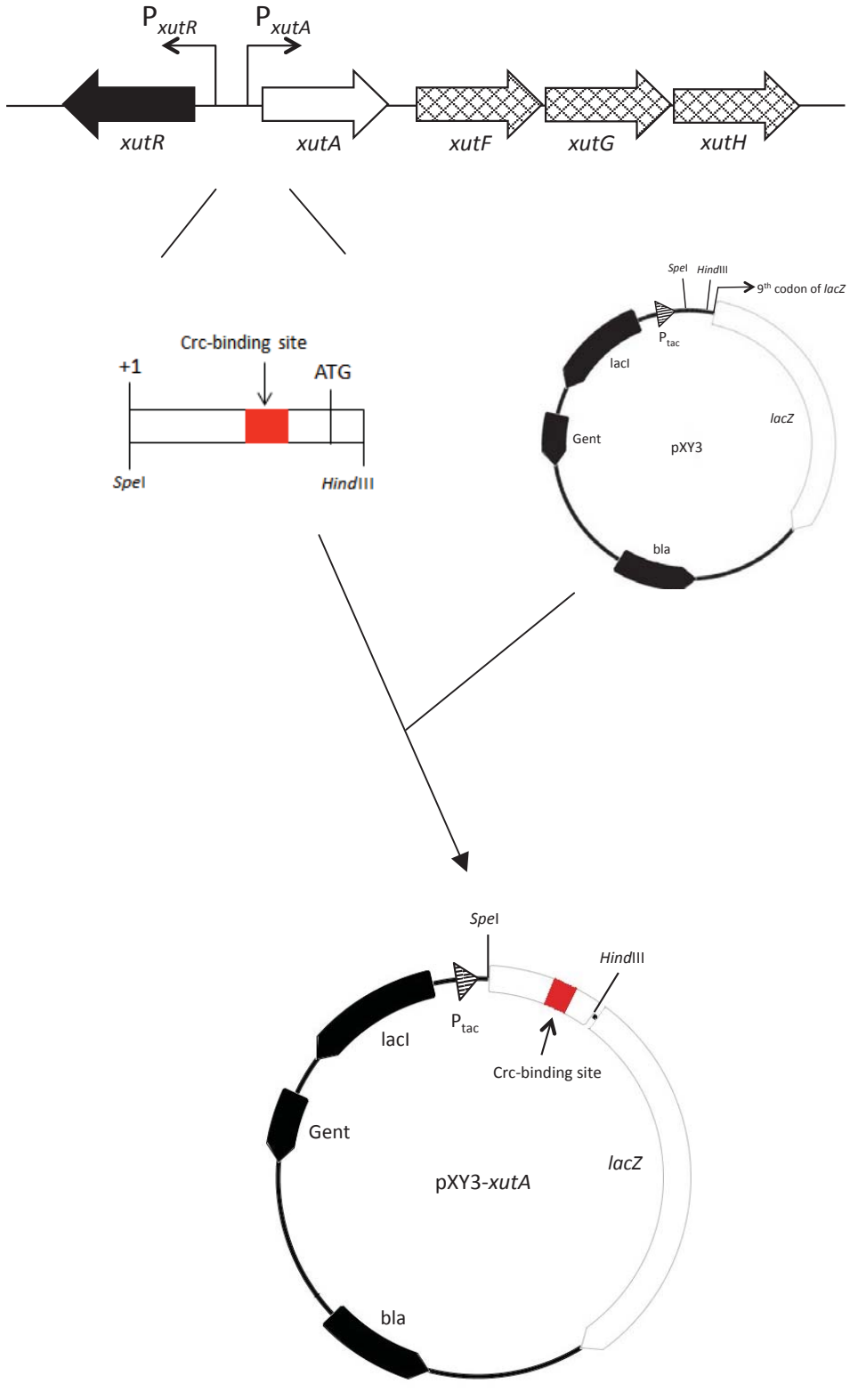

Figure 5.12. Construction of pXY3-*xutA*. A DNA fragment which includes the transcription start site of *xutA*, the Crc-binding site and a part of *xutA* coding region was obtained by PCR and ligated to the 9th codon of *lacZ* gene in pXY3. The expression of *xutA* is under the control of the P_{tac} promoter in pXY3.

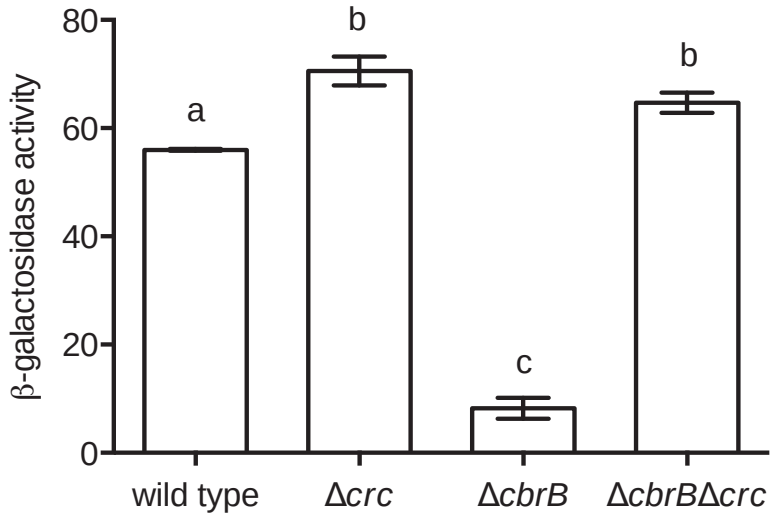

Figure 5.13. Effect of Crc on expression of pXY3-*xutA*. β-galactosidase activities (μM 4MU OD_{600}^{-1} min^{-1}) of *xutA-lacZ* translational fusions (pXY3-*xutA*) in wild-type SBW25, Δ*crc*, Δ*cbrB* and Δ*cbrB*Δ*crc* mutants were measured in MSM supplemented with succinate as a sole carbon source at mid-exponential phase (OD_{600} = 0.4~0.5). The expression of *xutA* was induced by the addition of IPTG (50 μM). Data are means and standard errors of three independent cultures. One-way ANOVA revealed a significant difference among means [$F_{(3,8)}$ = 224.6, $P < 0.0001$]. Bars that are not connected by the same letter (shown above bars) are significantly different ($P < 0.05$) by Tukey's HSD.

5.2.7 Molecular interaction between Crc and *xut* mRNAs: overexpression and purification of Crc protein

To demonstrate the predicted Crc binding *in vitro* with *xutA* and *xutR* mRNAs, the first step was to purify Crc protein from *P. fluorescens* SBW25. This was achieved by cloning the *crc* gene into plasmid pTrc99A. Plasmid pTrc99A is a general cloning vector that has been widely used for the regulated expression of genes in *Escherichia coli* (Amann et al., 1988). It has a strong hybrid *trp*/*lac* (*trc*) promoter whose activity is repressed by the $LacI^q$ repressor (Figure 5.14). Expression of the cloned gene is induced by addition of IPTG in growth media. There is a unique *Nco*I restriction site (CCATGG) located 8 bp downstream of the *lacZ* ribosomal binding site (RBS) for cloning. It also provides the ATG start codon for gene translation.

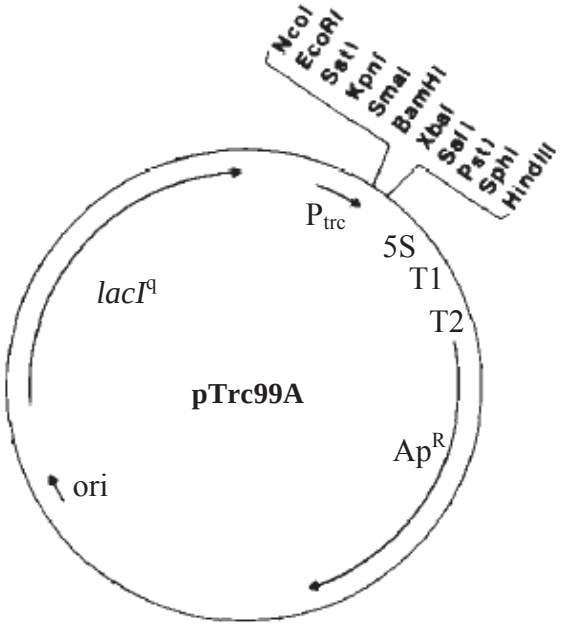

Figure 5.14. The map of pTrc99A expression vector (Amann et al., 1988). ori: origin of replication. $lacI^q$: autorepressor. P_{trc}: trc promoter. 5S: 5S rRNA. T1&T2: transcriptional terminator of the *rrnB* operon. Ap^R: ampicillin resistance gene. Direction of transcription and orientation of genes are indicated by arrows.

To express the *crc* gene in pTrc99A, a pair of primers Crc_ProF (5' – GCCATGGGCCGGATCATCAGTGTGAACGTT – 3') and Crc_ProR (5' – GAAGCTTTCA**GTGGTGGTGGTGGTGGTG**GATGGTCAATGTCCAGTCGTA – 3') was designed to amplify the coding region of *crc* from *P. fluorescens* SBW25. Restriction sites *Nco*I and *Hind*III (underlined) were incorporated into the primers to facilitate directional cloning. A C-terminal hexa-histidine tag (shown in bold letter) was incorporated for subsequent purification of Crc proteins.

A ~790 bp DNA fragment was amplified by PCR and cloned into pCR8/GW/TOPO® vectors (Invitrogen) following the manufacturer's instruction. After sequence identity was verified by DNA sequencing, the *crc* fragment was cloned into *Nco*I/*Hind*III-digested pTrc99A. The resulting plasmid was designated pTrc99A-*crc*. Restriction analysis of pTrc99A-*crc* produced two bands: a 4.2 kb band for the vector pTrc99A and a 790 bp fragment insert for *crc* (Figure 5.15).

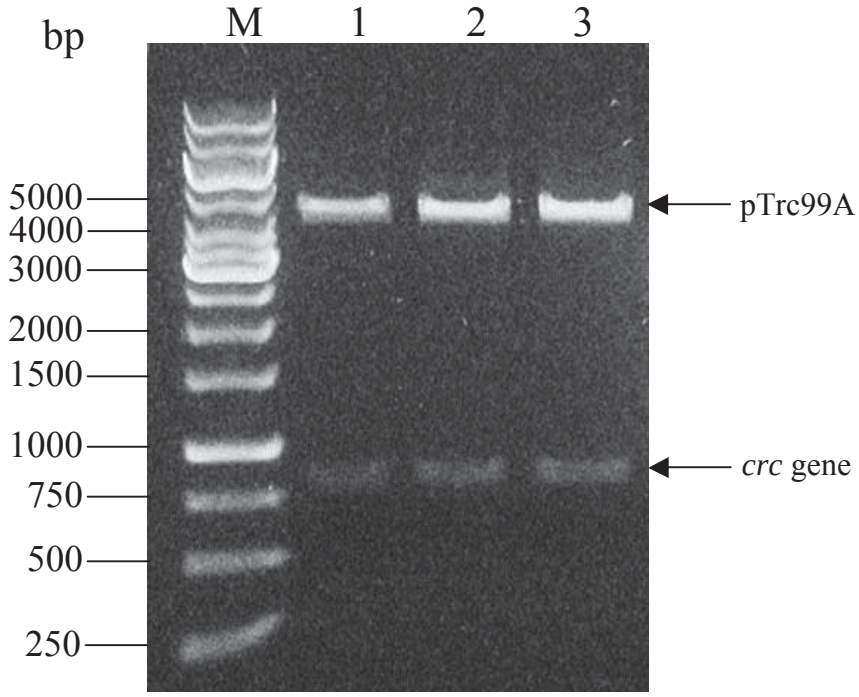

Figure 5.15. Restriction enzyme digestion of pTrc99A-*crc*. Expression plasmid pTrc99A-*crc* was digested with *Nco*I and *Hind*III. Lane 1-3: pTrc99A-*crc* cut with both *Nco*I and *Hind*III. M: 1kb DNA ladder.

5.2.7.1 Small-scale expression and solubility test of Crc protein

To test whether Crc protein can be induced by IPTG, plasmids pTrc99A-*crc* and pTrc99A were transformed into *E. coli* BL21 (DE3). Cells were grown in 20 ml LB broth to OD_{600} of 0.6 – 0.7 and expression of *crc* was induced by 1.0 mM IPTG at 37ºC. After 4 hours induction, aliquots of cells were taken and subjected to SDS-PAGE analysis. Results are shown in Figure 5.16. An additional protein band at the molecular weight of ~30 kDa was observed in cells harbouring pTrc99A-*crc* (lane 2) and it was absent in the control pTrc99A (lane 1). The predicted molecular weight of His_6-Crc is 29.8 kDa. The ~ 30 kDa protein is most likely the desired Crc protein.

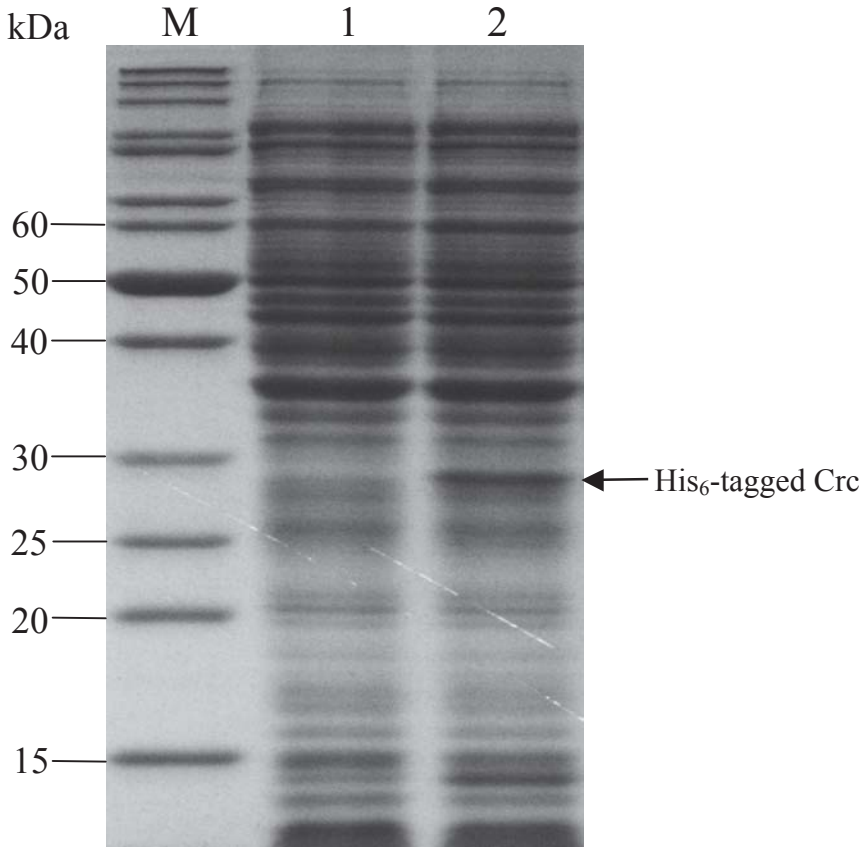

Figure 5.16. SDS-PAGE analysis of Crc expression at 37ºC. Total cellular bacterial proteins were separated by 12% SDS-PAGE and visualized by staining with Coomassie blue. M: protein molecular marker. Lane 1: whole cell of *E. coli* BL21 (DE3) containing pTrc99A. Lane 2: whole cell of *E. coli* BL21 (DE3) containing pTrc99A-*crc*.

To prepare Crc from the soluble fraction of the cell extract, IPTG-induced cells were treated with lysozyme and disrupted by sonication. The soluble and insoluble fractions were then analysed by SDS-PAGE. The intensity of the band representing Crc was strong in the insoluble fraction whereas it was weak in the soluble fraction (lane 2 and 3, Figure 5.17). The result indicates that Crc is partially soluble when it is overexpressed at 37ºC.

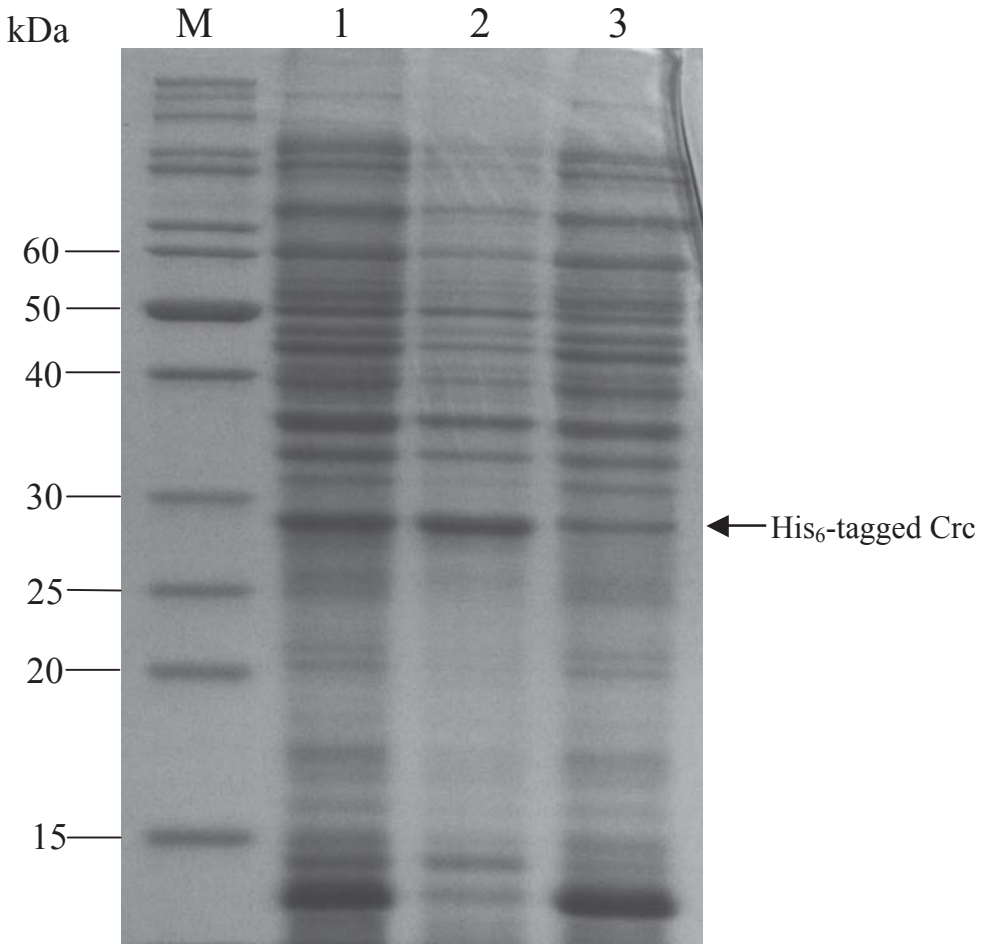

Figure 5.17. SDS-PAGE analysis of the solubility of expressed Crc protein. Bacterial cells were induced with 1.0 mM IPTG at 37ºC. The induced cells were lysed. The insoluble and soluble fractions were separated by centrifugation and analysed by 12% SDS-PAGE. Lane 1: induced whole cell lysate. Lane 2: insoluble fraction of cell lysate. Lane 3: soluble fraction of cell lysate. M: protein molecular weight marker.

5.2.7.2 Large-scale expression and purification of Crc

To prepare a large amount of Crc for biochemical analysis, *E. coli* BL21 (DE3) containing pTrc99A-*crc* was grown in 500 ml LB broth in a two-litre flask. After induction with IPTG (1.0 mM) cells were harvested and lysed with lysozyme and sonication. The soluble and insoluble fractions of the cell lysate were separated by centrifugation. His_6-tagged Crc proteins were purified from the soluble fraction of cell lysate using immobilized metal affinity chromatography resin (IMAC) charged with cobalt ions. Eluted fractions from a cobalt-IMAC gravity column were analysed by SDS-PAGE. As shown in Figure 5.18, Crc was eluted with 200 mM imidazole and was more than 95% pure as judged by SDS-PAGE. It was then concentrated using Vivaspin 6 concentrators with 10 kDa molecular weight cut-off.

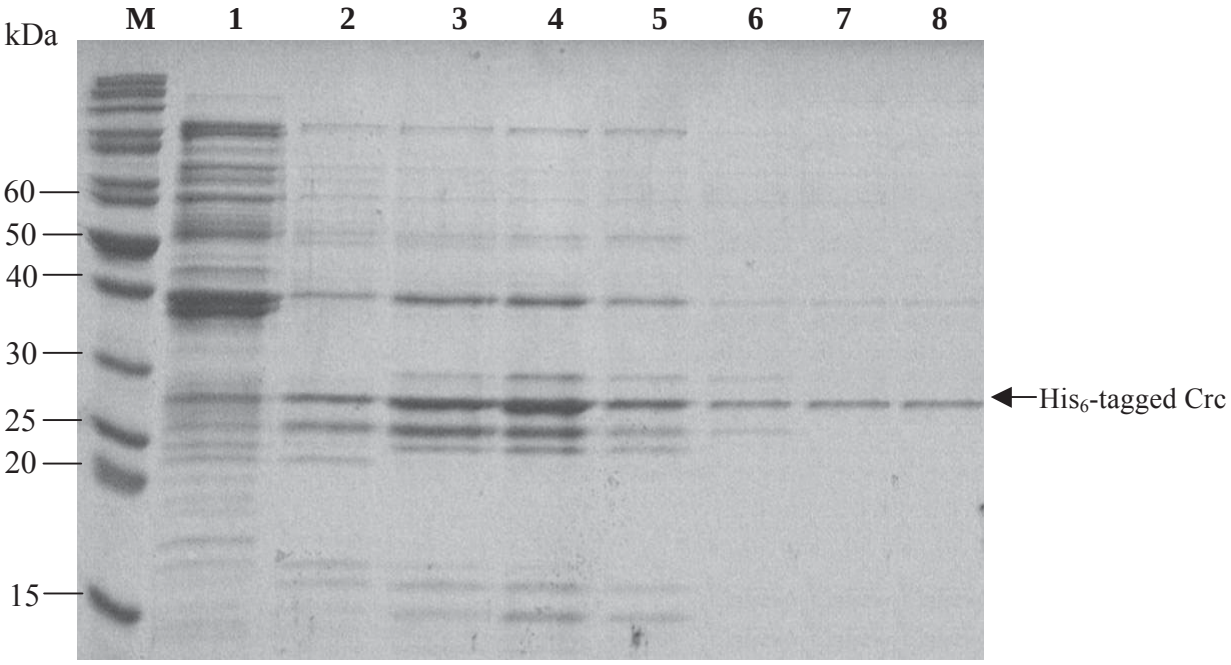

Figure 5.18. Purification of His_6-Crc using cobalt-IMAC. The soluble fraction of cell lysate was loaded to a gravity column containing IMAC resin charged with cobalt ions. The column was washed and eluted with buffer containing a stepped imidazole gradient. The eluted fractions were analysed by 12% SDS-PAGE. M: protein molecular weight marker. Lane 1: soluble fraction of cell lysate. Lane 2: wash fraction with 10 mM imidazole. Lane 3: wash fraction with 50 mM imidazole. Lane 4-8: fractions from elution step with 200 mM imidazole.

5.2.8 Molecular interaction between Crc and *xut* mRNAs: Crc binds to *xutR* and *xutA* mRNAs *in vitro*

xutR and *xutA* mRNA fragments used in this study were synthesized by *in vitro* transcription (see Materials and Methods). As shown in Figure 5.19, both *xutR*(1-122) and *xutA*(1-112) contain a putative Crc-binding site. The mRNA fragments were 3' end-labelled with biotin and then subjected to electrophoretic mobility shift assays (EMSAs) using the purified His_6-Crc. Results are shown in Figure 5.20, a single band (free *xutR* or *xutA*) was observed in the absence of Crc (lane 1). An additional band with lower mobility was observed when Crc was added. This band corresponds to a complex of Crc and *xutR* or *xutA* mRNAs. Significantly, band intensity of the Crc/RNA complex gradually increased along with increasing concentration of Crc (lane 2 to 6). Meanwhile, the intensity of free *xutR* or *xutA* mRNAs gradually decreased with increasing concentration of Crc. The binding activity was specific as addition of an excess amount of the same unlabelled RNA fragments almost abolished binding (lane 7). As a negative control, BSA was unable to interact with RNA fragments (lane 8). These results indicate that Crc is able to specifically bind to both *xutR* and *xutA* mRNAs.

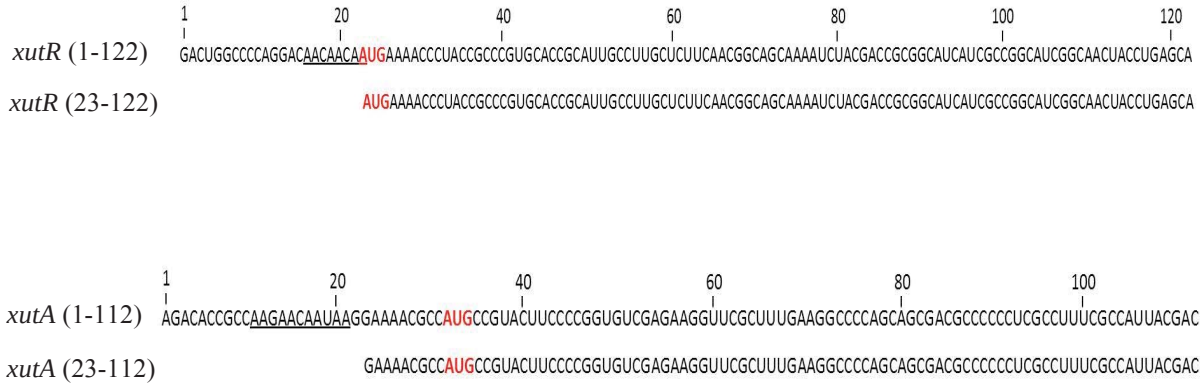

Figure 5.19. *xutA* and *xutR* mRNA fragments used in EMSAs. The putative Crc-binding site (the A-rich sequence) in *xutA* and *xutR* mRNA is underlined. The AUG translation start codon is marked in red.

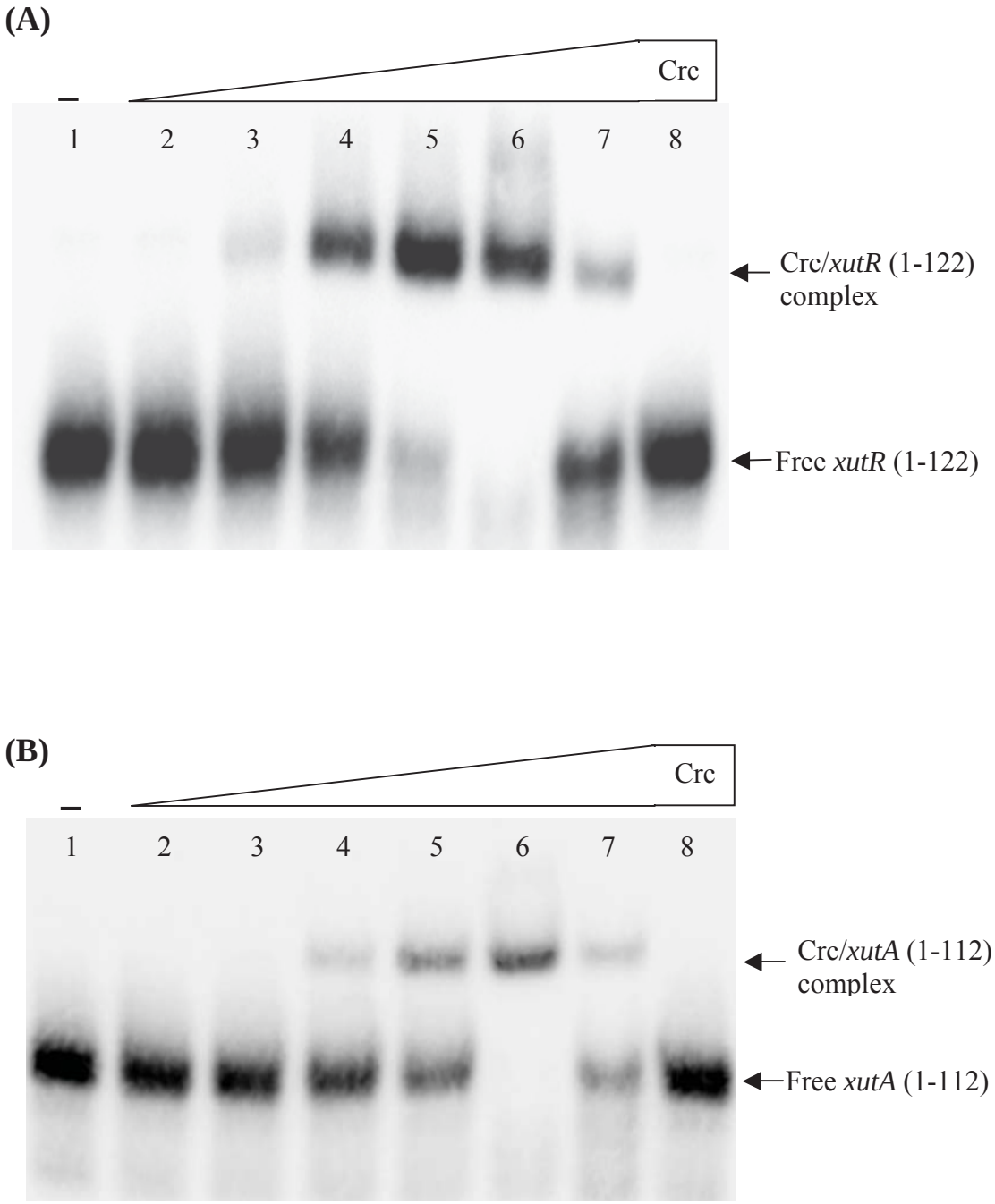

Figure 5.20. Binding of Crc to *xutR* (A) or *xutA* (B) mRNA *in vitro*. EMSA reaction contained 3' end biotin-labelled *xutR* or *xutA* mRNA, 1 µg of yeast tRNA and varying concentrations of purified Crc. The concentrations of Crc in lane 1 to 7 were 0, 50, 100, 200, 400, 800 and 800 nM, respectively. Unlabelled *xutR* or *xutA* mRNA was added as a specific competitor in lane 7. BSA (instead of Crc) was used in lane 8 as a negative control. Protein-RNA complexes were resolved on a 6% nondenaturing polyacrylamide gel. The positions of free *xutR* or *xutA* mRNA and Crc-bound *xutR* or *xutA* complexes are indicated.

To determine whether the A-rich sequence near the translation initiation region of *xutA* and *xutR* is required for Crc binding, two short transcripts [*xutR* (23-122) and *xutA* (23-112)] without the A-rich sequence for putative Crc binding (Figure 5.19) were synthesized by *in vitro* transcription and then end-labelled with biotin. The ability of purified Crc to bind to these short transcripts was analysed by EMSA and the results are shown in Figure 5.21. Only one band corresponding to free mRNAs was observed with and without the addition of Crc. Crc was unable to interact with these short transcripts. These results indicate that the A-rich sequence is essentially required for Crc binding to the *xutR* and *xutA* transcripts.

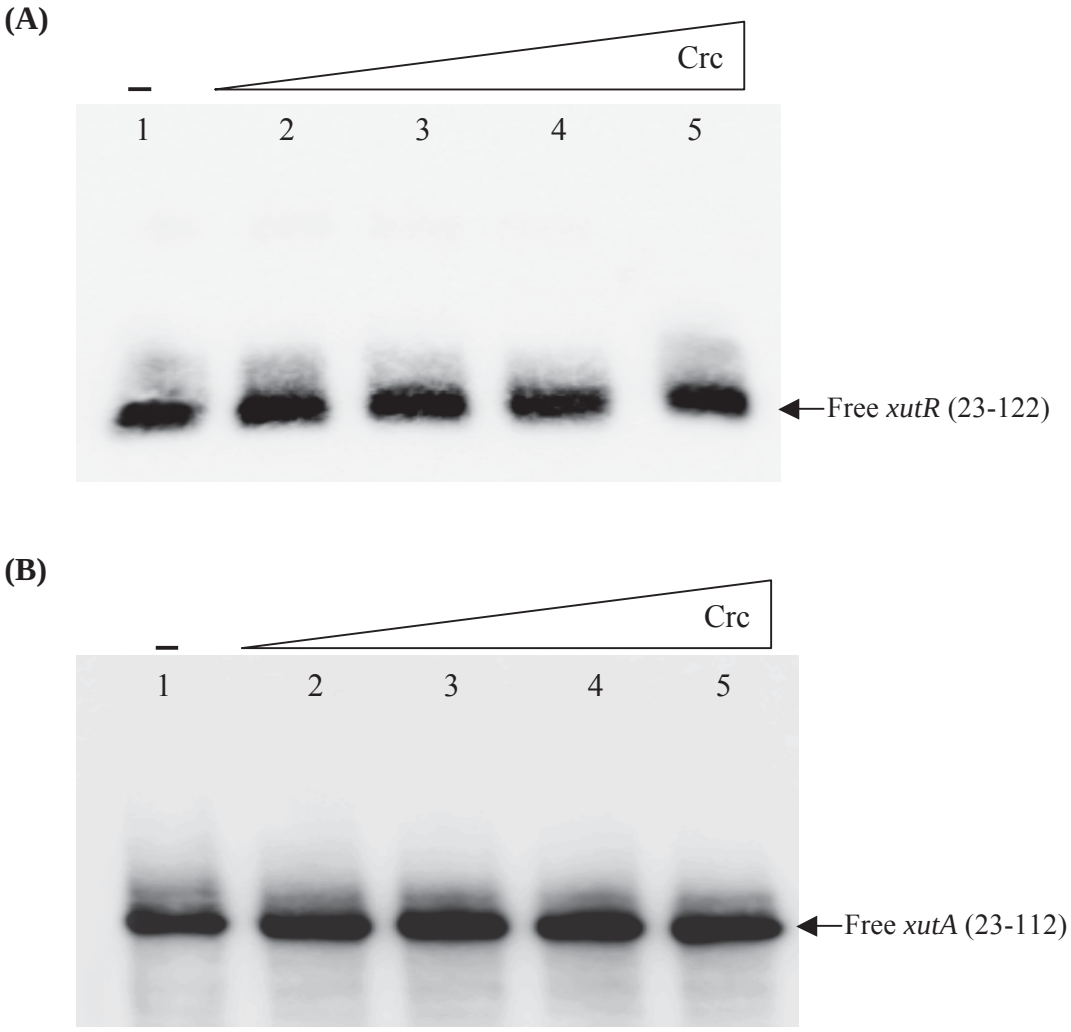

Figure 5.21. Binding of Crc to short *xutR* (A) or *xutA* (B) mRNA *in vitro*. EMSA reaction contained 3' end biotin-labelled *xutR* (23-122) or *xutA* (23-112) transcripts, 1 μg of yeast tRNA and purified Crc. The concentrations of Crc in lane 1 to 5 were 0, 100, 200, 400, 800 nM, respectively. The positions of free *xutR* or *xutA* transcripts are indicated.

5.2.9 Identification of two small non-coding RNAs under the control of CbrAB

In *P. aeruginosa*, CbrB activates a non-coding RNA (*crcZ*), which de-represses the Crc activity (Sonnleitner *et al.*, 2009). If the same holds for *P. fluorescens* SBW25, I would expect a Xut$^-$ phenotype for the Δ*crcZ* mutant. However, in previous work (Zhang *et al.*, 2010), we have shown that *crcZ* encodes a non-coding RNA under the control of CbrAB, but the *crcZ* deletion mutant did not show any of growth defects that were observed for Δ*cbrB*, including xylose utilization. This led to an interrogation of the SBW25 genome and identification of a *crcZ* homologue located in the intergenic region between *pflu3887* and *pflu3888* (termed *crcY*). It is predicted that CrcY could be functionally redundant and thus be able to complement the *crcZ* gene deletion. Indeed, when a double deletion mutant Δ*crcY*Δ*crcZ* was constructed, it showed no growth on xylose. By contrast, mutants devoid of either *crcY* or *crcZ* grew normally as the wild-type strain (Figure 5.22).

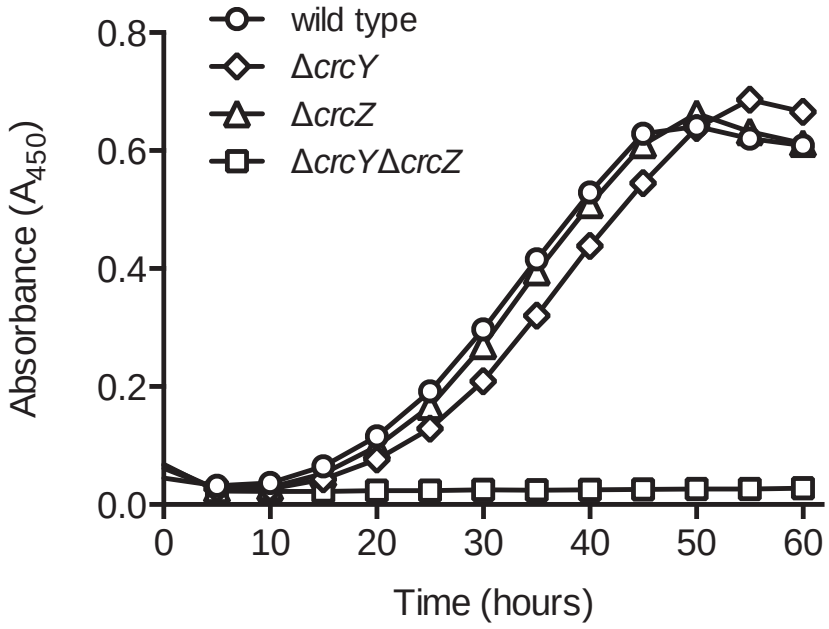

Figure 5.22. Growth dynamics of wild-type SBW25, Δ*crcY*, Δ*crcZ* and Δ*crcY*Δ*crcZ* mutants on xylose. Growth (OD_{450}) was measured for wild-type SBW25 (circles), mutants Δ*crcY* (diamonds), Δ*crcZ* (triangles), and Δ*crcY*Δ*crcZ* (squares) in MSM supplemented with xylose (20mM) as a sole carbon source. Results are means and standard deviations of six independent cultures. Data were collected at 5-min intervals

It was subsequently shown that *crcZ* is transcribed from a σ^{54}-type promoter (P_{crcZ}); deletion of *cbrB* compromised the promoter activity (Zhang *et al.*, 2010). To investigate the *crcY* promoter, the transcriptional start site of *crcY* was determined by 5'-RACE analysis (see Materials and Methods). Results are shown in Figure 5.23. Immediately upstream of the transcription start site of *crcY* is a short DNA sequence (TGGCAC-N5-CTGCT) that shows strong similarity to the consensus σ^{54}-dependent promoter (TGGCAC-N5-TTGCW).

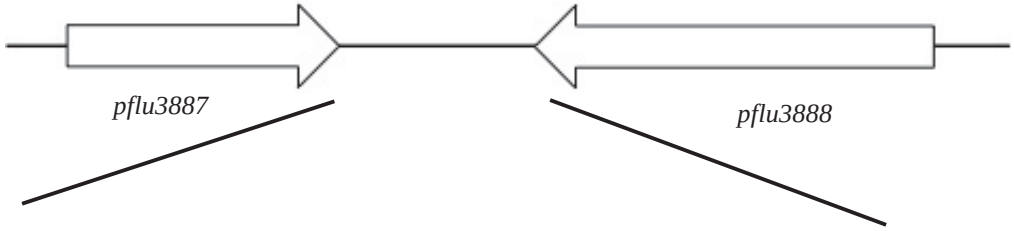

pflu3887 (stop codon)

TTGAGTAGCGTAGCCGTGACAATGTGTTACCGCACGTCTACACATCGAGTA

ACACGGGAACATATTTTGTCGTATTTGCCGCAGGACATTTCCCACCAAAAA

ATCAAGCCACTGATTTTAAAGGCTTTTTAAAAGTTGGCACGGCTTCTGCTA

-24 -12

TCTCTATGGCATAACAAGAATAAAAAGCACCAAGCCTAATAAAAATAAGA

+1

CGAAACGACTCTGACATAACAAAAACAACACGGCAGAGACGCAGCTAAC

AGATTTTTTTGGAGAAGATGTGCTTCGCAGGGTACGGCGTGCCGAAACCCG

CAACCGGTTAGAGAAAAATAAAACTACCTCAGGTAGCTACCCACTGGTTG

GATCGATAACGAAGAAGCAGATCAGCGCTCAAAAAAATACGTTTGCTCTT

GACCCCGAATGGGGGTCGCCCAAAACAGCGGTAAAGGGTAACGGTTGCCA

AAAACAACAATAGACCGCCCCTCAATAATAAAAAAAGAGCACGCAACGA

CAAATTAAAGGGGACCCTCGGGTCCCCTTTGTGCTTTCTGCGTTTCGTTCAT

GTGTTGATTCACCGCAGCCAACATGTGAGGGAGCAAGCCCCCTGCCTCATG

GGTTCTGTGGTGTTA

pflu3888 (stop codon)

Figure 5.23. Location of *crcY* in *P. fluorescens* SBW25. The transcription start site of *crcY* determined by 5'-RACE analysis is indicated by '+1' and an arrowed line. Predicted σ^{54}-type promoter is underlined. Predicted transcriptional terminator is indicated by inverted arrows.

To test if CbrB is the σ^{54} activator required for *crcY* expression, a transcriptional *crcY-lacZ* was constructed by cloning the *crcY* promoter region into pUIC3 (Rainey, 1999). The resulting plasmid was mobilized and integrated into the genome of wild type SBW25 and its derived Δ*cbrB* mutant. β-galactosidase activity was measured in cells grown under non-CCR-conditions, i.e., MSM with xylose and glycerol. Results showed that *cbrB* deletion caused a ~20-folds reduction in *crcY* expression (Figure 5.24). Together, the data indicate that CbrAB activates expression of both *crcY* and *crcZ*.

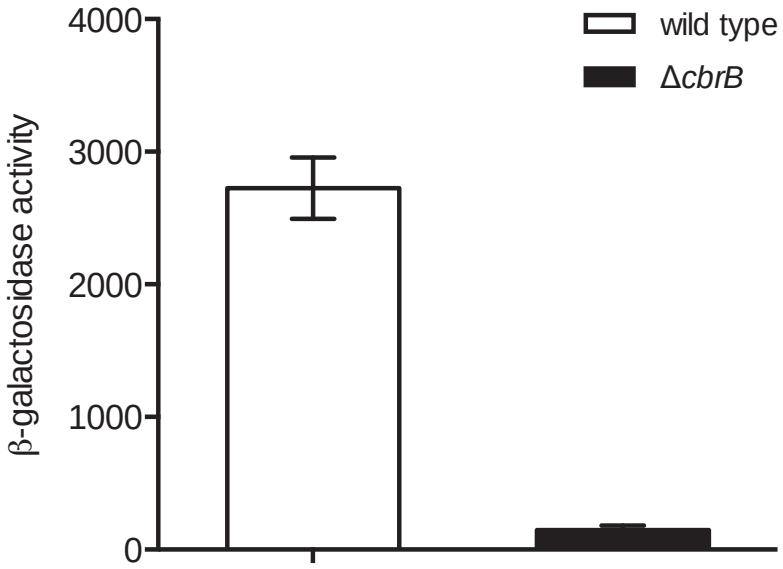

Figure 5.24. Expression of *crcY* is activated by CbrB. β-galactosidase activity (μM 4MU OD_{600}^{-1} min^{-1}) of *crcY-lacZ* transcriptional fusions was measured in wild-type SBW25 and the Δ*cbrB* mutant grown in MSM supplemented glycerol (20mM) plus xylose (20mM) at mid-exponential phase. Data are means and standard errors of three independent cultures. The t-test shows a significant difference among means ($P < 0.0001$).

5.2.10 Molecular interaction between Crc protein and CrcY and CrcZ

The predicted secondary structures of CrcY and CrcZ are shown in Figure 5.25 and Figure 5.26, respectively. Both contain a total of six A-rich sequences that are located in the unpaired region for putative Crc binding. To demonstrate Crc binding to CrcY and CrcZ *in vitro*, EMSA was performed using biotin-labelled CrcY and CrcZ.

Results are shown in Figure 5.27. A single band (free CrcY or CrcZ) was observed in the absence of Crc (lane 1). A smear band with lower mobility was observed and its intensity increased with increasing concentration of Crc. Meanwhile, the band intensity of free CrcZ or CrcY was gradually decreased with increasing concentration of Crc. The smeared band corresponds to a complex of Crc and CrcZ or CrcY. The protein/RNA complex was barely visible with addition of unlabelled CrcY or CrcZ at excess (lane 8), suggesting that the binding is specific. Together, the data indicate that both CrcY and CrcZ can bind to Crc and thus relieve Crc-mediated repression of catabolic genes.

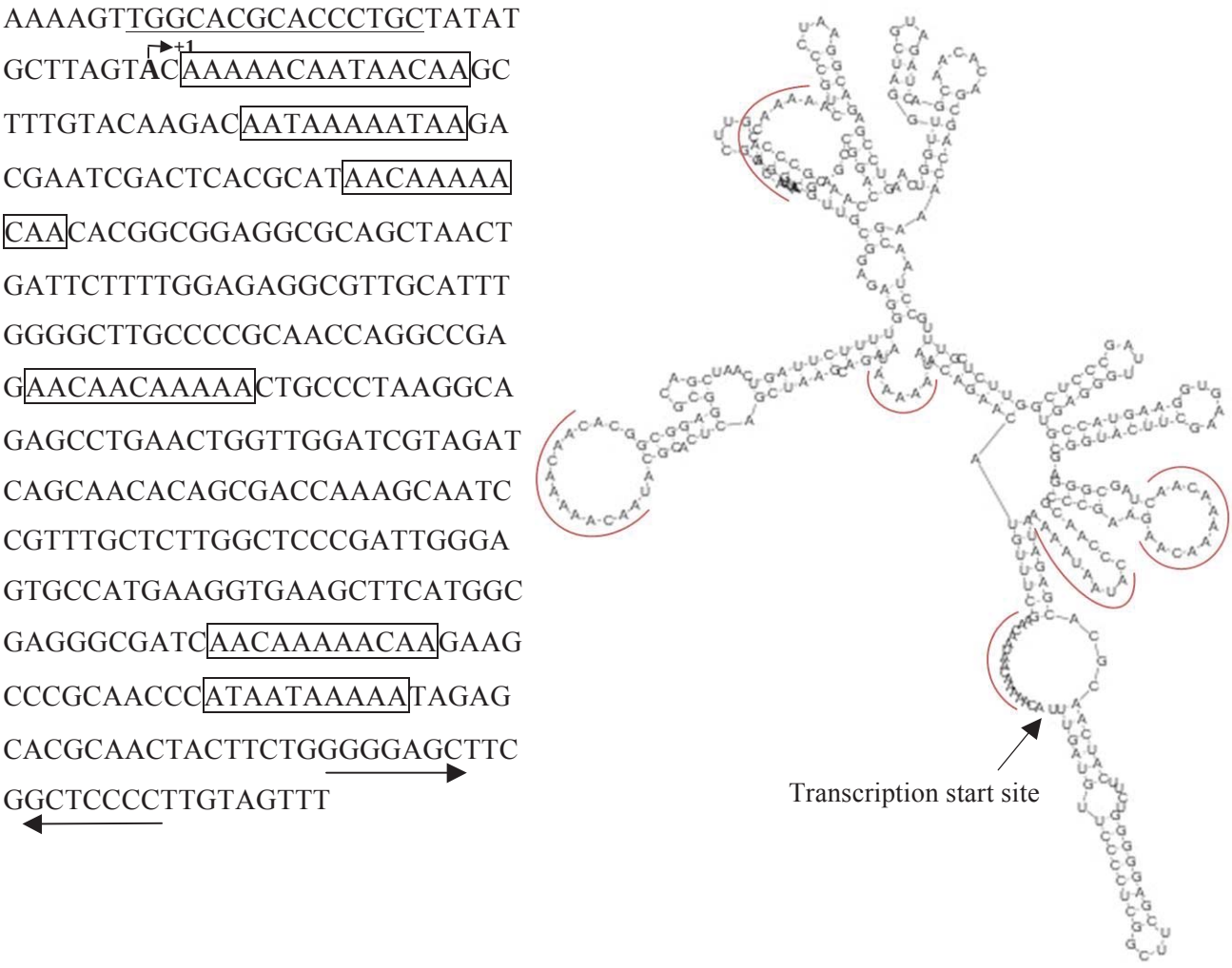

Figure 5.25. Sequence of *crcZ* (Zhang *et al.*, 2010) and its predicted secondary structure. The predicted σ^{54} promoter is underlined. The transcription start site of *crcZ* is indicated by '+1' and an arrow. Six putative Crc-binding motifs are boxed. Palindromic sequences marked by inverted arrows might function as a transcriptional terminator. The secondary structure of CrcZ is predicted by Geneious Pro. Crc-binding motifs are marked by red contour lines.

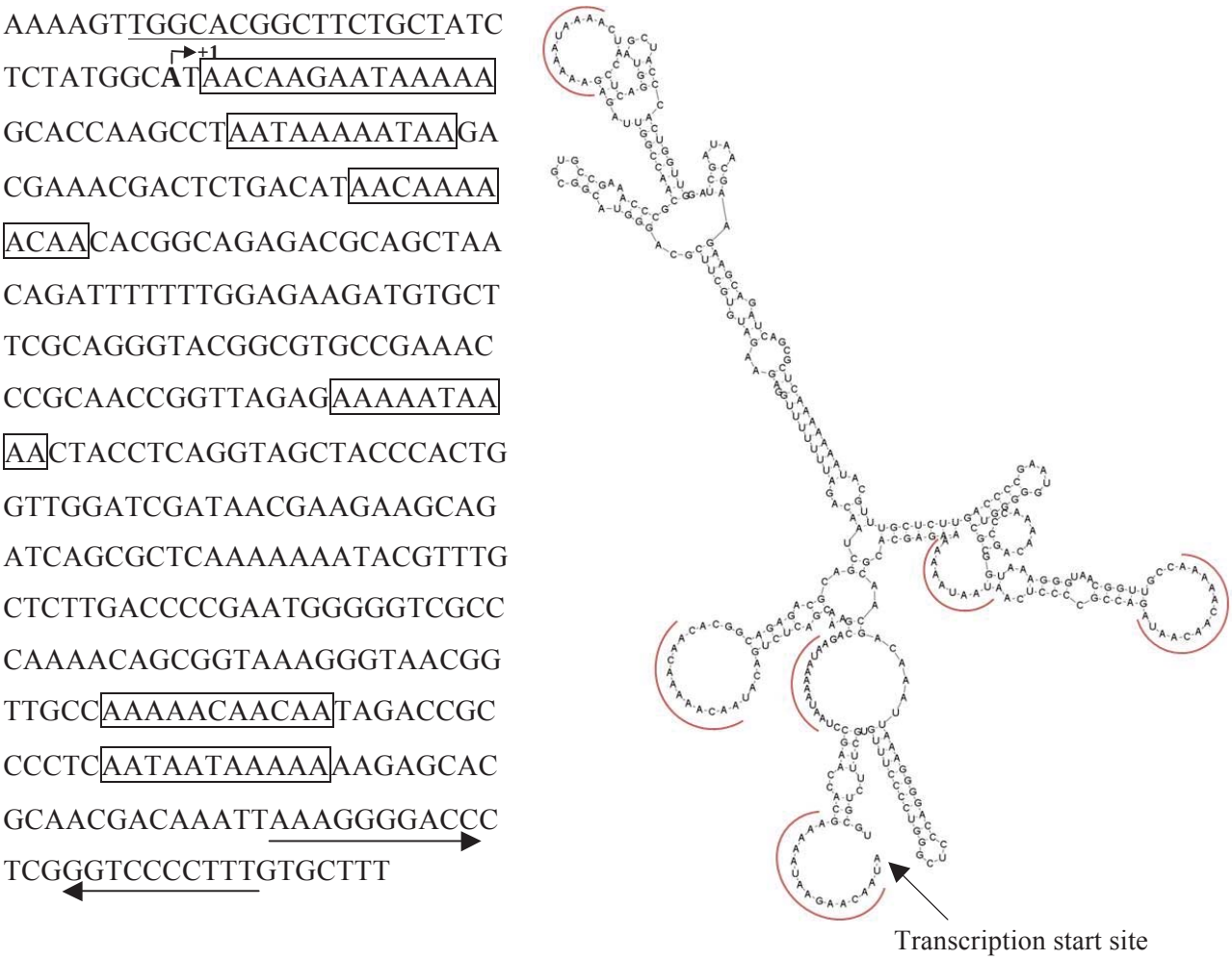

Figure 5.26. Sequence of *crcY* and its predicted secondary structure. The predicted σ54 promoter is underlined. The transcription start site of *crcY* is indicated by '+1' and an arrow. Six putative Crc-binding motifs are boxed. Palindromic sequences marked by inverted arrows might function as a transcriptional terminator. The secondary structure of CrcY is predicted by Geneious Pro. Crc-binding motifs are marked by red contour lines.

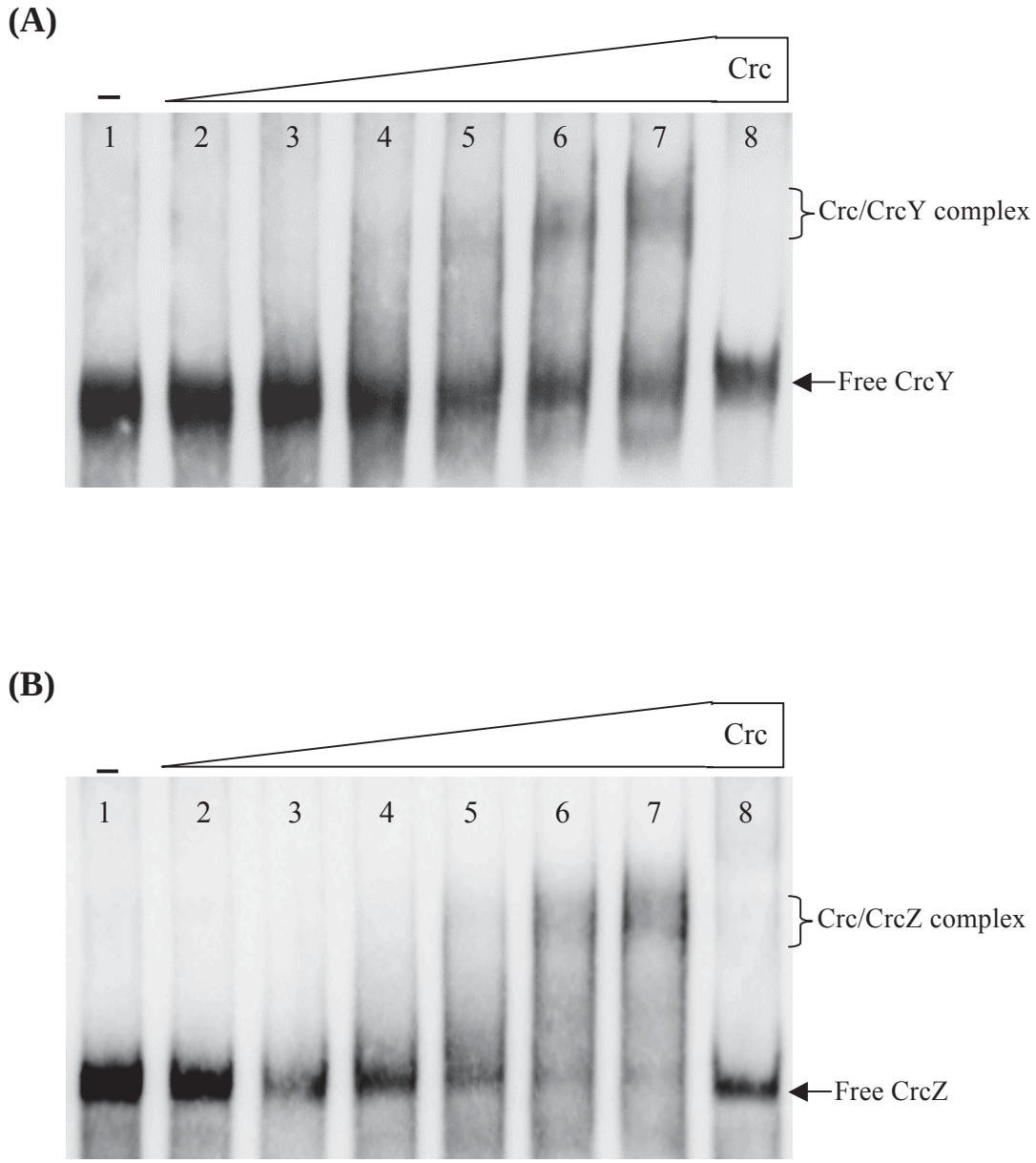

Figure 5.27. Binding of purified Crc to CrcY (A) and CrcZ (B) *in vitro*. EMSA reaction contained the biotin-labelled CrcY or CrcZ, 1 μg of yeast tRNA and purified His_6-Crc. The concentrations of His_6-Crc in lane 1 to 8 were 0, 25, 50, 100, 200, 400, 500 and 500 nM respectively. Unlabelled CrcY or CrcZ was added as a specific competitor in lane 8. Protein-RNA complexes were resolved on a 5% nondenaturing polyacrylamide gel. The positions of free CrcY or CrcZ and the Crc-bound sRNA complexes are indicated.

5.3 Conclusion and Discussion

Data presented in this chapter have identified genetic components that are involved in CCR control of *xut* genes for xylose utilization. The CbrA/CbrB two-component signal transduction system resides at the top of the regulatory hierarchy; and it regulates expression of two small non-coding RNAs (CrcY and CrcZ), which in turn sequester the Crc/Hfq complex and relieve the repression of catabolic genes, such as the *xut* operons. On the basis of the genetic and biochemical data, a regulatory model for CCR in *P. fluorescens* SBW25 is proposed (Figure 5.28). In the presence of succinate, the Crc/Hfq protein complex binds to the 5'-end of *xutAFGH* and *xutR* transcripts at positions near the translational start site, repressing their translation. However, when succinate disappears, CbrAB is activated and stimulates expression of *crcY* and *crcZ*. The small non-coding RNAs CrcY and CrcZ will sequester cellular Crc proteins at high affinity, causing de-repression of *xut* genes.

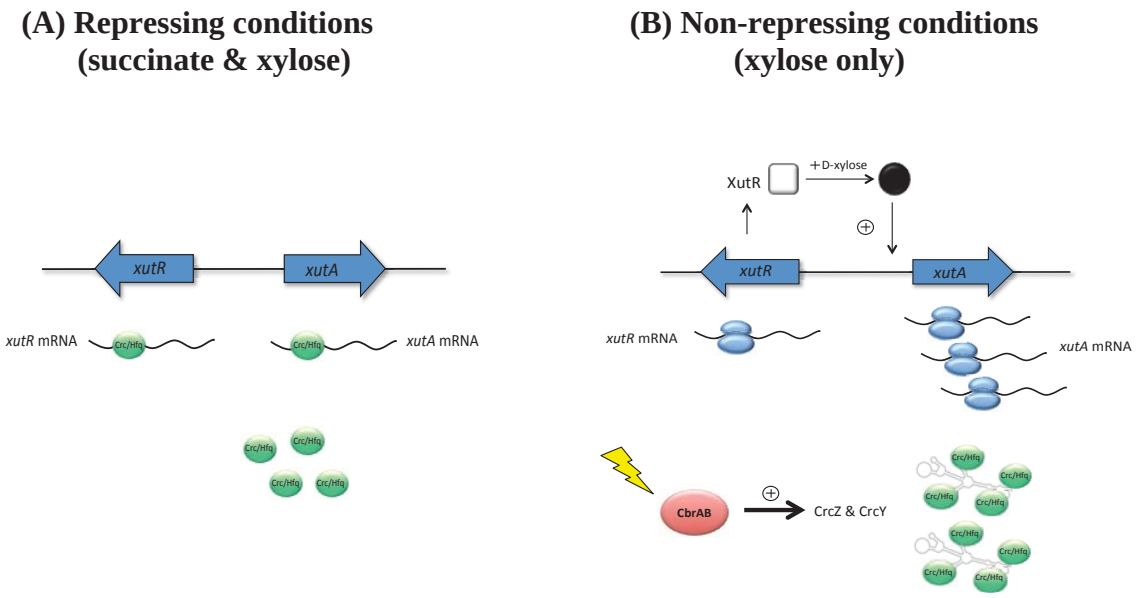

Figure 5.28. The proposed model of CCR in *P. fluorescens* SBW25. (A) When the preferred carbon source succinate is present, Crc/Hfq complex binds to the translation initiation region and blocks translation of mRNAs. (B) When succinate disappears, the two-component system CbrAB stimulates expression of *crcY* and *crcZ*, which sequester the protein complex of Crc/Hfq. This prevents the Crc/Hfq complex from binding to the target mRNAs (e.g. *xyl* genes) and allows ribosome binding and translation of mRNAs.

A combination of site-directed mutagenesis and chromosome integrated *lacZ* reporter fusion has been used to demonstrate the regulatory steps involved in the proposed CCR model. Specifically, I have shown that CbrB activates expression of *crcY* as well as *crcZ* in a σ^{54}-dependent manner. Crc represses expression of not only the structural gene *xutA* but also the regulator *xutR*; and moreover, I show that repression occurs at the post-transcriptional level, instead of the transcriptional level. Crc proteins from *P. fluorescens* SBW25 were successfully purified, and binding of Crc to its candidate mRNA targets was analysed by EMSA. The results show that Crc is capable of binding to 5'-end of *xutA* and *xutR* mRNAs specifically; and more importantly, Crc is also capable of binding to small RNAs CrcY and CrcZ. These empirical data provide sufficient support for the proposed model. However, some critical details are still missing.

First, the precise role of Hfq in CCR remains unclear. The involvement of Hfq in CCR was identified in this work by random transposon mutagenesis in a genome-wide search for regulators in the CbrAB regulon that mediate CbrAB-regulated expression of *xut* genes. Hfq was identified in two of 16 suppressor mutants (others inactivated *crc*). Site-directed mutagenesis analysis showed that Hfq plays similar roles as Crc in repression of *xut* genes. However, biochemical characterization has been focused on the function of Crc. The Hfq protein will be purified and characterized in future follow-up studies. Research of CCR in other *Pseudomonas* species, such as *P. aeruginosa* and *P. putida*, suggests that Hfq can be co-purified with Crc; Hfq instead of Crc directly binds to mRNAs (Sonnleitner & Blasi, 2014; Moreno *et al.*, 2015). While the molecular interaction between Hfq and Crc remain elusive, it is clear that Hfq and Crc form a protein complex and act in a coordinate manner to modulate gene expression at the translation level.

Second, Crc regulates xylose utilization by repressing translation of not only *xut* structural genes but also the activator XutR. The translation of *xutA* mRNA, which encodes the first enzyme of the xylose degradation pathway, is repressed by Crc. A stronger inhibition of *xutA* expression (3~5 folds) than that of *xutR* (~1.5 folds) has been observed. Presumably, this is due to the combined effects of Crc on translation of both *xutR* and *xutA*. A similar regulatory strategy exerted by Crc has been reported

for the toluene/xylene assimilation pathway encoded in the *P. putida* pWW0 plasmid (Moreno *et al.*, 2010), alkane utilization pathway encoded in the *P. putida* OCT plasmid and the benzoate degradation pathway encoded in *P. putida* KT2440 chromosome (Hernandez-Arranz *et al.*, 2013). In these cases, translation of transcriptional activators and some structural genes responsible for the uptake and assimilation of substrates is inhibited by Crc under catabolite repression conditions. Despite limited empirical information available for Crc-regulated metabolic pathways, a computational analysis of twelve fully genome-sequenced *Pseudomonas* species predicted specific targets of Crc which includes transcriptional regulators, transporters and catabolic enzymes of corresponding pathways (Browne *et al.*, 2010). This suggests that Crc-targeting of catabolic genes, transporters and regulators is a common CCR strategy for *Pseudomonas* species.

In *P. aeruginosa,* the small non-coding RNA CrcZ relieves catabolite repression by binding to and sequestering Crc (Sonnleitner *et al.*, 2009). The homologue of CrcZ was also identified in *P. fluorescens* SBW25 (Zhang *et al.*, 2010). In this study, in addition to CrcZ, a homologue sRNA (CrcY) was found. The EMSA showed that both CrcZ and CrcY are able to interact with purified Crc. It suggests that both sRNAs act coordinately to control the amount of free Crc and thus mediate catabolite repression. Under non-repressing growth conditions (xylose only), deletion of either *crcZ* or *crcY* did not affect growth while simultaneous lack of both sRNAs completely abolished cell growth. Moreover, expression of both *crcZ* and *crcY* is activated by the two-component system CbrAB. These results suggest functional redundancy between CrcZ and CrcY. It would be interesting to further elucidate the possible functional difference of CrcY and CrcZ.

Finally, it is interesting but challenging to understand why such a complex regulatory system has evolved in *Pseudomonas* for CCR control of catabolic genes. It may reflect the fact that *Pseudomonas* strains are ubiquitously found in various nutrient-complex environments ranging from water, soil to eukaryotic hosts. The multiple steps of regulation would benefit *Pseudomonas* strains to acclimate to rapid changes of nutrient availability.

5.4 References

Bao, Y., Lies, D. P., Fu, H., & Roberts, G. P. (1991). An improved Tn7-based system for the single-copy insertion of cloned genes into chromosomes of gram-negative bacteria. *Gene, 109*(1), 167-168.

Browne, P., Barret, M., O'Gara, F., & Morrissey, J. P. (2010). Computational prediction of the Crc regulon identifies genus-wide and species-specific targets of catabolite repression control in *Pseudomonas* bacteria. *BMC Microbiol, 10*, 300.

Collier, D. N., Hager, P. W., & Phibbs, P. V., Jr. (1996). Catabolite repression control in the *Pseudomonads*. *Res Microbiol, 147*(6-7), 551-561.

Giddens, S. R., Jackson, R. W., Moon, C. D., Jacobs, M. A., Zhang, X. X., Gehrig, S. M., & Rainey, P. B. (2007). Mutational activation of niche-specific genes provides insight into regulatory networks and bacterial function in a complex environment. *Proc Natl Acad Sci U S A, 104*(46), 18247-18252.

Görke, B., & Stülke, J. (2008). Carbon catabolite repression in bacteria: many ways to make the most out of nutrients. *Nat Rev Microbiol, 6*(8), 613-624.

Hernandez-Arranz, S., Moreno, R., & Rojo, F. (2013). The translational repressor Crc controls the *Pseudomonas putida* benzoate and alkane catabolic pathways using a multi-tier regulation strategy. *Environ Microbiol, 15*(1), 227-241.

Liu, Y., Rainey, P. B., & Zhang, X. X. (2014). Mini-Tn7 vectors for studying post-transcriptional gene expression in *Pseudomonas*. *J Microbiol Methods, 107*, 182-185.

Moreno, R., Ruiz-Manzano, Ana, Yuste, Luis, & Rojo, Fernando. (2007). The *Pseudomonas putida* Crc global regulator is an RNA binding protein that inhibits translation of the AlkS transcriptional regulator. *Mol Microbiol, 64*(3), 665-675.

Moreno, R., Fonseca, P., & Rojo, F. (2010). The Crc global regulator inhibits the *Pseudomonas putida* pWW0 toluene/xylene assimilation pathway by repressing the translation of regulatory and structural genes. *J Biol Chem, 285*(32), 24412-24419.

Moreno, R., Hernandez-Arranz, S., La Rosa, R., Yuste, L., Madhushani, A., Shingler, V., & Rojo, F. (2015). The Crc and Hfq proteins of *Pseudomonas putida* cooperate in catabolite repression and formation of ribonucleic acid complexes with specific target motifs. *Environ Microbiol, 17*(1), 105-118.

Rainey, P. B. (1999). Adaptation of *Pseudomonas fluorescens* to the plant rhizosphere. *Environ Microbiol, 1*(3), 243-257.

Rojo, F. (2010). Carbon catabolite repression in *Pseudomonas* : optimizing metabolic versatility and interactions with the environment. *FEMS Microbiol Rev, 34*(5), 658-684.

Sonnleitner, E., Abdou, L., & Haas, D. (2009). Small RNA as global regulator of carbon catabolite repression in *Pseudomonas aeruginosa*. *Proceedings of the National Academy of Sciences, 106*(51), 21866-21871.

Sonnleitner, E., & Blasi, U. (2014). Regulation of Hfq by the RNA CrcZ in *Pseudomonas aeruginosa* carbon catabolite repression. *PLoS Genet, 10*(6), e1004440.

Vogel, J., & Luisi, B. F. (2011). Hfq and its constellation of RNA. *Nat Rev Microbiol, 9*(8), 578-589.

Zhang, X. X., & Rainey, P. B. (2008). Dual involvement of CbrAB and NtrBC in the regulation of histidine utilization in *Pseudomonas fluorescens* SBW25. *Genetics, 178*(1), 185-195.

Zhang, X. X., Liu, Y. H., & Rainey, P. B. (2010). CbrAB-dependent regulation of pcnB, a poly(A) polymerase gene involved in polyadenylation of RNA in *Pseudomonas fluorescens*. *Environ Microbiol, 12*(6), 1674-1683.

Chapter 6

Concluding remarks and future directions

6.1 Genetic identification and functional analysis of xylose utilization (*xut*) genes

D-Xylose is a five-carbon sugar prevalent in the hemicellulose fraction of biomass. In nature, xylose is mostly present in the form of polymers (i.e. xylan) (Lee, 1997). However, current evidence shows that xylose is also present in monomers in various natural environments, including the surfaces of plants (Shallom & Shoham, 2003) where it is one of the major sugars in plant exudates (Dakora & Phillips, 2002). The overall aim of this project was to understand the genetic basis of xylose utilization by plant-associated bacteria, and moreover, the ecological significance of plant-derived xylose for successful bacterial colonization on plant surfaces. The work has been performed on a model organism - the plant growth-promoting bacterium *P. fluorescens* SBW25. It was based on previous studies that showed xylose utilization genes to be expressed at elevated levels during the process of bacterial colonization of sugar beet seedlings (Rainey, 1999).

Chapter 3 described the characterization of genes involved in xylose utilization by *P. fluorescens* SBW25. The results of genetic and biochemical analysis revealed a novel mechanism of xylose utilization in terms of not only the metabolic genes but also the mode of gene regulation. Importantly, the results of fitness assays using a Xut$^-$ mutant indicate that xylose utilization is an important trait for *P. fluorescens* SBW25 and *xut* genes contribute to the competitiveness of this bacterium in the plant environment.

Bacterial degradation of xylose is sequentially mediated by two enzymes - an isomerase (XutA) and a xylulokinase (XutB) - with xylulose as an intermediate. My work with *P. fluorescens* SBW25 shows that xylose is metabolised through the two-enzyme pathway established in bacteria; however, SBW25 does not carry a xylulokinase gene specific for xylose utilization. I functionally identified two xylulokinase-encoding genes *xutB1* and *xutB2*. Both contribute to bacterial growth on

xylose, but their primary roles are the utilization of mannitol, arabitol and some other unknown substrates (Brunker *et al.*, 1998). Significantly, expression of *xutB1* is specifically induced by xylose. This finding raises the question as to which AraC-type activator (XutR versus MtlR) is responsible for the xylose-induced expression of *xutB1*. Next, experiments were carefully designed to identify the regulator of *xutB1*. The data led to the conclusion that the xylose-induced *xutB1* expression is mediated by the mannitol-responsive activator MtlR, but not XutR. However, xylulose rather than xylose is the direct inducer molecule of MtlR. Xylulose is a common intermediate of catabolic pathways for xylose and arabitol, and it can also be present in natural environments as SBW25 is capable of growth on xylulose as a sole source of carbon and energy. Together, the data indicate a complex overlapping cellular response to xylose and other structurally similar sugars such as mannitol, sorbitol, fructose as well as ribose.

With focus on the regulation of xylose utilization genes, my results show that expression of *xut* genes in *P. fluorescens* SBW25 is controlled by two AraC-type activators (XutR and MtlR) instead of only one as found in other bacteria, such as *E. coli* (XylR) (Song & Park, 1997; Ni *et al.*, 2013). Both XutR and MtlR possess a characteristic 100-residue region with two helix-turn-helix (HTH) DNA-binding motifs (Gallegos *et al.*, 1997). Interestingly, XutR and MtlR have distinct but overlapping substrate specificities. The data show that XutR can recognize three carbon substrates: xylose, xylulose and ribose, whereas MtlR can be activated by mannitol and xylulose. Strikingly, XutR plays no apparent role in ribose utilization, as the *xutR* deletion mutant grew normally as the wild type on ribose. A plausible explanation for ribose-induced expression of the *xutAFGH* operon is that *xutFGH* encode an ABC-type transporter with a functional role in ribose uptake. The Δ*xutFGH* mutant displayed a reduced growth phenotype on xylose, suggesting that XutFGH functions as a xylose-specific transporter. However, the possible involvement of XutFGH in the uptake of xylulose and ribose remains to be determined.

Transcriptional activators of the AraC family typically use DNA-looping to modulate levels of gene expression. For example, DNA-looping mediated by the xylose

responsive regulator XylR allows simultaneous activation of the two divergently organized promoters of the *xylAB* and *xylFGH* operons in *E. coli* (Ni *et al.*, 2013). In the present study, the XutR regulator was subjected to a detailed genetic and biochemical characterization, including electrophoretic mobility shift assays (EMSA) and DNase I footprinting analysis. The DNA targeting site of XutR has been identified, and the molecular data presented here allowed me to propose an unconventional mechanism of XutR action that does not involve DNA-looping. Specifically, XutR appears to function as a dimer that recognizes two inverted repeat sequences; but binding to one half site is very weak, requiring inducer molecules such as xylose for activation.

6.2 Molecular mechanism of carbon catabolite repression (CCR) of xylose utilization (*xut*) genes

Xylose is present in abundance in natural environments, but it does not support fast growth of *P. fluorescens* SBW25. It is therefore not surprising that xylose is a non-preferred carbon source for *P. fluorescens* SBW25. Accordingly, expression of *xut* genes for xylose utilization is repressed in the presence of preferred carbon sources, such as succinate. This is a typical of a phenomenon known as carbon catabolic repression (CCR) (Görke & Stülke, 2008). CCR has been well studied in *E. coli* where it is mediated by the catabolite-activating protein (CAP) charged with cAMP. However, this paradigm does not hold for many non-enteric bacteria, including bacteria belonging to the closed related genus *Pseudomonas* (Rojo, 2010). It is known that CCR in *Pseudomonas* occurs at the post-transcriptional level involving a RNA-binding protein Crc (Moreno *et al.*, 2007), but the precise molecular mechanism remains unclear.

To study the mechanism of succinate-mediated CCR control of xylose utilization genes, it was necessary to construct genetic tools suitable for monitoring gene expression at the post-transcriptional level. To this end, I constructed and validated a panel of five mini-Tn*7* vectors for analysis of post-transcriptional gene expression in *Pseudomonas*. The mini-Tn*7* vectors have advantages over plasmid vectors in that they deliver reporter fusions into the chromosome in a site- and orientation-specific manner. Mini-Tn*7* allows cloned genes to be integrated into the chromosome at a

single site (attTn*7*), which can stably maintained in the absence of antibiotic selection. Four vectors (namely pXY1 to pXY4) allow construction of translational fusions to β-galactosidase (*lacZ*), while the fifth (pXY5) is designed for functional analysis of noncoding RNA genes.

In this work, carbon catabolite repression of xylose utilization genes was studied based on a previous finding that the two-component regulatory system CbrAB is required for activation of *xut* genes (Zhang & Rainey, 2008). A *cbrB* mutant lost ability to use xylose (and other substrates such as arginine, histidine) as a sole carbon source. To identify genetic components in the CbrAB regulon responsible for activation of *xut* genes, random transposon mutagenesis was used to identify suppressor mutants that can grow on xylose. This led to the identification of suppressor mutations in two genes, *crc* and *hfq*. Given that Crc is known to be a key regulator of CCR in *Pseudomonas*, CbrAB is implicated in CCR.

I next performed a combination of genetic and biochemical analyses that showed the regulatory role of CbrAB in modulating Crc activity to be mediated by two small non-coding RNAs, termed CrcY and CrcZ. Both CrcY and CrcZ can specifically bind to the purified Crc protein, thus have the potential to sequester intracellular Crc. Moreover, CrcY and CrcZ are under the transcriptional control of the same regulator CbrAB. My data indicate that CrcY and CrcZ are functionally redundant. Notably, only one copy (CrcZ) is involved in CCR of other *Pseudomonas* species, such as *P. aeruginosa* (Sonnleitner *et al.*, 2009). In future work, it will be interesting to seek evidence, both experimental and theoretical, to explain why SBW25 has two regulatory RNAs for CCR control.

Given the central role of the Crc protein in CCR of *Pseudomonas*, I performed *in vitro* protein-mRNA binding assays to test the molecular interaction between Crc and target RNAs. Crc with a C-terminal His_6-tag was expressed and prepared from *E. coli* cells. EMSA analysis showed that Crc is capable of binding to CrcY, CrcZ, *xutA* and *xutR* RNA molecules. Taken together, these data enabled me to propose a regulatory model for CCR in *P. fluorescens* SBW25 (Figure 5.28). When succinate is present in the environment, Crc/Hfq protein complex binds to the 5-end of *xutA* and *xutR* transcripts at positions near the translational start sites, repressing their translation.

When succinate disappears, CbrAB is activated and stimulates expression of *crcY* and *crcZ*. Non-coding RNAs CrcY and CrcZ then sequester the Crc protein, causing de-repression of *xut* genes. Of note is that the regulatory role of the RNA chaperon protein Hfq in CCR control is not fully understood. Further work will likely focus on the molecular interaction between Crc and Hfq.

Finally, it is interesting to note that Crc regulates xylose utilization by targeting the mRNA transcripts of both the catabolic gene *xutA* and its regulator *xutR*. It may be that this mode of regulation ensures a rapid response (or a shift of cellular metabolism) towards the preferred substrate (e.g., succinate) and would be much slower were regulation to target the transcriptional response determined by a regulator. However, a rapid response to the presence of succinate would mean a slow response to the disappearance of a preferred substrate. One possibility is the existence of additional steps of regulation (that are yet to be determined) that might reduce the possibility of a slow response. This would be understandable given the nutritional versatility of *Pseudomonas* and its *r*-selected (weed-like) ecological strategy – a strategy that does not delay in taking advantage of every – and any – opportunity for rapid uptake of nutrients.

6.3 References:

Brunker, P., Altenbuchner, J., & Mattes, R. (1998). Structure and function of the genes involved in mannitol, arabitol and glucitol utilization from *Pseudomonas fluorescens* DSM50106. *Gene, 206*(1), 117-126.

Dakora, F., & Phillips, D. (2002). Root exudates as mediators of mineral acquisition in low-nutrient environments. *Plant and Soil, 245*(1), 35-47.

Gallegos, M. T., Schleif, R., Bairoch, A., Hofmann, K., & Ramos, J. L. (1997). Arac/XylS family of transcriptional regulators. *Microbiol Mol Biol Rev, 61*(4), 393-410.

Görke, B., & Stülke, J. (2008). Carbon catabolite repression in bacteria: many ways to make the most out of nutrients. *Nat Rev Microbiol, 6*(8), 613-624.

Lee, J. (1997). Biological conversion of lignocellulosic biomass to ethanol. *J Biotechnol, 56*(1), 1-24.

Moreno, R., Ruiz-Manzano, Ana, Yuste, Luis, & Rojo, Fernando. (2007). The *Pseudomonas putida* Crc global regulator is an RNA binding protein that inhibits translation of the AlkS transcriptional regulator. *Mol Microbiol, 64*(3), 665-675.

Ni, L., Tonthat, N. K., Chinnam, N., & Schumacher, M. A. (2013). Structures of the *Escherichia coli* transcription activator and regulator of diauxie, XylR: an AraC DNA-binding family member with a LacI/GalR ligand-binding domain. *Nucleic Acids Res, 41*(3), 1998-2008.

Rainey, P. B. (1999). Adaptation of *Pseudomonas fluorescens* to the plant rhizosphere. *Environ Microbiol, 1*(3), 243-257.

Rojo, F. (2010). Carbon catabolite repression in *Pseudomonas* : optimizing metabolic versatility and interactions with the environment. *FEMS Microbiol Rev, 34*(5), 658-684.

Shallom, D., & Shoham, Y. (2003). Microbial hemicellulases. *Curr Opin Microbiol, 6*(3), 219-228.

Song, S., & Park, C. (1997). Organization and regulation of the D-xylose operons in *Escherichia coli* K-12: XylR acts as a transcriptional activator. *J Bacteriol, 179*(22), 7025-7032.

Sonnleitner, E., Abdou, L., & Haas, D. (2009). Small RNA as global regulator of carbon catabolite repression in *Pseudomonas aeruginosa*. *Proceedings of the National Academy of Sciences, 106*(51), 21866-21871.

Zhang, X. X., & Rainey, P. B. (2008). Dual involvement of CbrAB and NtrBC in the regulation of histidine utilization in *Pseudomonas fluorescens* SBW25. *Genetics, 178*(1), 185-195.

Appendix I

MASSEY UNIVERSITY
GRADUATE RESEARCH SCHOOL

STATEMENT OF CONTRIBUTION TO DOCTORAL THESIS CONTAINING PUBLICATIONS

(To appear at the end of each thesis chapter/section/appendix submitted as an article/paper or collected as an appendix at the end of the thesis)

We, the candidate and the candidate's Principal Supervisor, certify that all co-authors have consented to their work being included in the thesis and they have accepted the candidate's contribution as indicated below in the *Statement of Originality*.

Name of Candidate: Yunhao Liu

Name/Title of Principal Supervisor: Prof. Paul Rainey

Name of Published Research Output and full reference:

Liu, Y., Rainey, P. B., & Zhang, X. X. (2014). Mini-Tn7 vectors for studying post-transcriptional gene expression in Pseudomonas. J Microbiol Methods, 107, 182-185

In which Chapter is the Published Work: Chapter 4

Please indicate either:

- The percentage of the Published Work that was contributed by the candidate:

  and / or

- Describe the contribution that the candidate has made to the Published Work:

  Yunhao was responsible for conducting all experimental work and contributed to the writing of the manuscript.

Yunhao Liu — Digitally signed by Yunhao Liu, DN: cn=Yunhao Liu, o=Massey University, ou=NZIAS, email=yunhao.liu.1@uni.massey.ac.nz, c=NZ, Date: 2015.03.30 14:19:51 +13'00'

Candidate's Signature — 15.04.2015 — Date

Paul Rainey — Digitally signed by Paul Rainey, DN: cn=Paul Rainey, o, ou=NZIAS, email=p.b.rainey@massey.ac.nz, c=NZ, Date: 2015.04.19 05:49:26 +01'00'

Principal Supervisor's signature — Date